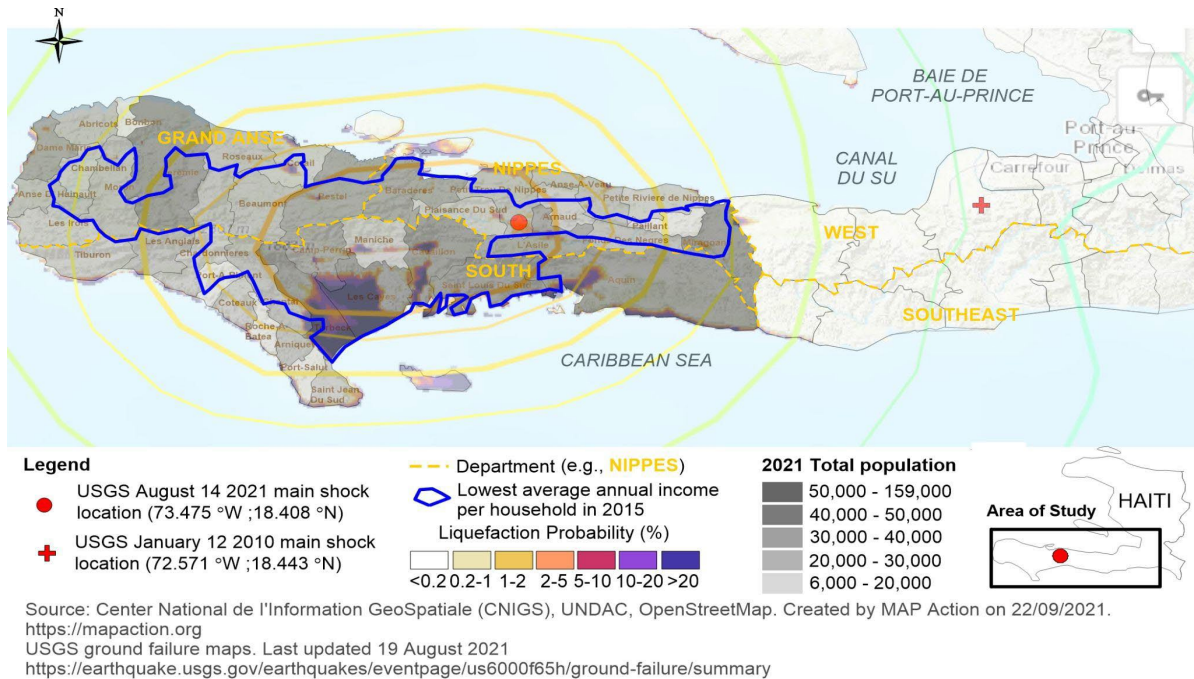


# RECONNAISSANCE FOLLOWING THE AUGUST 14, 2021 HAITI EARTHQUAKE: PERSPECTIVES FROM GEOTECHNICAL ENGINEERING AND SOCIAL/POLITICAL SCIENCES

Geotechnical Extreme Events Reconnaissance (GEER) Report No. 073

doi:10.18118/G60090

Version 1.0: February 3, 2021



## Editors:

Shideh Dashti, Geotechnical Engineering Team Lead (University of Colorado Boulder, USA)  
Nazife Emel Ganapati, Social Science Team Lead (Florida International University, USA)

## Contributing Authors (alphabetical order):

Nancy Ingabire Abayo (North Carolina State University, USA)  
Ashly Cabas (North Carolina State University, USA)  
Santina Contreras (University of Southern California, USA)  
Joseph Emmanuel Dessable (Geosciences at Faculte Des Sciences of UEH, Haiti)  
Estefan Garcia (University of Michigan, USA)  
Kelly Guerrier (Université d'Etat d'Haïti, Haiti)  
Yu-Wei Hwang (University of Colorado Boulder & University of Texas at Austin, USA)  
Tarah Jeannot (Civil Engineer at National Transport et Construction)

Chunyang Ji (North Carolina State University, USA)  
Richard Lagesse (ARUP, UK)  
Marvens Logiste (la Faculté des sciences de UEH, Haiti)  
Cristina Lorenzo-Velazquez (North Carolina State University, USA)  
Louis HERNs Marcelin (University of Miami, USA)  
Sary Nicolas (ARUP, USA)  
Jenny Ramirez (Geosyntec Consultants, USA)  
Christa Remington (University of South Florida, USA)  
Joanne Perodin (Florida International University, USA)  
Newdeskari Saint Fleur (Université d'Etat d'Haïti, Haiti)  
Michelle Shriro (ARUP, USA)  
Santiana Vissière (Geosciences at Faculte Des Sciences of UEH, Haiti)  
Michael Whitworth (AECOM and EEFIT, UK)

## CONTENTS

ACKNOWLEDGEMENTS .....	1
1. INTRODUCTION.....	1
2. TEAM STRUCTURE AND DATA COLLECTION APPROACH.....	2
3. REGIONAL TECTONICS .....	4
3.1. Historical Seismicity .....	6
4. GEOLOGIC SETTING.....	9
4.1. Bedrock Geology .....	9
4.2. Surficial Geology .....	11
4.2.1 Local hydrogeologic and geomorphologic conditions.....	17
5. SEISMOLOGICAL ASPECTS AND GROUND MOTION CHARACTERISTICS.....	20
5.1. Past Recorded Earthquakes .....	20
5.2. Main Event Characteristics and Aftershocks.....	24
5.3. Recorded Ground Motions from the 2021 Nippes Earthquake.....	27
6. SIMULTANEOUS HAZARDS AND CRISES IN HAITI AFFECTING VULNERABILITY..	34
6.1. Natural Hazards.....	34
6.2. Governance Challenges.....	35
6.3. Security Challenges.....	37
6.4. Developmental Challenges.....	38
6.5. Mental Health Challenges.....	40
7. GEOTECHNICAL HAZARDS .....	42
7.1. Ground Failure along the Fault.....	43
7.2. Seismic Slope Stability and Landslides.....	56
7.3. Liquefaction and Cyclic Softening.....	86
7.4. Performance of Roads, Bridges, Retaining Structures, and other Infrastructure.....	96
7.5. Damage to Building Structures due to Geotechnical Effects .....	105
8 INTERSECTION OF SOCIAL AND ENGINEERING OBSERVATIONS .....	107
8.1. Pre-Earthquake Conditions .....	107
8.2. Population Displacement following the Mw7.0, 2010 Earthquake.....	108
8.3. The 2012 Hurricane Sandy .....	109
8.4. The 2016 Hurricane Matthew .....	110
8.5. The 2021 Mw7.2 Nippes Earthquake.....	111

<b>9. FUTURE RESEARCH AGENDA AND RECOMMENDATIONS</b> .....	113
<b>9.1. Engineering</b> .....	113
<b>9.2. Social Science</b> .....	113
<b>10. GUIDING PRINCIPLES FOR POST-DISASTER RESPONSE, RECOVERY, AND MITIGATION IN HAITI</b> .....	114
<b>11. REFERENCES</b> .....	116

## LIST OF TABLES

<b>Table 3.1.</b> Significant (>6.0 Mw) historical and recent earthquakes for the island of Hispaniola.....	8
<b>Table 4.1.</b> Recording stations with available records from the 2021 Nippes mainshock.....	13
<b>Table 4.2.</b> Proxy-based Vs30 and NEHRP (BSSC, 2003) site classification at locations of interest in Haiti based on proxy-based values of Vs30 from USGS.....	14
<b>Table 5.1.</b> Code, name, and location of the stations within the AY – Haitian Seismic Network operated by BME (FDSN; last accessed November 2021).....	22
<b>Table 5.2.</b> Ground motion characteristics of the records corresponding to the 2021 Nippes earthquake. ....	28
<b>Table 6.1.</b> Haiti’s Economic Profile.....	39
<b>Table 6.2.</b> Largest Official Development Assistance Recipients in the Americas in 2019. ....	39

## LIST OF FIGURES

- Figure 3.1.** Summary of tectonics in the Caribbean region and the epicenter location corresponding to the 2021 M7.2 Nippes, Haiti earthquake (modified after USGS, last accessed October 2021)...4
- Figure 3.2.** The complex tectonic regime characterizing the seismicity in Haiti. The Septentrional Fault in the north and the Enriquillo-Plantain Garden Fault are shown in the northern and southern parts, respectively. Historical seismicity in the region is also depicted (Modified after New York Times, January 26, 2010; credit Jonathan Corum). ..... 5
- Figure 3.3.** Crustal Faults are shown in red and green, while subduction zones are shown in blue. The black star shows the epicenter of the M7.0 12 January 2010 Haiti earthquake with respect to Port-au-Prince (denoted as “P”), while the red star depicts the epicenter of the M7.2 14 August 2021 Haiti earthquake (modified after Frankel et al 2011)..... 6
- Figure 3.4.** Estimated locations of historical events on or near the Enriquillo fault shown as orange stars. The location of the epicenter of the 12 January 2010 event is depicted as a white star (after Bakun et al 2012). ..... 7
- Figure 4.1.** Geographic Provinces of Haiti showing the extent of the mountain range of La Hotte (Woodring et al. 1924.).....10
- Figure 4.2.** Regional geological map highlighting the locations where ground failure or damage was observed [Modified after Bureau des mines et de l’énergie d’Haïti (1986)] ..... 11
- Figure 4.3.** Location of stations that recorded ground motions from the 2021 Nippes earthquake overlaid on a map of the spatial distribution of proxy-based Vs30 values in Haiti. The cities of Nippes and Les Cayes, which experienced significant damage due to the 2021 Nippes earthquakes are shown, along with Haiti’s capital city, Port au Prince. .... 12
- Figure 4.4.** Regional map with the locations of interest overlaid on the proxy-based Vs30 distribution map of Haiti (from USGS). ..... 15
- Figure 4.5.** Comparison of the approximated Vs30 proxy maps with the regional geologic maps within the regions of interest and the corresponding NEHRP (BSSC, 2003) soil classification.. 16
- Figure 4.6.** Surface water resources map [Modified after Knowles et al. 1999] ..... 18
- Figure 4.7.** Groundwater Resources map [Modified after Knowles et al. 1999] ..... 19

<b>Figure 5.1.</b> Locations of four Kinematics K2 seismographs (accelerometer) stations deployed by Eberhald et al (2013) during their reconnaissance mission after the 12 January 2010 Port-au-Prince earthquake. ....	20
<b>Figure 5.2.</b> Location of seismograph and strong-motion stations installed in Haiti (left) and their status (right) as of October 2017 (after Bent et al. 2018). EPGF refers to the Enriquillo Plantain Garden fault, NHF is the North Hispaniola fault, and SF refers to the Septentrional fault. ....	21
<b>Figure 5.3.</b> Location of stations (red triangles) in the AY – Haitian Seismic Network operated by the Bureau of Mines and Energy of Haiti. (modified after FDSN; last accessed November 2021). ....	22
<b>Figure 5.4.</b> Locations of low-cost Raspberry Shake sensors in Haiti (modified after Witze 2021). The image on the right shows more detailed locations of the Raspberry sensors that are part of the Ayiti-Seismes, citizen science network ( <a href="https://ayiti.unice.fr/ayiti-seismes/">https://ayiti.unice.fr/ayiti-seismes/</a> ; last accessed November 2021) .....	23
<b>Figure 5.5.</b> Macroseismic Intensity Map in Haiti for the 2021 Nippes main event (USGS, last accessed October 2021). ....	25
<b>Figure 5.6.</b> Peak ground acceleration ShakeMap in Haiti for the 2021 main event (USGS, last accessed October 2021). ....	26
<b>Figure 5.7.</b> Magnitude and location of more than 400 aftershocks associated with the 2021 Nippes earthquake between August 14-23, 2021 ( <a href="https://ayiti.unice.fr/ayiti-seismes/">https://ayiti.unice.fr/ayiti-seismes/</a> ; last accessed November 2021). ....	26
<b>Figure 5.8.</b> Acceleration time series observed at station AM.R50D4 during the 2021 Nippes Earthquake. ....	29
<b>Figure 5.9.</b> Acceleration time series observed at station AY.NQUSE during the 2021 Nippes Earthquake. ....	30
<b>Figure 5.10.</b> Velocity time series observed at station AM.R50D4 during the 2021 Nippes Earthquake. ....	31
<b>Figure 5.11.</b> Comparison of the Fourier amplitude spectra in the two orthogonal horizontal directions observed at stations AM.R50D4 and AY.NQUSE. The AM.R50D4 may indicate potential directivity effects in the amplification of low-frequency motions in the north-south component. ....	32
<b>Figure 5.12.</b> Comparison of the acceleration response spectra (5%-damped) in the two orthogonal horizontal directions observed at stations AM.R50D4 and AY.NQUSE. The AM.R50D4 may	

indicate potential directivity effects in the amplification of long-period motions in the north-south component..... 33

**Figure 6.1.** Percentage of Haitian population impacted by three or more events by department (region) between 2014-2016.....35

**Figure 7.1.** Route 1 taken by the October 9-10 GEER Team. Point A: Les Cayes. Point B: Pestle. Point C: Camp-Perrin..... 42

**Figure 7.2.** Route 2 taken by the October 9-10 GEER Team. Point A: Les Cayes. Point B: L'Asile. Point C: Balou. Point D: Cavaillon..... 43

**Figure 7.3.** Locations of geotechnical observations nearest to the Enriquillo-Plaintain Garden Fault (courtesy of Google Earth). The Enriquillo-Plaintain Garden Fault is delineated in red by Saint Fleur et al. (2020). The pins correspond to the location of subsequent figures..... 44

**Figure 7.4.** Rockfall next to road RC-204 (Lat: 18.37306, Lon: -73.53889)..... 45

**Figure 7.5.** Possible surface fault rupture next to road RC-204 (Lat: 18.37306, Lon: -73.53889). ..... 45

**Figure 7.6.** Slope failure near Balou (Lat: 18.37866, Lon: -73.51278). ..... 46

**Figure 7.7.** Possible earthquake-induced landslide near RC-204A between L'Asile and Balou (Lat: 18.37528, Lon: -73.46333). ..... 47

**Figure 7.8.** Upslope view of scarp associated with ground failure near L'Asile (Lat: 18.37444, Lon: -73.43278). For scale, person in (b) is 1.6 meters in height. .... 48

**Figure 7.9.** Downslope views of ground failure near L'Asile (Lat: 18.37444, Lon: -73.43278). 49

**Figure 7.10.** Ground cracking associated with ground failure near L'Asile shown in Figs. 7.8 and 7.9 (Lat: 18.37444, Lon: -73.43278)..... 50

**Figure 7.11.** Additional views of the ground failure shown in Figs. 7.8-7.10 (Lat: 18.37444, Lon: -73.43278)..... 51

**Figure 7.12.** Foundation damage associated with ground failure shown in Figs. 7.8-7.11 (Lat: 18.37444, Lon: -73.43278). ..... 52

**Figure 7.13.** Ground failure scarp near L'Asile (Lat: 18.3744, Lon: -73.4325)..... 52

**Figure 7.14.** Landslide adjacent to river in Saint Ange (Lat: 18.37333, Lon: -73.43278) ..... 53

<b>Figure 7.15.</b> Rockfall along RC-204a between L’Asile and Mornes (Lat: 18.36833, Lon: -73.39417). .....	54
<b>Figure 7.16.</b> Surface cracks with evidence of sand ejecta immediately adjacent to the cracks (Lat: 18.38574, Lon: -73.41023). Photos taken on August 25, 2021, courtesy of Dr. Newdeskarl Saint Fleur. ....	55
<b>Figure 7.17.</b> Surface cracks with evidence of sand ejecta immediately adjacent to the cracks (Lat: 18.35, Lon: -73.70694). Photos taken on August 28, 2021, courtesy of Dr. Newdeskarl Saint Fleur. ....	55
<b>Figure 7.18.</b> Landslide susceptibility base map in Haiti (the sources are provided in the figure legend).....	56
<b>Figure 7.19.</b> Satellite views of Pic Macaya National Park. (a) Imagery from August 10, 2021. (b) Imagery from August 29, 2021. Landslides are interpreted from the removed vegetation in the second image. Images courtesy of Planet Labs (planet.com). ....	57
<b>Figure 7.20.</b> Locations of slope instabilities identified by the remote GEER Team between October 9-10 (courtesy of Google Earth). Red pins are locations of rockfalls. Yellow pins are locations of landslides. Fault traces are delineated in red by Saint Fleur et al. (2020).....	58
<b>Figure 7.21.</b> Landslide along RN2 between Saint Louis du Sud and Meyance (Lat: 18.25861, Lon: -73.52694). .....	59
<b>Figure 7.22.</b> Landslide near Champlois (Lat: 18.3718016, Lon: -73.8393673). ....	60
<b>Figure 7.23.</b> Satellite imagery of Landslide (roughly outlined in red) shown in Fig. 7.22 (courtesy of Google Earth). ....	60
<b>Figure 7.24.</b> Landslide and rockfall adjacent to Saut-Mathurine (Lat: 18.3690876, Lon: -73.8495348). .....	61
<b>Figure 7.25.</b> Google Earth imagery of Saut Mathurine (a) before the earthquake on February 26, 2021, and (b) after the earthquake on August 27, 2021. ....	61
<b>Figure 7.26.</b> Slope failure along RN7 with water tank at top of slope (Lat: 18.3652708, Lon: -73.8791013). .....	62
<b>Figure 7.27.</b> Pre-event and post-event satellite imagery of landsliding along RN7 west of Champlois (courtesy of Planet Labs, planet.com): (a) February 26, 2021. (b) August 27, 2021. 62	

<b>Figure 7.28.</b> Locations of landslides and rockfalls observed along RN7 east of Duchity and West of Champlois. Mapped fault strand shown in red from Saint Fleur et al. (2020). Imagery date October 9, 2021.....	63
<b>Figure 7.29.</b> Slope failure along RN7 associated with 1.6 km stretch of landslide activity (Lat: 18.3688969905183, Lon: -73.8789592310786). .....	64
<b>Figure 7.30.</b> Rockfall along RN7 associated with 1.6 km stretch of landslide activity (Lat: 18.369867, Lon: -73.8784972). Photo taken September 27, 2021. ....	64
<b>Figure 7.31.</b> Slope failure along RN7 associated with 1.6 km stretch of landslide activity (Lat: 18.371743, Lon: -73.8773852). .....	65
<b>Figure 7.32.</b> Rockfall along RN7 (Lat: 18.3718874, Lon: -73.8773472)......	65
<b>Figure 7.33.</b> Rockfall along RN7 (Lat: 18.3737682, Lon: -73.8769681)......	66
<b>Figure 7.34.</b> Rockfall along RN7 (Lat: 18.37430287, Lon: -73.87626537). Photo taken September 28, 2021.....	66
<b>Figure 7.35.</b> Rockfall along RN7 (Lat: 18.3745397, Lon: -73.8762437). Photo taken September 28, 2021.....	67
<b>Figure 7.36.</b> Rockfall along RN7 (Lat: 18.374679, Lon: -73.8760854)......	67
<b>Figure 7.37.</b> Rockfall along RN7 (Lat: 18.3757585, Lon: -73.8739482)......	67
<b>Figure 7.38.</b> Rockfall along RN7 (Lat: 18.376124, Lon: -73.8739723). Photo taken September 28, 2021.....	68
<b>Figure 7.39.</b> Rockfall along RN7 (Lat: 18.3771116, Lon: -73.8734214)......	68
<b>Figure 7.40.</b> Rockfall along RN7 (Lat: 18.3777911, Lon: -73.8750105)......	68
<b>Figure 7.41.</b> Landslide near RN7 with an average slope 47% over length of ~0.4 km as measured in Google Earth (Lat: 18.385256, Lon: -73.869594). (a) February 26, 2021. (b) August 27, 2021. ....	69
<b>Figure 7.42.</b> Locations of landslides (yellow pins) and rockfalls (red pins) observed along RN7 (courtesy of Google Earth). Imagery date October 9, 2021.....	69
<b>Figure 7.43.</b> Rockfall along RN7 in Catiche (Lat: 18.4030031, Lon: -73.8747026).....	70
<b>Figure 7.44.</b> Rockfall along RN7 in Catiche (Lat: 18.4048258, Lon: -73.8767197).....	70

<b>Figure 7.45.</b> Landslide along RN7 (Lat: 18.4053372, Lon: -73.8777936).....	71
<b>Figure 7.46.</b> Rockfall along RN7 (Lat: 18.407487, Lon: -73.8794692).....	71
<b>Figure 7.47.</b> Landslide with boulder debris along RN7 (Lat: 18.4072403, Lon: -73.8819915)..	72
<b>Figure 7.48.</b> Rockfall along RN7 (Lat: 18.4073275, Lon: -73.8825593).....	72
<b>Figure 7.49.</b> Rockfall along RN7 (Lat: 18.4082712, Lon: -73.8832756).....	72
<b>Figure 7.50.</b> Locations of landslides and rockfalls along RN7 (courtesy of Google Earth). Imagery date October 15, 2019.....	73
<b>Figure 7.51.</b> Slope failure along RN7 (Lat: 18.4166156, Lon: -73.9020873).....	73
<b>Figure 7.52.</b> Slope failure along RN7 (Lat: 18.418817, Lon: -73.9027543).....	74
<b>Figure 7.53.</b> Debris flow on RN7 (Lat: 18.4189306, Lon: -73.903528).....	74
<b>Figure 7.54.</b> Smaller rockfall along RN7 (Lat: 18.427099, Lon: -73.9020971).....	75
<b>Figure 7.55.</b> Landslide above Riviere Glace (Lat: 18.4271578, Lon: -73.9020508).....	75
<b>Figure 7.56.</b> Landslide above Riviere Glace (Lat: 18.4277291, Lon: -73.9014994).....	75
<b>Figure 7.57.</b> Satellite imagery for landslide shown in Figs. 7.29 and 7.30 (courtesy of Planet Labs, planet.com). Marker shown is where the photos in Fig. 7.29 were taken. (a) August 10, 2021. (b) August 30, 2021.....	76
<b>Figure 7.58.</b> Possible failure of rockface along RN7 (Lat: 18.429466, Lon: -73.8998361).....	76
<b>Figure 7.59.</b> Possible landslide with boulder debris that may have occurred sometime prior to the August 14 earthquake, judging based on satellite imagery (Lat: 18.429649, Lon: -73.899932)..	77
<b>Figure 7.60.</b> Locations of rockfalls observed along RN7 (courtesy of Google Earth). Imagery date October 15, 2019.....	77
<b>Figure 7.61.</b> Rockslide along RN7 (Lat: 18.456184, Lon: -73.919748).....	78
<b>Figure 7.62.</b> Rockslide along RN7 (Lat: 18.4561665, Lon: -73.9199208).....	78
<b>Figure 7.63.</b> Rockfall along RN7 (Lat: 18.46123, Lon: -73.919987).....	78
<b>Figure 7.64.</b> Northernmost locations of rockfalls documented by the GEER Team (courtesy of Google Earth). Imagery date October 15, 2019.....	79

<b>Figure 7.65.</b> Rockfall between Joly Guirbert and Nan Dance (Lat: 18.5009437, Lon: -73.7815141). .....	79
<b>Figure 7.66.</b> Rockfall along Highway 218 near Pestel (Lat: 18.5323424, Lon: -73.7988606) ..	80
<b>Figure 7.67.</b> Rockfall along Highway 218 near Pestel (Lat: 18.5326725, Lon: -73.7988475). ..	80
<b>Figure 7.68.</b> Rockfall along Highway 218 near Pestel (Lat: 18.5371693, Lon: -73.8009462). ..	80
<b>Figure 7.69.</b> Locations of slope failures observed in Nippes on September 23, 2021. Courtesy of Google Earth. ....	81
<b>Figure 7.70.</b> Toppling slope failure in Nippes. (a) Lat: 18.43791138, Lon: -73.49213398. (b) Lat: 18.437773, Lon: -73.4922458. Photos taken September 23, 2021. ....	81
<b>Figure 7.71.</b> Slope failure in Nippes. (Lat: 18.39118189, Lon: -73.54879741). Photo taken September 23, 2021. ....	82
<b>Figure 7.72.</b> Slope failure in Nippes. (Lat: 18.3905122, Lon: -73.5280873). Photo taken September 23, 2021. ....	82
<b>Figure 7.73.</b> Locations of rockfalls observed along the northern coast of the southern peninsula of Haiti on September 29, 2021. Courtesy of Google Earth. ....	83
<b>Figure 7.74.</b> Rockfall along northern coast of southern peninsula of Haiti (Lat: 18.59722, Lon: -73.94528). Photo taken September 29, 2021 courtesy of Dr. Newdeskarl Saint Fleur. ....	83
<b>Figure 7.75.</b> Rockfall along northern coast of southern peninsula of Haiti (Lat: 18.59556, Lon: -73.94944). Photo taken September 29, 2021, courtesy of Dr. Newdeskarl Saint Fleur. ....	84
<b>Figure 7.76.</b> Rockfall along northern coast of southern peninsula of Haiti (Lat: 18.59583, Lon: -73.94417). Photo taken September 29, 2021, courtesy of Dr. Newdeskarl Saint Fleur. ....	84
<b>Figure 7.77.</b> Rockfall along northern coast of southern peninsula of Haiti (Lat: 18.5925, Lon: -73.95222). Photo taken September 29, 2021, courtesy of Dr. Newdeskarl Saint Fleur. ....	85
<b>Figure 7.78.</b> Rockfall along northern coast of southern peninsula of Haiti (Lat: 18.60111, Lon: -73.96167). Photo taken September 29, 2021, courtesy of Dr. Newdeskarl Saint Fleur. ....	85
<b>Figure 7.79.</b> Rockfall along northern coast of southern peninsula of Haiti (Lat: 18.62389, Lon: -73.79583). Photo taken September 29, 2021, courtesy of Dr. Newdeskarl Saint Fleur. ....	86
<b>Figure 7.80.</b> Liquefaction susceptibility base map. ....	87

<b>Figure 7.81.</b> Locations of liquefaction observation by the in-ground GEER team. ....	87
<b>Figure 7.82.</b> Reported observations of liquefaction during the August 14 <sup>th</sup> Nippes Earthquake (Lat: 18.5435502, Lon: -73.7921043). ....	88
<b>Figure 7.83.</b> Ground cracking near the coast in Pestel (Lat: 18.5422912, Lon: -73.7904188)....	89
<b>Figure 7.84.</b> Ground cracking near the coast in Pestel (Lat: 18.5423509, Lon: -73.7906552)....	89
<b>Figure 7.85.</b> Ground cracking near the coast in Pestel (Lat: 18.5424493, Lon: -73.7910169)....	89
<b>Figure 7.86.</b> Drone observations of liquefaction in Les Cayes (courtesy of Google Earth).....	90
Figure 7.87. Coast and slope damage near south Les Cayes: (a) before the earthquake; (b) after the earthquake. Coordinates: 18.181111, -73.758611. Images courtesy of OpenstreetMap (Pierre Béland, <a href="https://pierzen.dev.openstreetmap.org/">https://pierzen.dev.openstreetmap.org/</a> ). ....	91
<b>Figure 7.88.</b> Coastal damage and possible evidence of liquefaction-induced lateral spreading in south Les Cayes. Coordinates: 18.189722, -73.748333. Images courtesy of OpenstreetMap (Pierre Béland, <a href="https://pierzen.dev.openstreetmap.org/">https://pierzen.dev.openstreetmap.org/</a> ). ....	91
<b>Figure 7.89.</b> Coastal damage and possible evidence of liquefaction-induced lateral spreading in south Les Cayes. Coordinates: 18.188056, -73.750556. Images courtesy of OpenstreetMap (Pierre Béland, <a href="https://pierzen.dev.openstreetmap.org/">https://pierzen.dev.openstreetmap.org/</a> ). ....	92
Figure 7.90. Possible lateral spreading in Les Cayes. Coordinates: 18.198611, -73.745833. Images courtesy of OpenstreetMap (Pierre Béland, <a href="https://pierzen.dev.openstreetmap.org/">https://pierzen.dev.openstreetmap.org/</a> )...	92
<b>Figure 7.91.</b> Damage and possible evidence of liquefaction-induced lateral spreading near river (Ravine du Sud) in Les Cayes. Coordinates: 18.195556, -73.759722. Images courtesy of OpenstreetMap (Pierre Béland, <a href="https://pierzen.dev.openstreetmap.org/">https://pierzen.dev.openstreetmap.org/</a> ). ....	93
<b>Figure 7.92.</b> Damage and possible lateral spreading near river (Ravine du Sud) in Les Cayes. Coordinates: 18.195 -73.760278. Images courtesy of OpenstreetMap (Pierre Béland, <a href="https://pierzen.dev.openstreetmap.org/">https://pierzen.dev.openstreetmap.org/</a> ).....	93
<b>Figure 7.93.</b> Damage and possible lateral spreading near river (Ravine du Sud) in Les Cayes. Coordinates: 18.196389, -73.760833. Images courtesy of OpenstreetMap (Pierre Béland, <a href="https://pierzen.dev.openstreetmap.org/">https://pierzen.dev.openstreetmap.org/</a> ).....	94
<b>Figure 7.94.</b> Damage and possible lateral spreading near river (Ravine du Sud) in Les Cayes. Coordinates: 18.361389 -73.770556. Images courtesy of OpenstreetMap (Pierre Béland, <a href="https://pierzen.dev.openstreetmap.org/">https://pierzen.dev.openstreetmap.org/</a> ).....	94

<b>Figure 7.95.</b> Damage and possible lateral spreading near river (Madan Samdi) in Les Cayes. Coordinates: 18.218333, -73.759444. Images courtesy of OpenstreetMap (Pierre Béland, <a href="https://pierzen.dev.openstreetmap.org/">https://pierzen.dev.openstreetmap.org/</a> ).....	95
Figure 7.96. Possible damage of water facility near river (Riviere L'Islet) in Les Cayes. Coordinates: 18.215278, -73.745833. Images courtesy of OpenstreetMap (Pierre Béland, <a href="https://pierzen.dev.openstreetmap.org/">https://pierzen.dev.openstreetmap.org/</a> ). .....	95
<b>Figure 7.97.</b> Damage and possible lateral spreading near river (Riviere de Cavaillon) in Cavaillon. Coordinates: 18.299167, -73.655833. Images courtesy of OpenstreetMap (Pierre Béland, <a href="https://pierzen.dev.openstreetmap.org/">https://pierzen.dev.openstreetmap.org/</a> ).....	96
<b>Figure 7.98.</b> Locations of damage to roads and highways (red pins) and retaining structures (yellow pins). Courtesy of Google Earth. ....	97
<b>Figure 7.99.</b> Retaining wall damage along RN7 (Lat: 18.403283, Lon: -73.8750032).....	97
<b>Figure 7.100.</b> Retaining wall damage along RN7 (Lat: 18.4046922, Lon: -73.8766514).....	98
<b>Figure 7.101.</b> Retaining wall damage along RN7 (Lat: 18.4262836, Lon: -73.9027722).....	98
<b>Figure 7.102.</b> Retaining wall damage 2 km north of Enriquillo-Plaintain Garden Fault in Bonne Fin (Lat: 18.38944, Lon: -73.61028). ....	99
<b>Figure 7.103.</b> Pavement damage on RN7. (Lat: 18.3631332, Lon: -73.8753663). ....	100
<b>Figure 7.104.</b> Pavement damage on RN7 (Lat: 18.3646397, Lon: -73.8785984). ....	101
<b>Figure 7.105.</b> Pavement damage on RN7 (Lat: 18.39580833, Lon: -73.87810833). Photo taken September 29, 2021. ....	102
<b>Figure 7.106.</b> Pavement damage on RN7 (Lat: 18.4039901, Lon: -73.8770421). ....	102
<b>Figure 7.107.</b> Pavement damage on RN7 (Lat: 18.40532455, Lon: -73.87818961). Photo taken September 29, 2021. ....	103
<b>Figure 7.108.</b> Pavement damage on RN7 (Lat: 18.4073805, Lon: -73.8794886). ....	104
<b>Figure 7.109.</b> Road embankment damage on RN7 (Lat: 18.4073147, Lon: -73.8823895). .....	104
<b>Figure 7.110.</b> Pavement damage on RN7 (Lat: 18.410061, Lon: -73.8873537). ....	105
<b>Figure 7.111.</b> Damaged building in Les Cayes (Lat: 18.1944, Lon: -73.7456).....	106
<b>Figure 7.112.</b> Damaged building in Les Cayes (Lat: 18.1956, Lon: -73.7456).....	106

<b>Figure 8.1.</b> Population density per commune in 2008 and 2021 in Haiti (source: Map Action, <a href="http://www.mapaction.org">www.mapaction.org</a> ).....	108
<b>Figure 8.2.</b> Social-political crises and natural disasters in Haiti since 2010, including the disaster new population displacements (sources noted in the legend).....	108
<b>Figure 8.3.</b> Map of population movements following the 2010 earthquake in Haiti (sources noted in the legend).....	109
<b>Figure 8.4.</b> Map of flooded areas during the 2012 Hurricane Sandy, including some landslide areas and locations of maximum human casualty (sources noted in the legend).....	110
<b>Figure 8.5.</b> Map of affected areas during the 2016 Hurricane Matthew and the lowest average annual income from 2015 in the study region (sources noted in the legend). ....	111
<b>Figure 8.6.</b> The USGS Liquefaction probability map and shaking intensity contours of the 2021 Nippes earthquake overlaid on the 2021 population map with the boundary of lowest average annual income within the study region in Haiti (sources noted in the legend).....	112
<b>Figure 8.7.</b> The USGS Landslide probability map and shaking intensity contours of the 2021 Nippes earthquake overlaid on the 2021 population map with the boundary of lowest average annual income within the study region in Haiti (sources noted in the legend).....	112

## **ACKNOWLEDGEMENTS**

The work of the GEER Association is based in part on work supported by the National Science Foundation through the Engineering for Civil Infrastructure Program under Grant No. CMMI1826118. Any opinions, findings, and conclusions or recommendations expressed in this material are those of the authors and do not necessarily reflect the views of the NSF. The authors would also like to express their gratitude to the USGS for providing access to hazard maps. In addition, the team benefited greatly from collaboration and coordination with members of StEER and GeoHazards International (GHI), who were collecting data on both structural and geotechnical hazards in Haiti immediately following the 2021 earthquake. StEER also provided access to the phone application Fulcrum, which greatly improved our ability to collect relevant perishable data on the ground.

# 1. INTRODUCTION

Haiti is located in the western part of the island of Hispaniola, which is one of the Greater Antilles Islands between Puerto Rico and Cuba. The Mw7.2 Nippes, Haiti earthquake occurred at 8:29 am local time on August 14, 2021 in Haiti's southwest peninsula. According to the USGS, the epicenter was located at 18.434°N 73.482°W, 10.6 km from the city of Petit Trou de Nippes, 38.6 km from Les Cayes, and 75 km west of the epicenter corresponding to the 2010 Mw 7.0 Port-au-Prince earthquake. The earthquake occurred in conjunction with significant social, economical, and political challenges and crises as well as other hazards (e.g., storm, tsunami, and a global pandemic) that made the population especially vulnerable to the aftermath of this earthquake. About 96% of Haiti's population are vulnerable to natural hazards (World Bank, 2021). Besides earthquakes, with 1,100 miles of coastline in the hurricane belt, the country is subject to severe storms during the hurricane season (June 1 to November 30). According to EM-DAT (2021), between 2010 and 2021, 233,562 Haitians lost their lives to disasters. Of these, 96.4% and 3% were associated with earthquakes and hurricanes, respectively. The remaining losses were due to such events as biological and technological disasters, floods, and droughts.

Due to the security challenges in Haiti at the time of the event, it was not possible to deploy an in-person reconnaissance team from the U.S. to Haiti. Instead, GEER (Geotechnical Extreme Events Reconnaissance) mobilized one interdisciplinary remote team from the U.S. to investigate the geotechnical and social/political effects of the August 14th, 2021 M7.2 Nippes event immediately following the event. The team was later able to partner with local academics and engineers who assisted in capturing additional higher quality data on the geotechnical hazards in affected regions. During this first phase of the reconnaissance, we collected data and observations on the following:

- Ground shaking characteristics, site effects, and directivity effects;
- Seismically induced landslides;
- Absence or presence of surface fault ruptures;
- Effects of liquefaction or cyclic softening on lateral spread, foundation failure, or damage to pipelines;
- Seismic damage to infrastructure (e.g., retaining structures, bridges, highways, roads, and pipelines);
- Social/economical/political context of this disaster and other crises in Haiti;
- Impact of multiple crises and social/economical/political environment on vulnerability to geotechnical and seismological hazards.

The results presented in this report are the outcome of a truly collaborative and interdisciplinary effort. This effort required the participation and collaboration of all remote and local team members as well as assistance from other organizations (detailed in Section 2). The goal of this first version of the GEER report is to summarize the preliminary findings of the team from the collaborative investigation and set the ground for future, more comprehensive investigations of the earthquake and other future hazards in Haiti.

## 2. TEAM STRUCTURE AND DATA COLLECTION APPROACH

The remote GEER team consisted of experts in geotechnical earthquake engineering, engineering geology and seismology, engineering geomorphology, and social and political implications of disasters. This team was led by Shideh Dashti of the University of Colorado Boulder (CU) on the engineering side, and N. Emel Ganapati of the Florida International University (FIU) on the social science side. The engineering team consisted of Yu-Wei Hwang (University of Texas at Austin, UTA); Jenny Ramirez (Geosyntec Consultants); Ashly Cabas, Nancy Ingabire Abayo, Cristina Lorenzo-Velazquez, and Chunyang Ji (North Carolina State University, NCSU); Estefan Garcia (University of Michigan, UM); Sary Nicolas, Michelle Shriro, and Richard Lagesse (ARUP), and Michael Whitworth at AECOM and EEFIT. The social science team consisted of Joanne Perodin (FIU); Santana Contreras (University of Southern California, USC); and Christa Remington (University of South Florida, USF). The GEER team members in Haiti consisted of Professors Kelly Guerrier and Newdeskari Saint Fleur (Université d'Etat d'Haïti, UEH), Santiana Vissière, Joseph Emmanuel Dessable (MS student in Geosciences at Faculte Des Sciences of UEH), Tarah Jeannot (Civil Engineer at National Transport et Construction), and Marvens Logiste (MS student at la Faculté des sciences de UEH).

Because of the nature of this event and lack of immediate physical presence of the team (due to safety and security concerns), we initially collected perishable data and information from a variety of sources as quickly as possible. For example, the team employed reports provided by the USGS, USAID, CNIGS, CNSA, UN, and World Bank, plus satellite imagery and drone data collected by the World Bank. We obtained ground motion recordings from IRIS, Raspberry Shake Citizen Science Network/Ayiti-Seismes of Haiti, and Observatorio Sismológico Politécnico Loyola (in Dominican Republic). Evidence of geotechnical damage in affected areas was initially collected from social media (primarily twitter) and mainstream media as well as satellite imagery (primarily Google Earth) during reconnaissance planning. Subsequently, field reconnaissance was conducted with local GEER team members in affected areas, mainly using the Fulcrum phone application made available to us by StEER. In parallel, the team benefited greatly from collaboration and coordination with members of StEER and GeoHazards International (GHI), who were collecting data on both structural and geotechnical hazards in Haiti immediately following the 2021 earthquake. Hence, the preliminary results and insights presented in this report come from a large variety of sources, which leads to varying levels of quality and resolution in information.

To create the intersectional maps, a simplified base map layer of the geographic extent of Haiti was first downloaded from the digital cartography collection of Porto Tapiquén (<http://tapiquensig.jimdofree.com>, last accessed October 20<sup>th</sup>, 2021). Subsequently, several maps that include different engineering data or social/economical information were superimposed as multiple base map layers either manually or digitally. For instance, unreferenced images (e.g., USGS liquefaction or landslides probability map images) were overlaid on the main base map by manually assigning map coordinates to some points on the image. Alternatively, images with stored data were automatically imported digitally (e.g., Enrique-Plantain fault from Saint Fleur

2021). Finally, to account for a few distinctive Haiti map features, the geographic extent map was manually reshaped using the georeferenced maps from MapAction.

Other map features included objects, data points, and contours to better visualize the available data. For example, some base map layers included a group of georeferenced objects that were manually traced (e.g., polygons that represent Haiti communes) with different attributes (e.g., total population per commune, flooded areas). Maps also consisted of layers with datapoints with coordinates such as the epicenter for both the 2021 Nippes earthquake and the 2010 Haiti earthquake. Some maps provided a visual representation of more qualitative as well as quantitative tabulated data (e.g., the disaster new population displacement map). When possible, the available data was processed for easier visual interpretation. For instance, earthquake intensity contours from the USGS (2021) were digitalized to more easily overlay them on the main base map layer.

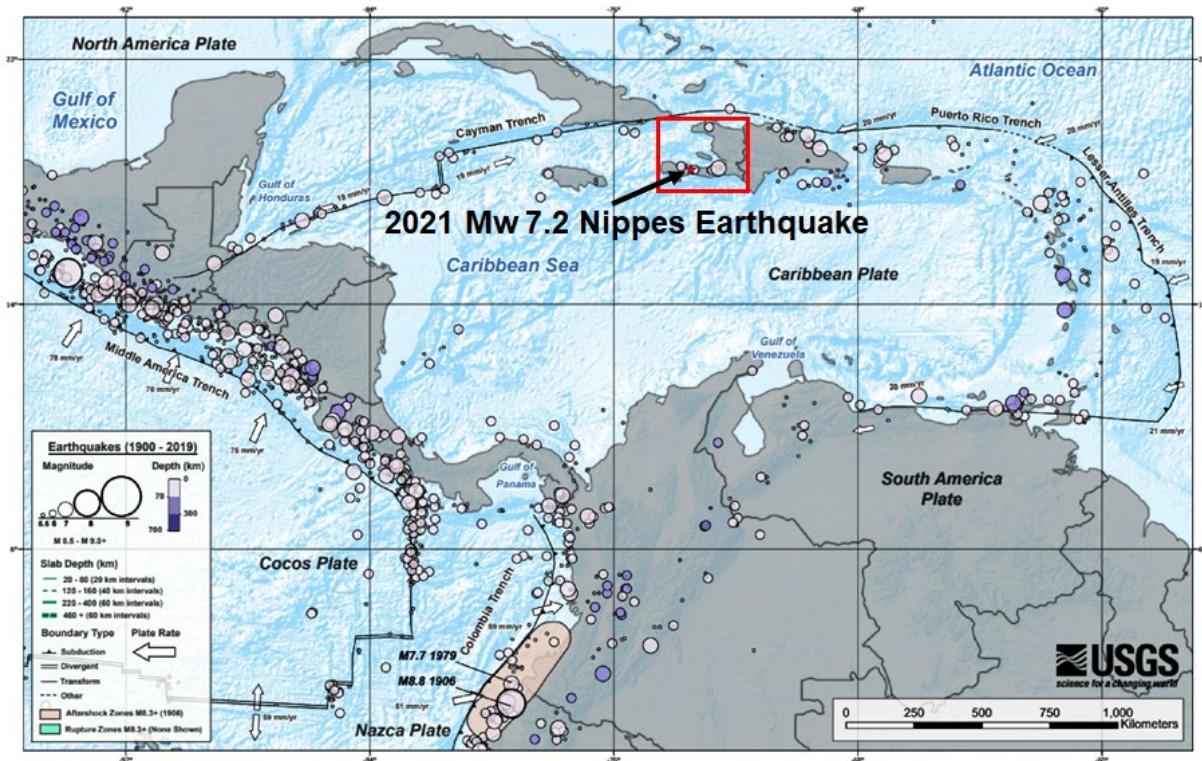
Social science data for this report is based on team members' prior research in Haiti and a review of secondary sources. After the 2010 Haiti earthquake, our social science team members conducted research on a number of issues, including shelter recovery, social capital, public participation, and work-related challenges faced by those involved in disaster response and recovery (e.g., emotional challenges, cultural competencies). This research was funded by such agencies as the National Science Foundation (NSF) and the National Institutes of Health (NIH). The work was based on interviews, surveys, focus groups, and Town Hall meetings with various stakeholders (e.g., international aid agency representatives, and Haitian government officials, community leaders, and Port au Prince residents) (see Contreras 2019; Ganapati & Mukherji 2019; Ganapati & Rahill 2017; Kroll et al. 2021; Mukherji, Ganapati & Rahill 2014; Rahill et al. 2016, 2014; Remington & Ganapati 2017 for details on the methods).

Secondary sources reviewed for this report, focusing on the effects of the 2021 Nippes Earthquake in Haiti, were mainly from: (1) Haitian government agencies (e.g., Ministry of Public Health [Ministère de la Santé Publique et de la Population]); (2) Haitian (e.g., Quisqueya University [Université Quisqueya]) and international universities, think-tanks, and research institutes (e.g., Pew Research Center); (3) Haitian (e.g., Le Nouvelliste) and international news sources (e.g., Reuters); (4) international aid agencies (e.g., the World Bank, the United Nations [UN] Development Programme, UN Office for Coordination of Humanitarian Assistance, UN International Organization for Migration, and UN Security Council); and, (5) disaster-focused databases (e.g., EM-DAT International Disaster Database).

The team is in the process of receiving the Institutional Review Board (IRB) approval for conducting stakeholder interviews and a PhotoVoice project, both from U.S. and Haitian institutions. The plan is to conduct online or phone interviews with Haitian government officials, international aid agency representatives working in Haiti, community leaders in Haiti, and the Haitian diaspora in the U.S. The results of these data collection activities will be included in the follow-up report.

### 3. REGIONAL TECTONICS

Haiti is geologically and tectonically relatively young and therefore quite dynamic and unstable. There is a complex tectonic regime that has developed in the last 12-15 million years. The North America, South America, Nazca and Cocos plates are located in the perimeter of the Caribbean Plate, and their relative motion characterizes complex and diverse tectonic regimes in the region (USGS, last accessed September 2021). Figure 3.1 shows a summary of the tectonics in the region, including the locations of earthquakes between 1900 and 2019. The red square highlights the location of Haiti, and the red star depicts the epicenter of the 2021 M7.2 Nippes, Haiti earthquake.



Hispaniola is situated on a complex plate boundary where the predominant tectonic motions are left-lateral strike-slip between the North America and Caribbean plates, but there are also two converging subducting slabs beneath the Greater Antilles Crust where Hispaniola is situated. Over time, the tectonic motions have imparted a complex set of fault systems over the region with a variety of focal mechanisms. The predominant fault system orientation is from NW to SE (Mann et al. 1990, 1995), which largely controls the topographic structure of the island. Shallow crustal earthquakes are prevalent with focal depths of local events suggesting that the seismogenic crust extends to a depth of approximately 45 km (Geomatrix, 2007). In addition, there is the potential for deeper subduction slab related events to occur.



weaker rocks along the fault zone (GEER, 2010). More information on evidence of surface fault rupture is provided in Section 7.1 of this report.

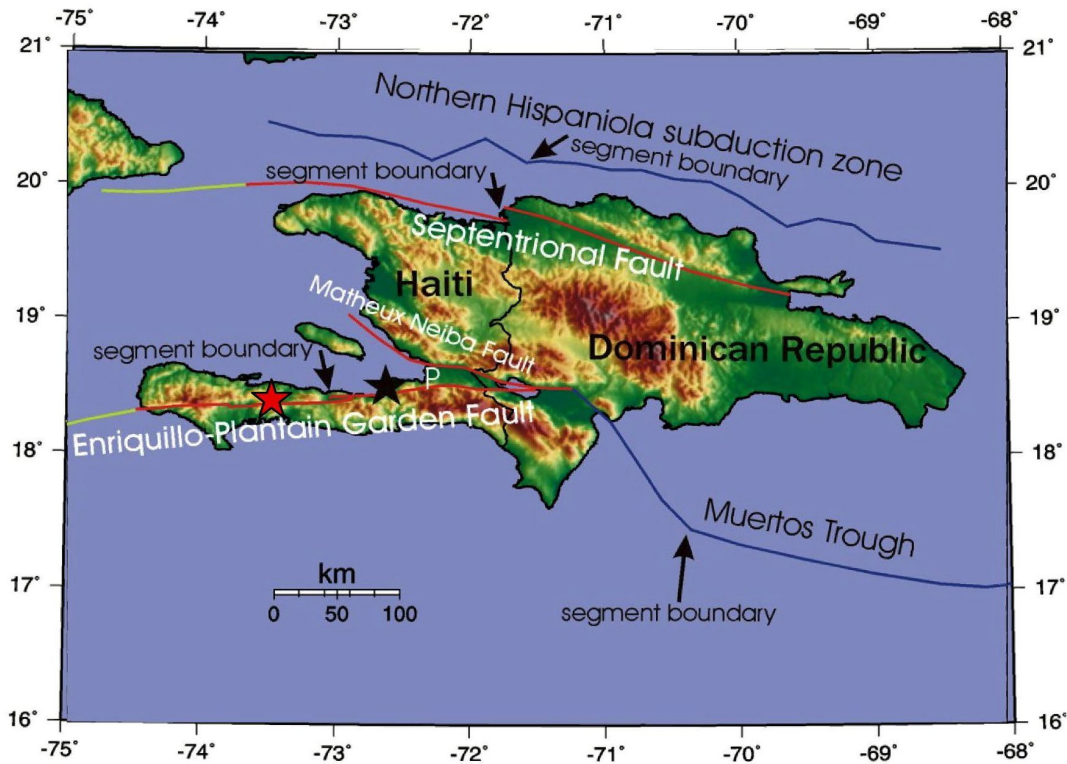


**Figure 3.3.** Crustal Faults are shown in red and green, while subduction zones are shown in blue. The black star shows the epicenter of the M7.0 12 January 2010 Haiti earthquake with respect to Port-au-Prince (denoted as “P”), while the red star depicts the epicenter of the M7.2 14 August 2021 Haiti earthquake (modified after Frankel et al 2011).

### 3.1. Historical Seismicity

Haiti remained seismically quiescent during the 20th century, and prior to the 12 January 2010 Port-au-Prince earthquake (Eberhard et al 2013). Earthquake catalogs indicate that only one event with magnitude larger than 4.0 occurred in the Port au Prince region before the M7.0 earthquake in 2010. However, Haiti’s historical seismicity includes very damaging earthquakes with magnitudes greater than 7.0 in 1701, 1751, 1770 and 1860 associated with the motion of the Enriquillo fault, as shown in Fig. 3.4 (Scherer, 1912; O’Loughlin and Lander, 2003). The regions of Port-au-Prince and Léogâne were particularly affected by these historical events, with collapsed buildings throughout those cities.

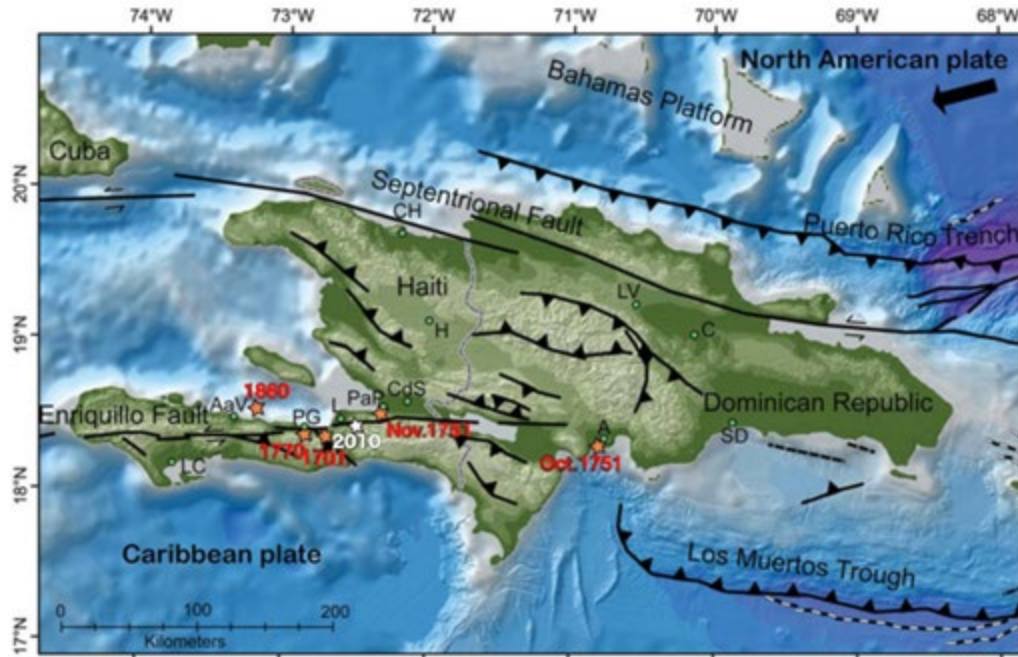


**Figure 3.4.** Estimated locations of historical events on or near the Enriquillo fault shown as orange stars. The location of the epicenter of the 12 January 2010 event is depicted as a white star (after Bakun et al 2012).

The 1701 event occurred near the location of the 2010 Haiti earthquake and with similar accounts of the shaking as those of the 2010 earthquake (Flores et al. 2012). The epicenter of the seismic event on October 18, 1751 was probably located in the Dominican Republic on the eastern side of the fault (Flores et al. 2012) as shown in Figure 3.4. The October 1751 event was followed by the November 21, 1751 earthquake (with lower intensity) and epicenter probably close to Port-au-Prince. Finally, this sequence of events includes the June 3, 1770 earthquake (with a similar intensity as the first event in the series) and located west to the 2010 event epicenter (Flores et al. 2012). The island of Hispaniola is situated in a region of high seismic activity and it has a historical record of seismicity since 1562 (de Utrera, 1995; ten Brink et al 2011). An inventory of significant earthquake events greater than Mw 6.0 since 1564 and up to 2018 is presented in Table 3.1. Focal depths are provided in km and magnitudes estimated by intensity proxies pre 1900, instrumental recordings post 1900, and modern instrumental recordings after 1964 (Geomatrix, 2007).

**Table 3.1.** Significant (>6.0 Mw) historical and recent earthquakes for the island of Hispaniola

<b>Year</b>	<b>Month</b>	<b>Day</b>	<b>Depth</b>	<b>Magnitude</b>	<b>Country</b>
1564	4	20	33	7	Dominican Republic
1691	1	1	33	7.7	Dominican Republic
1701	11	9	10	6.6	Haiti
1751	10	18	33	8	Dominican Republic
1751	11	21	33	7.5	Haiti
1770	6	3	10	7.5	Haiti
1776	1	30	0	6.3	Dominican Republic
1784	7	29	33	6.8	Haiti
1830	4	14	10	6.6	Dominican Republic
1842	1	1	33	7.7	Haiti
1860	10	23	33	6.6	Haiti
1897	12	29	33	6.6	Dominican Republic
1911	10	6	0	6.9	Dominican Republic
1916	4	25	80	7.2	Dominican Republic
1918	10	11	60	7.5	Dominican Republic
1943	7	29	25	7.9	Dominican Republic
1946	8	4	60	8.1	Dominican Republic
1946	10	4	50	6.5	Dominican Republic
1953	5	31	33	7.2	Dominican Republic
1962	1	8	33	6.5	Dominican Republic
1971	6	11	57	6.5	Dominican Republic
1972	9	19	33	6.1	Dominican Republic
1979	3	23	80	6.1	Dominican Republic
1984	6	24	20	6.6	Dominican Republic
2003	9	22	10	6.4	Dominican Republic
2010	1	12	13	7.0	Haiti
2018	10	7	24	5.9	Haiti

## 4. GEOLOGIC SETTING

### 4.1. Bedrock Geology

The Southern peninsula of Haiti, especially the region within the mountain range of La Hotte (Massif de la Hotte, Figure 4.1), was the most strongly affected by the 2021 Nippes earthquake. This region is geologically and topographically diverse. The topography is relatively rugged, with steep mountain ranges and hill fronts, deeply incised streams and narrow intermountain stream valleys, and broad coastal delta fans, valleys, and alluvial plains (GEER, 2010). It is characterized with sedimentary and igneous rocks that range in age. The igneous rocks that represent approximately  $\frac{1}{4}$  of the region include andesites, basalts, and other volcanic rocks as well as traces of dacites and other intrusive rocks (Butterlin et al. 1960). The igneous rocks represent the oldest rocks in the region from the Late Cretaceous period. The sedimentary rocks comprise most of the region with ages from the Cretaceous period to more recent deposits. Figure 4.2 presents the published regional geologic map [modified and geo-referenced after Bureau des mines et de l'énergie d'Haïti (1986)] for the western end of the southern Haiti peninsula, where most of the impacts of the 2021 Nippes earthquake were observed. Locations of interest to the GEER team, identified as areas with highly concentrated damage, are depicted with filled red circles in Fig. 4.2.

Cretaceous rocks dominate the Macaya formation within the Massif de la Hotte, which is composed of limestones with traces of shale and other clayey rocks with some rock fragments. The colors of the rocks can be diverse from yellow brown to green. Calcite veins are a commonly found throughout the Macaya formation. The characteristic deposits of this kind are found along the Les Cayes-Jérémie route in the Valley of Riviere glace. This formation is overlaid by the Cenozoic Era deposits through an angular discontinuity (Butterlin et al. 1960).

Sedimentary Rocks from the Paleocene and Eocene epochs represent approximately one-half of the region of Massif de la Hotte. They are represented by the Marigot Formation, which is characterized by various conglomerates, shales, and limestones. The characteristics of these rocks are consistent with marine deposits. While there are some rocks corresponding to the Oligocene epoch, they are not as dominant in the Massif de la Hotte. These are found in the Northern part of Les Cayes plains, and at the south of Roseaux. These are typically white – yellow chalky limestones (Butterlin et al. 1960).

The Miocene epoch is represented by the Grise River formation with brown limestones, loam with folded layers. These are found in the Valley of Grande Anse (Woodring et al. 1924), on the Jérémie-Léon route, Jérémie-Brassac route, Port-au-Prince-Cayes national route, and at Port-à-Piment. These rocks are of marine origin. Based on the structural orientation relative to the Miocene rocks, the rocks within the Tapion de Petit Goave are associated with the Pliocene Epoch. Contacts between the Miocene and Mio-Pliocene units are commonly faulted, and small folds and possible thrust faults have deformed the Mio-Pliocene bedrock in response to a regional northeast-southwest compression, oblique to the trend of the strike-slip motion along the EPGFZ (GEER, 2010).

Within the Valleys of Camp-Perrin and L'Asile there are continental rocks, which are also from the Miocene Epoch. This includes highly folded conglomerates, sandstones, shales, and limestones. These deposits are about 500 m thick and cover the Pic Macaya Formation though an angular discontinuity. The valley of L'Asile hosts the Grande Rivière de Nippes fluvial system, from which alluvial rocks are produced in the region. It is possible that these deposits are separated from the older limestones by a fault system. A remarkable length of the coasts of the Massif de la Hotte consists of reef limestones, with 3-4 km extent in width. Within the valleys of the rivers and coastal plains, especially the region of Les Cayes, the quaternary alluvial formation dominates. These include lithified and loose sediments (Butterlin et al. 1960).

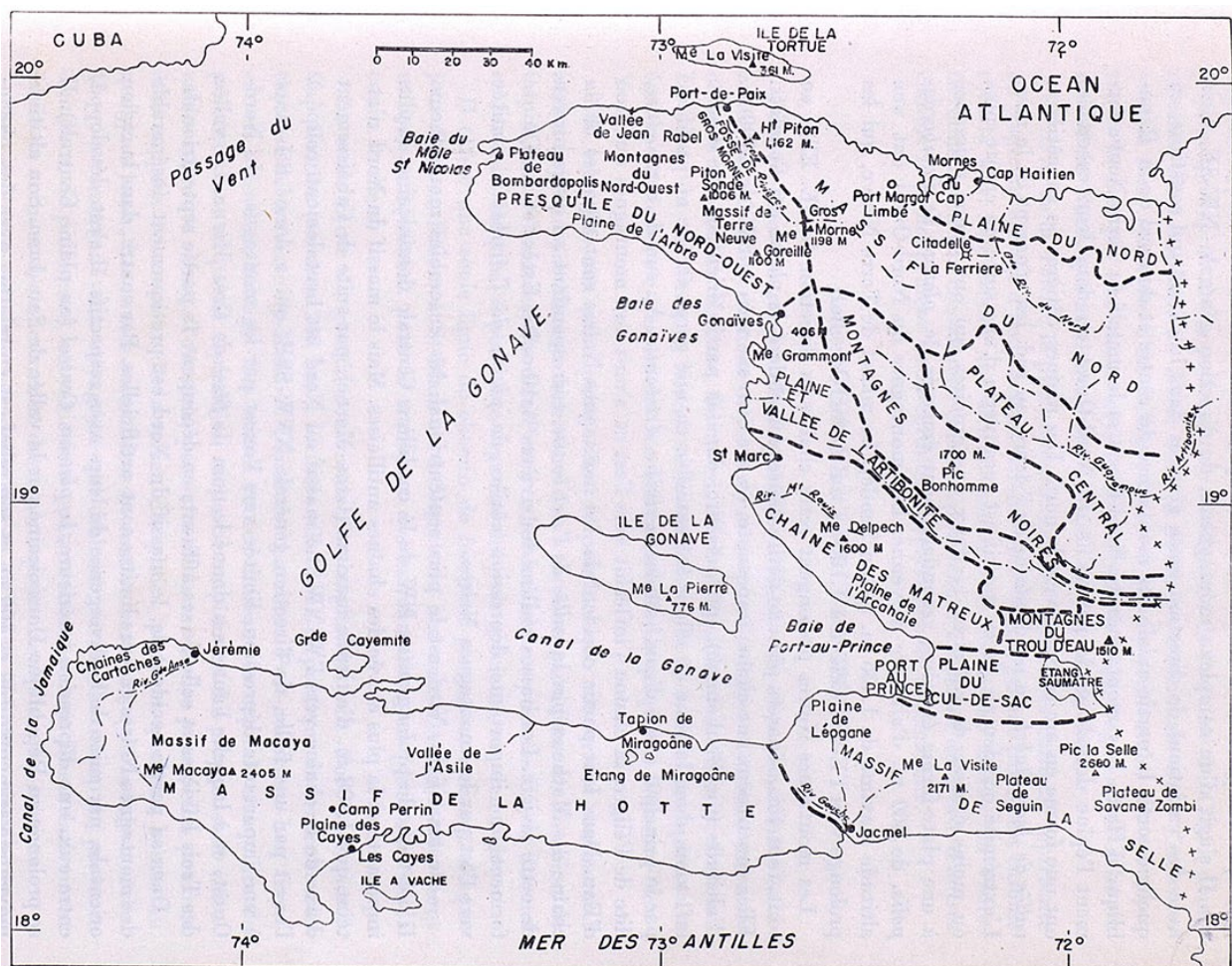


**Figure 4.1.** Geographic Provinces of Haiti showing the extent of the mountain range of La Hotte (Woodring et al. 1924.)

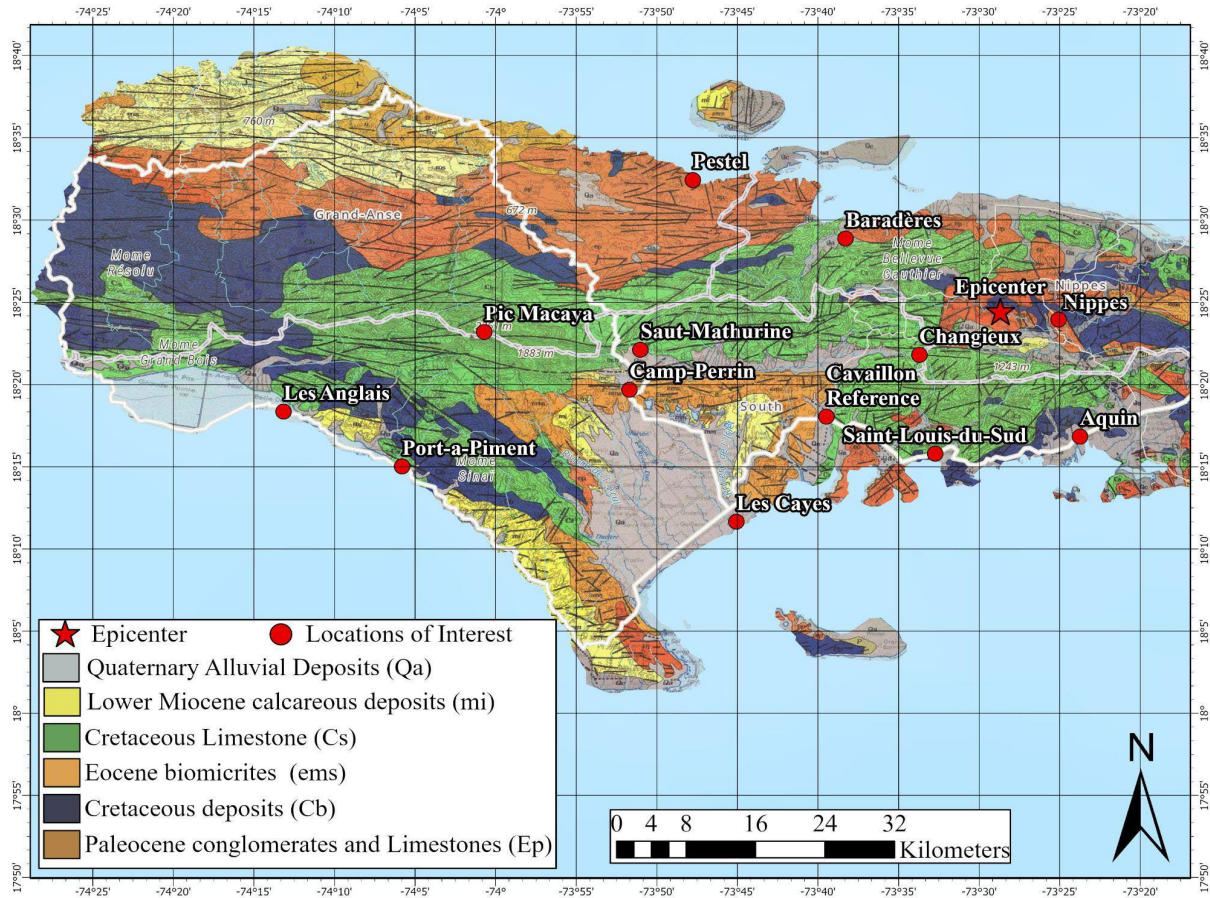


**Figure 4.2.** Regional geological map highlighting the locations where ground failure or damage was observed [Modified after Bureau des mines et de l'énergie d'Haïti (1986)]

## 4.2. Surficial Geology

The regions where significant ground deformations were observed are presented in Figure 4.2 as *locations of interest* to the GEER team, but the resolution of the current map may not be capturing the most recent deposits associated with quaternary alluvium (Butterlin, 1960). Within the region of Les Cayes, lateral spreading was observed along the port and the riverside. Based on the geomorphic and hydro-geological conditions of Les Cayes as well as the relative age of the sediment, liquefaction-induced deformations were expected. In the region of L'Asile, specifically in Nippes and Changeux, lateral spreading was expected and observed in addition to landslides and rockfalls. This region comprises quaternary alluvium that are susceptible to liquefaction triggering and its consequences based on the geologic history detailed by Butterlin (1960). Although the region of Pestel is composed of older deposits, there were sand boils and lateral spreading. Rockfalls and landslides were also observed in Camp-Perrin, as detailed later in this report.

Given the diverse and complex geology and seismicity in the area, the need to understand potential site effects is crucial. Site conditions (i.e., soil stiffness, geology, depth to bedrock, impedance contrasts) can modify the frequency content, duration, and amplitude of ground motions, which can lead to local ground motion amplifications. Our understanding of the local site conditions in the region can be advanced through the integration of knowledge of the surface geology and time-averaged shear wave velocities for the top 30 m ( $V_{s30}$ ). Due to the lack of sufficient data in the study area, proxy-based  $V_{s30}$  values were extracted from a  $V_{s30}$  mosaic based on the Wald and Allen (2007) topographic slope model downloaded from the U.S. Geological Survey (USGS) database. The spatial distribution of proxy-based  $V_{s30}$  values and the location of ground motion recording stations that recorded the 2021 Nippes earthquake are shown in Figure 4.3.

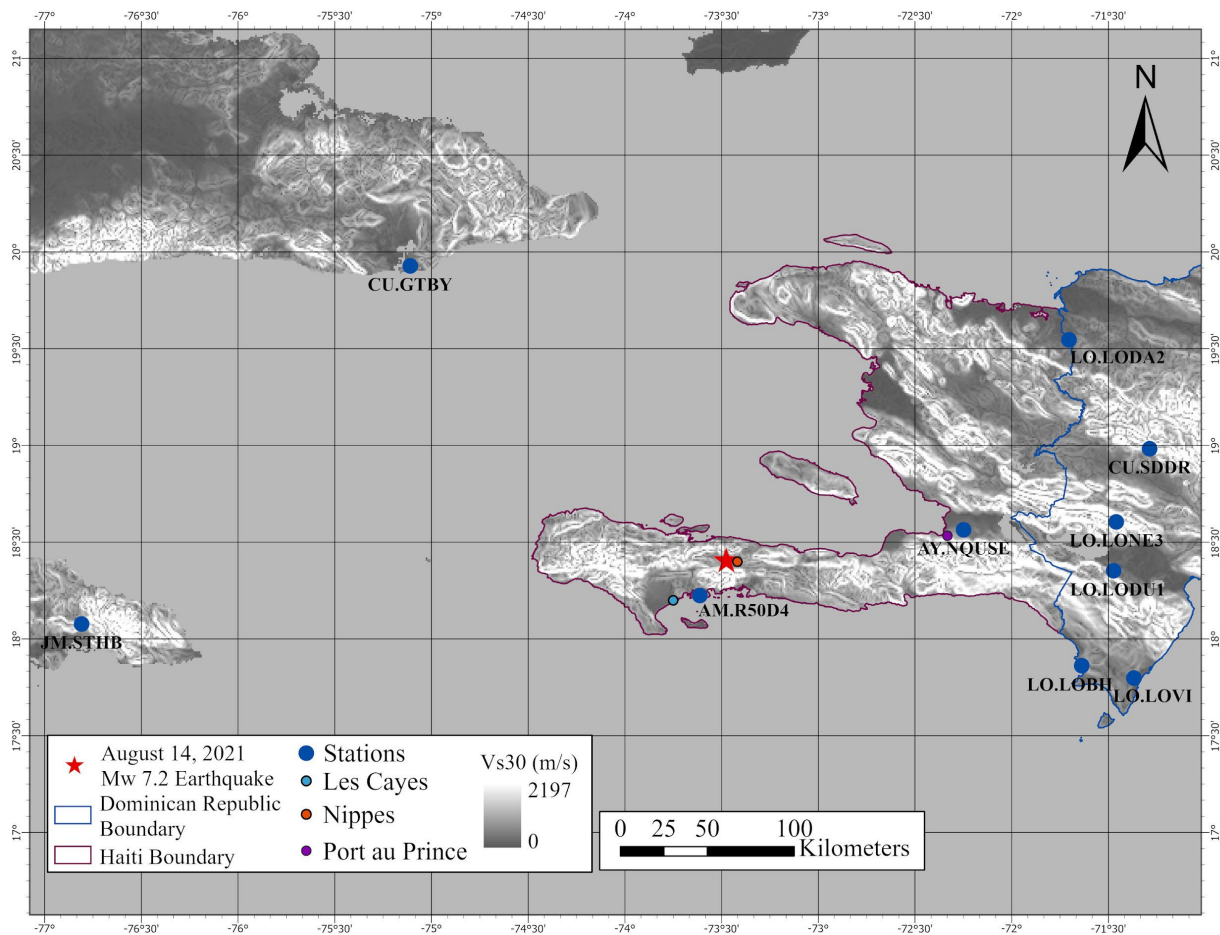


Table 4.1 lists ten recording stations that recorded ground motions from the 2021 Nippes earthquake in Haiti, Dominican Republic, Cuba, and Jamaica. As shown in Figure 4.3, only two stations where recorded ground motions from the 2021 Nippes earthquake passed the signal processing quality checks from the USGS (i.e., gmprocess software; Hearne et al. 2019) are located in Haiti. Those stations correspond to a Raspberry Shake station (AM.R50D4) and the US Embassy strong motion station (AY.NQUSE) at 25 km and 130 km from the epicenter, respectively (both highlighted in gray in Table 4.1). The five stations from the LO network correspond to the Observatorio Sismologico Politecnico Loyola in Dominican Republic (<http://ospl.ipl.edu.do/>; last accessed November 2021). The proxy-based Vs30 values obtained from the USGS database allowed the site classification of the station locations based on the National Earthquake Hazards Reduction Program (NEHRP; BSSC, 2003), as detailed in Table 4.1. AM.R50D4 and AY.NQUSE are located on sites classified as NEHRP site class C and D, where C corresponds to values of Vs30 between 360 and 760 m/s, and D between 180 and 360 m/s. Table 4.1 also presents back azimuths, epicentral distances, latitude, longitude, elevation, proxy-based Vs30 values (from USGS) and the corresponding NEHRP site class (BSSC, 2003) for the selected stations.

**Table 4.1.** Recording stations with available records from the 2021 Nippes mainshock.

Network	Data Provider	Station Code	Station ID	Station Description / Location	Sampling Rate (Hz)	Back Azimuth (degree)	Epicentral Distance (km)	Latitude (N)	Longitude (W)	Station Elevation (m)	Vs30 (m/s)	NEHRP Site Class
AM	SeisComp, Raspberry Shake	R50D4	AM.R50D4.EN	Raspberry Shake Citizen Science Station	100	35.7	24.9	18.2252	73.6128	0.1	475	C
AY	IRIS-DMC	NQUSE	AY.NQUSE.HN	US Embassy, Port au Prince, Haiti	200	262.6	130.74	18.5640	72.2482	78	296	D
CU	IRIS-DMC	GTBY	CU.GTBY.HN	Guantanamo Bay, Cuba	100	134.07	240.54	19.9268	75.1108	79	354	D
CU	IRIS-DMC	SDDR	CU.SDDR.HN	Presa de Sabenta, Dominican Republic (DR)	100	254.95	239.33	18.9821	71.2878	589	575	C
JM	IRIS-DMC	STHB	JM.STHB.HN	Stoney Hill, Jamaica	100	83.56	354.5	18.0774	76.8094	456	553	C
LO	IRIS-DMC	LOBH	LO.LOBH.EH	Bahia de las Aguilas, DR	100	287.56	203.53	17.8620	71.6387	45.4	408	C
LO	IRIS-DMC	LODA2	LO.LODA2.EH	ITESIL, Dajabon, DR	100	236.28	224.96	19.5448	71.7045	42	267	D
LO	IRIS-DMC	LODU1	LO.LODU1.EH	El Espartillar-Duverge, DR	100	271.97	211.58	18.3527	71.4740	123.3	286	D
LO	IRIS-DMC	LONE3	LO.LONE3.EH	El Aguacate, Bahoruco, DR	100	264.48	214.06	18.6047	71.4587	1145	761	B
LO	IRIS-DMC	LOVI	LO.LOVI.EH	El Cautin, Oviedo, DR	100	287.16	233.05	17.7983	71.3678	34.4	359	D

The locations of interest shown in Figure 4.2 are listed in Table 4.2 along with reference latitude and longitude pairs used to represent each area, and their corresponding proxy-based Vs30 (from USGS) and NEHRP site class. Figure 4.4 also shows these areas where ground damage was observed by the GEER team or identified through secondary reports (e.g., landslides or lateral spread). During the 2021 Nippes earthquake, ground damage (in the form of landslides and rockfalls) was documented even as far away from the epicenter as the Pic Macaya National Park, with a B site classification. In Changeux and Nippes, near the epicenter, sites classified as C often exhibited ground failure patterns such as lateral spreading, landslide, and rockfall. Also, evidence of foundation and structural damage caused by ground failure was later found in Pestel, Saut-Mathurine, Camp-Perrin, and Les Cayes city. The Pestel commune within the Grand'Anse

department suffered from lateral spread along the port area and sand boils near structures. Les Cayes city on the coast of southern Haiti, a location that has been classified as NEHRP site class D, was particularly devastated with many cases of structural damage. It is important to note that evidence of sand boils was found in multiple locations within the affected area near structures that had suffered considerable damage and even collapse. The other locations that suffered foundation and structural damage possibly due to different forms of ground failure were Camp-Perrin and Saut-Mathurine (classified as D and C, respectively), where landslide and rockfall took place. The geotechnical damage observations are discussed later in the report.

**Table 4.2.** Proxy-based Vs30 and NEHRP (BSSC, 2003) site classification at locations of interest in Haiti based on proxy-based values of Vs30 from USGS.

Location of Interest	Latitude (N)	Longitude (W)	V <sub>s30</sub> (m/s)	NEHRP Site Class
Epicenter	18.4340	73.4820	420	C
Les Cayes city	18.1939	73.7525	275	D
Camp-Perrin	18.3283	73.8614	255	D
Saut-Mathurine	18.3689	73.8503	491	C
Changeux	18.3681	73.5644	745	C
Nippes	18.4011	73.4183	443	C
Pic Macaya National Park	18.3906	74.0119	900	B
Pestel	18.5403	73.7958	600	C

Figure 4.5 compares the subsurface conditions based on both the regional geologic map and the Vs30 proxy-based values from the USGS for some *locations of interest*. The city of Les Cayes showed consistency between the two maps, with a proxy-based Vs30 of 275 m/s (at the latitude/longitude pair indicated in Table 4.2) and site class D based on NEHRP classification (BSSC, 2003) and the presence of quaternary alluvial deposits according to the geologic map. Similarly, the location of interest at Camp-Perrin was classified as D, which was in agreement with the relative age of the deposits compared to the surrounding environment. The deposits around the region of Saut-Mathurine are relatively older than those at Camp Perrin, but the locations of interest are identified within the same geomorphic unit. This observation is also consistent at Nippes and Changeux, which were classified as class C based on proxy Vs30 values. These locations correspond to Cretaceous and Eocene deposits that are relatively older than the aforementioned locations.

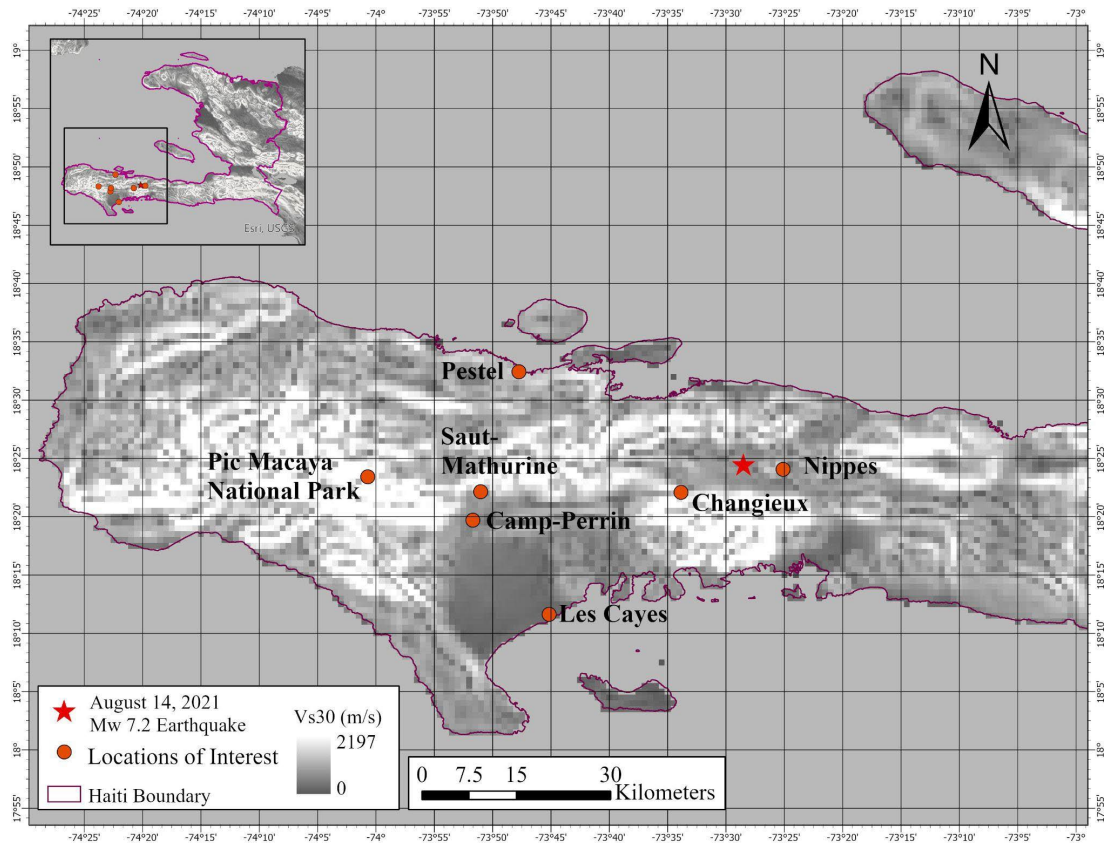


**Figure 4.4.** Regional map with the locations of interest overlaid on the proxy-based Vs30 distribution map of Haiti (from USGS).

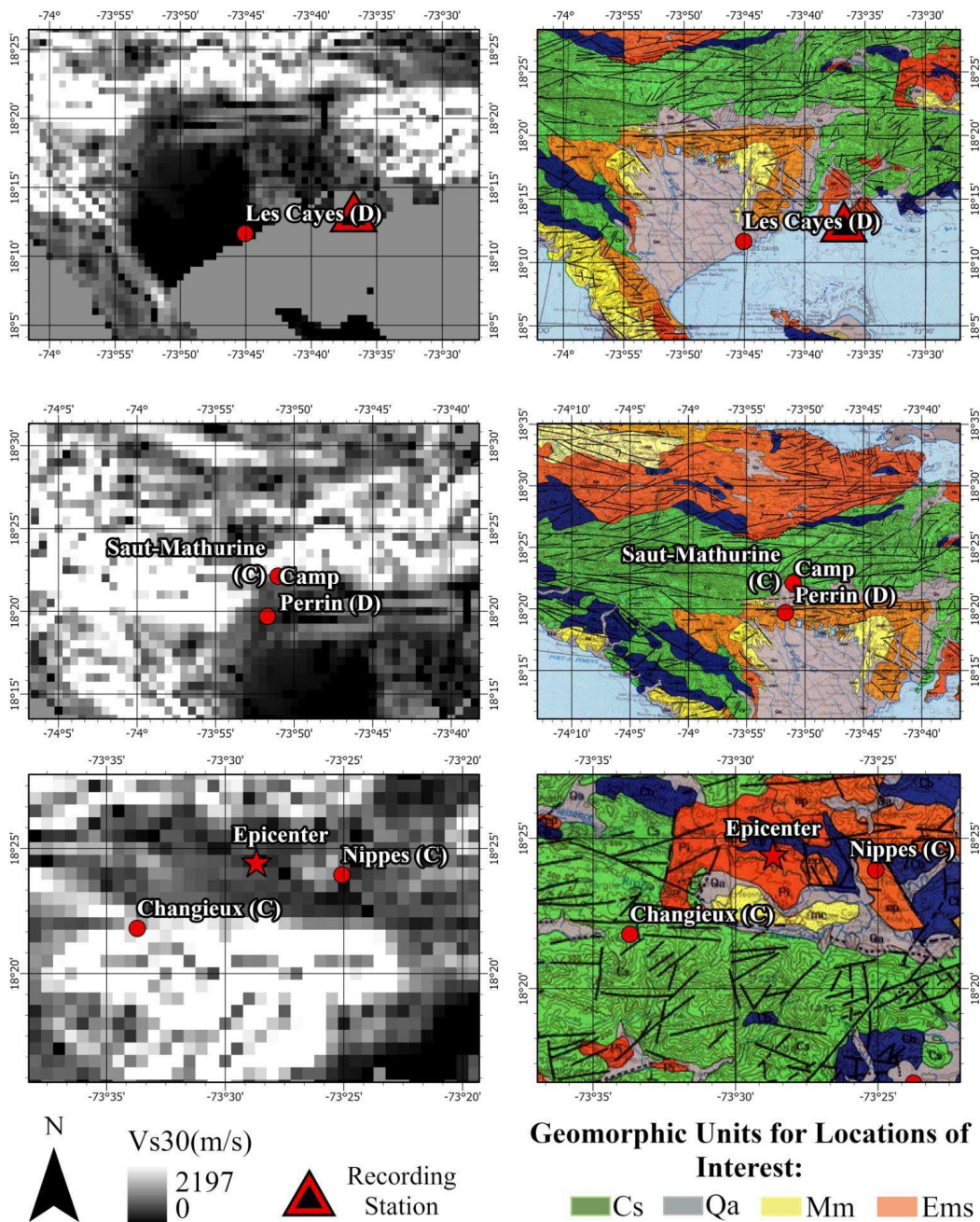


**Figure 4.5.** Comparison of the approximated Vs30 proxy maps with the regional geologic maps within the regions of interest and the corresponding NEHRP (BSSC, 2003) soil classification.

The geomorphic conditions as well as the proxy-based Vs30 values from the USGS support the observed damage patterns in the *locations of interest*. Sample Vs profiles obtained by Jeudy Betegard (GeoTechMap, 2013) also agree with both the NEHRP classifications and the geologic

conditions. However, it is important to consider the proximity to the epicenter, since the geologic conditions alone cannot explain the observed damage.

One of the seismic stations that recorded the 2021 Nippes earthquake (i.e., AY.NQUSE) is located at the US Embassy in Port au Prince as shown in Table 4.1. Cox et al. (2011) performed a microzonation study within and around Port au Prince, following the 2010 event. The study involved determining  $V_s30$  using multi-channel analysis of surface wave (MASW) testing at 36 sites, which is a rapid and non-intrusive method. The testing locations corresponded to ground motion stations and areas of interest where strong site effects (e.g., soft-soils or topographic amplification) were identified by the GEER team (Rathje et al. 2010). From the tests performed, the sites were classified based on their  $V_s30$ , as either NEHRP Site Class C or D. The sites corresponding to NEHRP Class C, were away from the foothills and underlain by Mio-Pliocene deposits with  $V_s30$  ranging between 360 and 490 m/s. The softer soils, classified as NEHRP class D, were located within a 0.5 to 10 km wide zone along the coast (Hough et al. 2011).

#### ***4.2.1 Local hydrogeologic and geomorphologic conditions***

Over 100 streams run through the mountains of Haiti into the Gonave gulf, Atlantic Ocean, and the Caribbean Sea. The flow rate is higher and more turbulent in the mountains. The streams are much slower in the plains and are mostly meandering rivers. The availability of flow is limited by increased deforestation in the region, in addition to evaporation and infiltration. The orientation of mountain ranges and their valleys leads to variability in quantity and distribution of precipitation (Knowles et al. 1999).

Surface and groundwater resources for the locations where notable damage was observed were reviewed and are presented here for each region. The largest river in the southern peninsula (the region within Haiti most affected by the 2021 Nippes earthquake) is the Rivière de Grand Anse, which flows through Jérémie. Within the region of Les Cayes, there are four main rivers/streams as follows: Ravine du sud, Riviere de l'Islet, Riviere de Torbeck and Riviere de l'Acul (Figures 4.6-4.7). This fluvial system supports the aforementioned geologic conditions belonging to quaternary alluvial soils, which are likely susceptible to liquefaction, and consistent with observations of sand boils. The region of Les Cayes is also characterized by a relatively shallow groundwater table (Figure 4.7). Similarly, the fluvial systems such as Riviere de Baraderes, Grande Riviere de Nippes, and the Riviere Mombin within the regions of Barades, Nippes, and Changeux, respectively, support the potential for liquefaction-induced deformations such as lateral spreading (detailed in later sections). Liquefaction was also expected and later observed in the alluvial deposits in the vicinity of the Riviere Brodequin and Rivière de Cavaillon in Aquin & Duverge as well as Cavaillon.

The region of Saint Louis du Sud, which is in the vicinity of one of the available recording stations lies on alluvial soil deposits, based on the available resolution. At the exact location of ground motion recording station, R50D4, there is evidence for competent soil that is likely not liquefiable. Further analyses such as time-frequency plots of accelerations can be used to assess the likelihood of significant soil softening at the recording stations. While a sand boil was observed

near structures, the geomorphic conditions which correspond to older Eocene-Paleocene carbonate deposits as well as the limited hydrogeologic resources did not indicate a strong likelihood for liquefaction in these regions. It is possible that the occurrence of sand boils or lateral spread was primarily concentrated near the free face of the ocean, or that the current geomorphic and hydrologic maps do not capture the right scale and resolution for a reliable evaluation of liquefaction susceptibility.

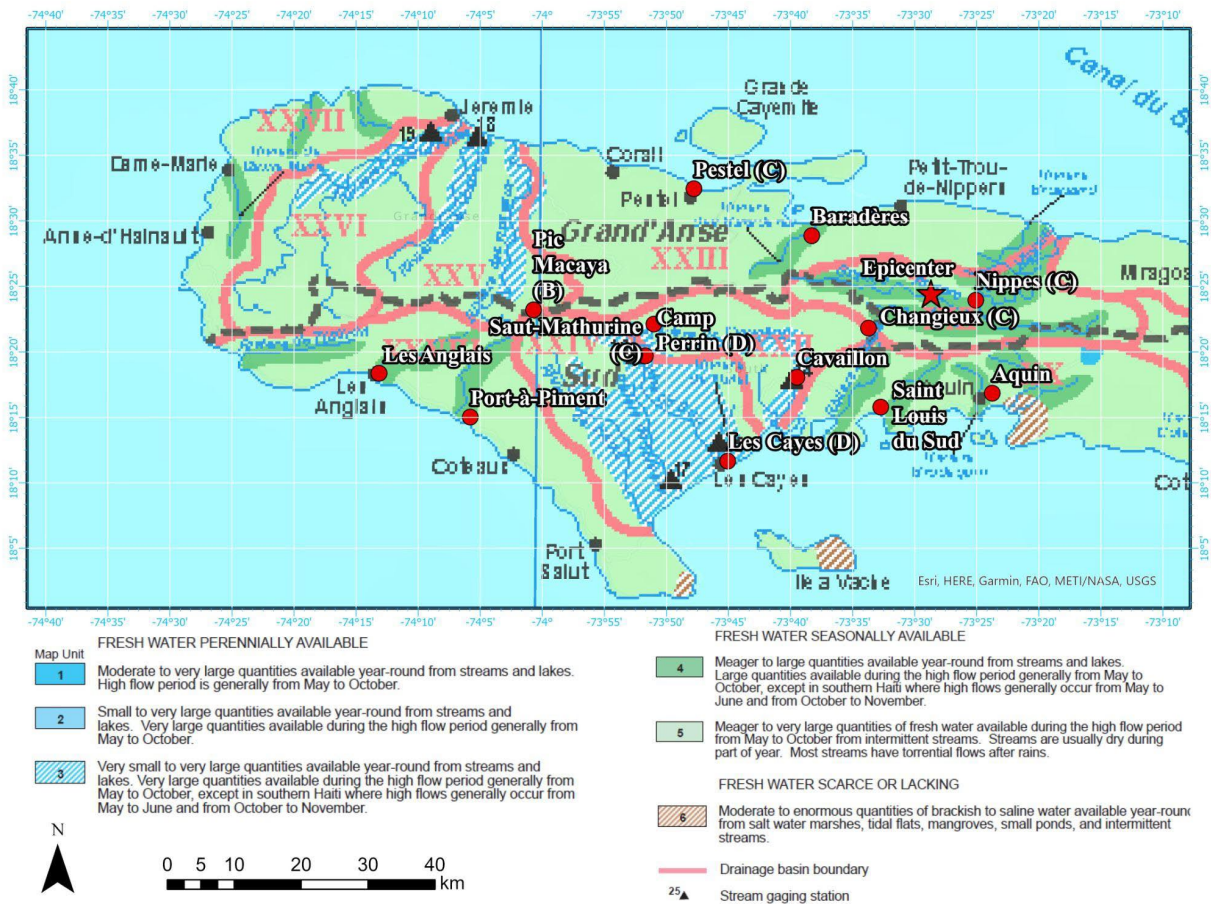
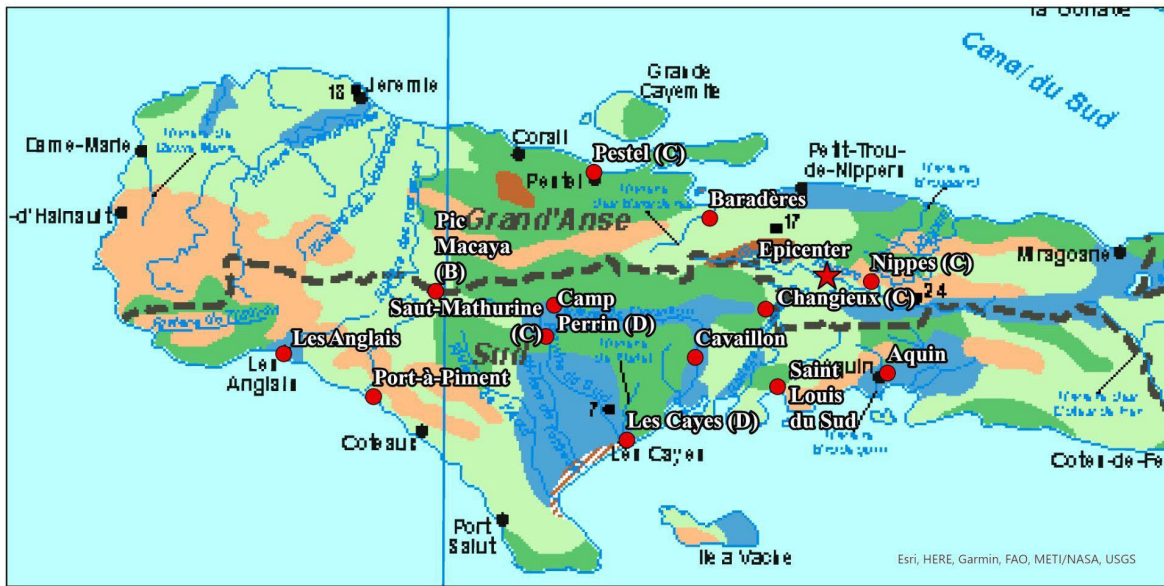


Figure 4.6. Surface water resources map [Modified after Knowles et al. 1999]



- |   |  |
|---|--|
| <p><b>FRESH WATER GENERALLY PLENTIFUL</b></p> <p>Map Unit<br/>1 Small to enormous quantities are available from Quaternary alluvial and carbonate aquifers in the Plaine du Nord, the Riviere Artibonite valley, the Plaine du Gonaïves, the Plaine du Cul-de-Sac, and in small coastal plains and river valleys. Depth to water is generally &lt;50 m.</p> <p><b>FRESH WATER LOCALLY PLENTIFUL</b></p> <p>2 Unsuitable to enormous quantities are available from Pleistocene reef deposits in the Plateau de Bombardopolis and the islands of Gonave and Tortue; and from Cretaceous to Eocene karstic or highly fractured limestones throughout the country. Depth to water is generally between 5 to 25 m, but in the mountains may be &gt;200 m.</p> <p>3 Unsuitable to moderate quantities are available from Cretaceous to Miocene limestones, sandstones, conglomerates, and schists that are slightly deformed with an uneven distribution of fractures. Depth to water is generally between 5 and 50 m, but in the mountains may be &gt;200 m.</p> | <p><b>FRESH WATER SCARCE OR LACKING</b></p> <p>4 Unsuitable to small quantities of fresh water are available from low-permeability Miocene and Pliocene shales, consolidated conglomerates, sandstones, marls, chalk, and other rock types. Depth to water is generally between 5 and 50 m, but in the mountains may be &gt;200 m.</p> <p>5 Unsuitable to small quantities of fresh water are available from Cretaceous to Quaternary igneous and metamorphic rocks. Depth to water may be &gt;100 m.</p> <p>6 Very small to very large quantities of brackish to saline water are available from Quaternary alluvial aquifers in Plaine du Nord near Fort Liberté, in the Riviere Artibonite delta, in large parts of the Plaine du Cul-de-Sac, around the Etang Saumatre, and in other alluvial deposits near the coast. Depth to water is generally from 10 to 75 m.</p> <p>28. Location of selected wells and springs with yields or quality data.</p> <p>Note: Map unit and well numbers refer to entries in table C-2.</p> |
|---|--|

## 5. SEISMOLOGICAL ASPECTS AND GROUND MOTION CHARACTERISTICS

### 5.1. Past Recorded Earthquakes

There were no seismograph stations deployed in Haiti to record ground motions from the 2010 Port-au-Prince mainshock or its strongest aftershocks. However, temporary networks were deployed a few days after the mainshock by different groups, including USGS researchers.

Eberhard et al. (2013) described the deployment of four Kinemetrics K2 accelerometer seismographs shown in Figure 5.1; with the first one installed on the grounds of the U.S. Embassy on January 27, 2010. Two days later, seismographs were also deployed in the towns of Grand Goâve and Oliver (located 58 km and 88 km west of the U.S. Embassy site, respectively; Eberhard et al. 2013), which are also shown in Figure 5.1. The last seismograph was installed at a hard-rock site at the Killick Naval Hospital in Port-au-Prince on February 2, 2010. Eberhard et al. (2013) intended for two of the deployed seismographs (i.e., the ones in the U.S. Embassy and Killick Naval Hospital) to remain operational indefinitely.

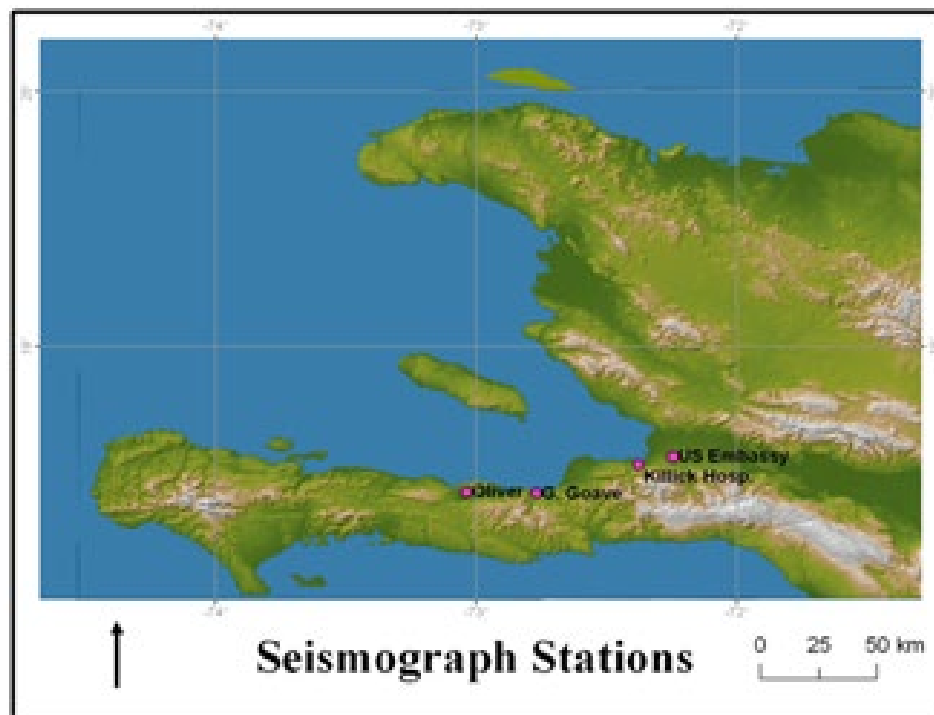


**Figure 5.1.** Locations of four Kinemetrics K2 seismographs (accelerometer) stations deployed by Eberhard et al (2013) during their reconnaissance mission after the 12 January 2010 Port-au-Prince earthquake.

After the 2010 seismic event, the Geological Survey of Canada (GSC) along with the U.S. Geological Survey (USGS) and Géoazur installed seismographs and strong-motion stations (Bent et al 2018). Three GSC stations consisting of collocated weak- and strong-motion instruments comprised the first real-time seismic network in Haiti, which were used to monitor aftershocks (Bent et al 2018). Haiti also established its own network consisting of two seismograph and five accelerograph stations with real-time data availability and three additional non-real-time strong-motion stations, which are maintained by the Bureau of Mines and Energy (BME) (Bent et al 2018; Calais et al 2020). Figure 5.2 shows the locations of the aforementioned stations as well as their status as evaluated by Bent et al. (2018).

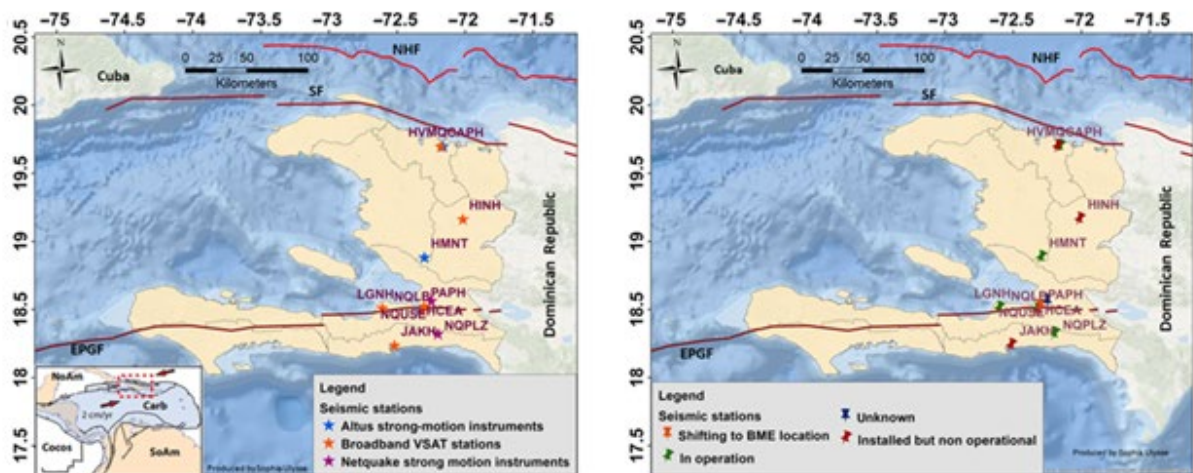


**Figure 5.2.** Location of seismograph and strong-motion stations installed in Haiti (left) and their status (right) as of October 2017 (after Bent et al. 2018). EPGF refers to the Enriquillo Plantain Garden fault, NHF is the North Hispaniola fault, and SF refers to the Septentrional fault.

The Unité Technique de Sismologie (UTS) was created in 2011 as part of a collaboration between the Haitian BME and the Seismological and Volcanological Observatory of Martinique (Bent et al. 2018). Technicians from the BME received training on monitoring seismic activity and managing the network, while experts from Martinique facilitated the creation of the national data center (Bent et al. 2018). Collectively, the two seismograph stations in Cap-Haïtien (CAPH) in the north and Hinche (HINH) in central Haiti, five strong motion NetQuakes instruments, and the three Kinematics (K2) accelerometers were designated with the network code AY.

Data from the seismograph and the NetQuake stations can be obtained from the IRIS-DMC, while the K2 data are not available in real time. However, “no data have been received from CAPH since October 2016 or from HINH since August 2014” (Bent et al 2018). Real-time regional data from four USGS stations located in Cuba, Jamaica, the Dominican Republic, and the Turks and Caicos as well as stations from the Dominican Republic seismograph network provide supplemental seismic information for the region (Bent et al. 2018).

Figure 5.3 provides the location of all the stations (red triangles) in the Haitian seismic network operated by the BME (according to the International Federation of Digital Seismographs Networks, FDSN, <https://www.fdsn.org/networks/detail/AY/>; last accessed November 2021) and highlights NQUSE, where one of the two ground motion records from the 2021 Nippes earthquake was recorded. The codes, names, as well as the latitude and longitude corresponding to each station in this network are provided in Table 5.1.

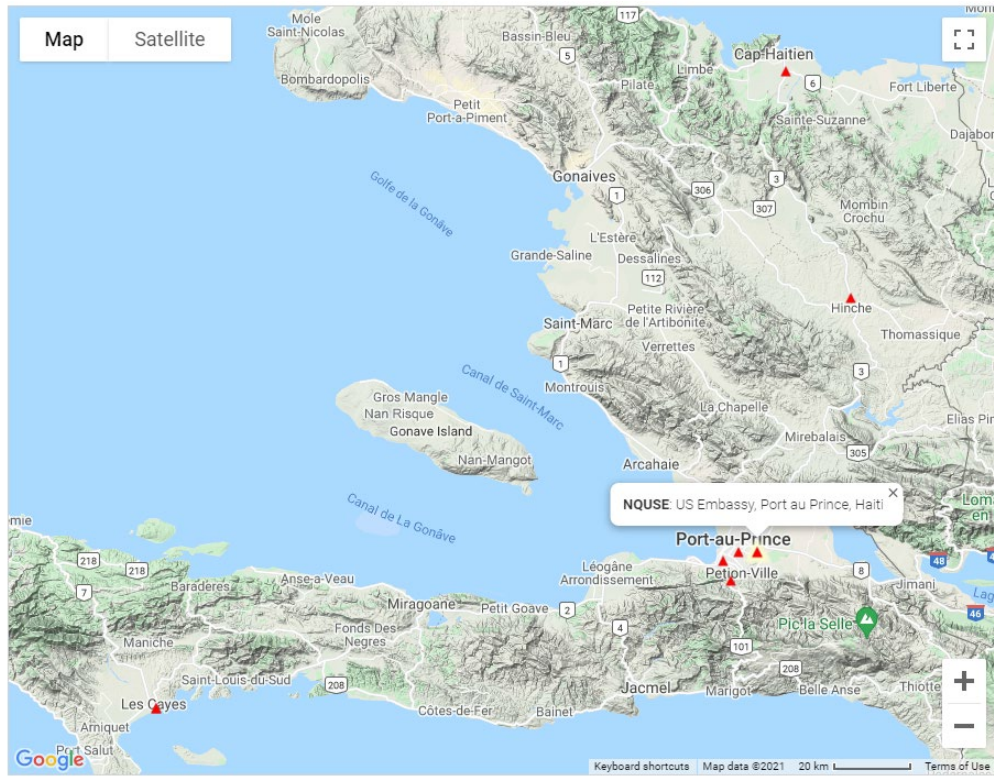


**Figure 5.3.** Location of stations (red triangles) in the AY – Haitian Seismic Network operated by the Bureau of Mines and Energy of Haiti. (modified after FDSN; last accessed November 2021).

**Table 5.1.** Code, name, and location of the stations within the AY – Haitian Seismic Network operated by BME (FDSN; last accessed November 2021).

Station Code	Station Name	Latitude	Longitude
CAPH	Cap-Haitien, NA	19.697599	-72.178398
HINH	Hinche, NA	19.1637	-72.015602
NQAFC	NQAFC, Haiti	18.193171	-73.749352
NQBME	BME, Port au Prince, Haiti	18.5627	-72.296768
NQPLZ	Rue Capois, Port au Prince, Haiti	18.542061	-72.334312

NQTMS	Rue Tousaint Louverture, Les Cayes, Haiti	18.191929	-73.749489
NQUSE	US Embassy, Port au Prince, Haiti	18.56402	-72.248177
NQWLB	Route de Kenscoff, Fermate, Haiti	18.49407	-72.315048

Unfortunately, Calais et al. (2020) reported that none of the Haitian seismic stations was functional when a magnitude 5.9 earthquake occurred on October 7, 2018 in the north-western part of Haiti. Bent et al. (2018) also indicated various levels of reliability associated with different sensors deployed as part of Haiti’s seismic network (see Figure 5.2). Thus, in 2019, a community-seismology project started to deploy low-cost Raspberry Shake sensors (i.e., geophones; raspberrysake.org, last accessed October 2021), which have simple installation and operation processes to record strong ground motion data. The name of the citizen science-based network is Ayiti-Seismes (<https://ayiti.unice.fr/ayiti-seismes/>; last accessed November 2021). Raspberry Shake sensors consist of a geophone, an amplifier, digitizer, and ARM processor to measure vibrations and store the data as miniSEED files. They were deployed in people’s homes and workplaces in different locations throughout Haiti as shown in Figure 5.4 (modified after Witze et al. 2021).

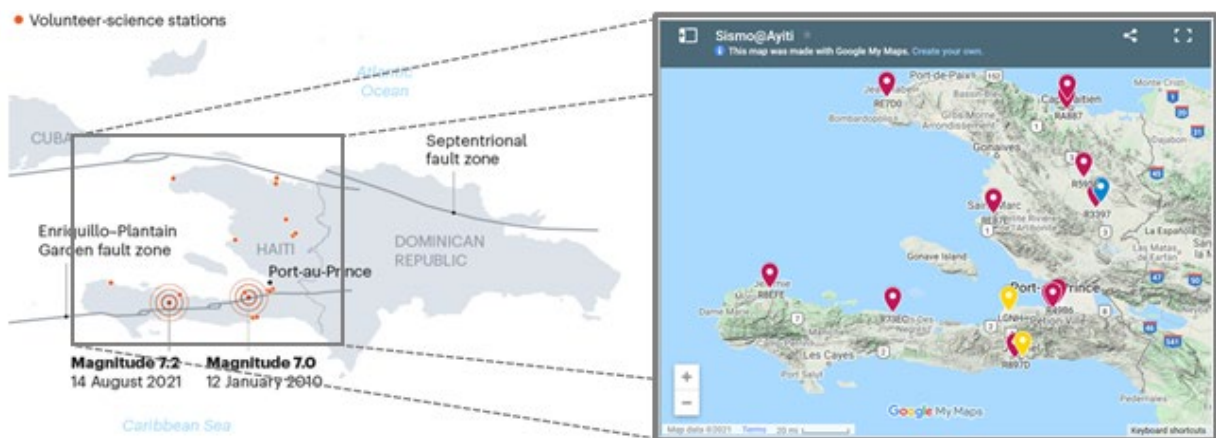


**Figure 5.4.** Locations of low-cost Raspberry Shake sensors in Haiti (modified after Witze 2021). The image on the right shows more detailed locations of the Raspberry sensors that are part of the Ayiti-Seismes, citizen science network (<https://ayiti.unice.fr/ayiti-seismes/>; last accessed November 2021)

The USGS Comprehensive Catalog (ComCat, Guy et al. 2015) was also used to search for recorded ground motions in Haiti with moment magnitudes larger than 5.0 since 2010. The earthquake source information retrieved from ComCat was last accessed on 6 September 2021.

Twenty-one events were found with 18 corresponding to aftershocks of the 2010 Haiti earthquake. The remaining three events corresponded to an earthquake of body wave magnitude Mb 5.0 in 2016 and 2 earthquakes of seismic moment magnitude Mw 5.4 and Mw 5.9 in 2018.

## **5.2. Main Event Characteristics and Aftershocks**

The 2021 Mw 7.2 Nippes, Haiti earthquake occurred at 12:29 pm local time on August 14, 2021 in Haiti's southwest peninsula. The epicenter was located at 18.434°N 73.482°W according to the USGS, 10.6 km from the city of Petit Trou de Nippes, 38.6 km from Les Cayes, and 75 km west of the epicenter corresponding to the 2010 Mw 7.0 Port-au-Prince earthquake (see Figure 5.4). Similar to the 2010 Haiti event, the fault mechanism for the 2021 Nippes earthquake indicates oblique faulting along the Enriquillo-Plantain Garden fault zone (EPGFZ; USGS, last accessed October 2021). Oblique faults result from a combination of shearing and tension or compressional forces, which means that they will have some component of dip-slip (e.g., normal or reverse) and some component of strike-slip. According to the USGS, this shallow event with a focal depth of 10 km occurred on either a reverse fault striking west and dipping to the north with a left-lateral slip component, or a fault striking southeast and dipping to the southwest with a right-lateral slip component. The local plate boundary at the location of the 2021 Nippes event is driven by left-lateral strike-slip motion and compressional forces, which makes the scenario with reverse faulting with a component of left-lateral strike slip faulting on the EPGFZ more likely (USGS, last accessed October 2021). Figures 5.5 and 5.6 provide the USGS Intensity and peak ground acceleration ShakeMaps, respectively.

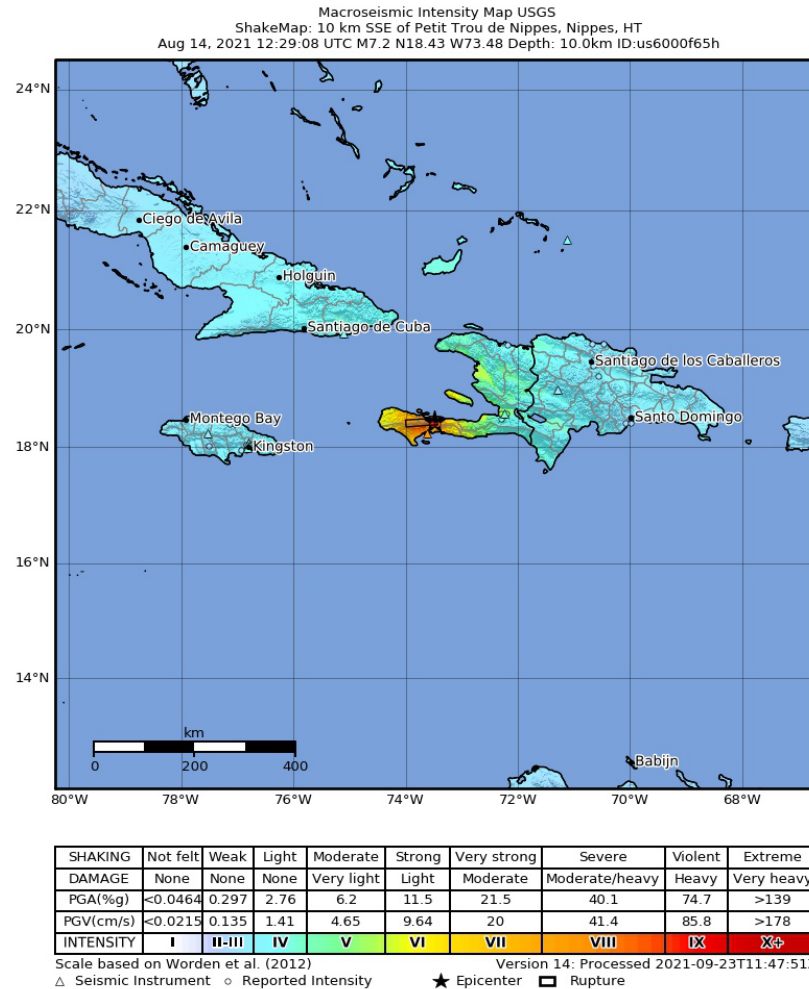


**Figure 5.5.** Macroscopic Intensity Map in Haiti for the 2021 Nippes main event (USGS, last accessed October 2021).

Twenty-four Did You Feel It (DYFI) reports were submitted after the mainshock, but only six from Haiti with maximum reported Modified Mercalli Intensities (MMI) of IX and VIII estimated at 8.56 km and 8.28 km from the epicenter, respectively. Three DYFI reports were submitted from areas nearby the US Embassy in Port-au-Prince (MMI from IV to V). The remaining DYFI data came from the Dominican Republic, Cuba, Puerto Rico, and Turks and Caicos Islands. Figure 5.7 shows the magnitude and location of more than 400 aftershocks associated with the 2021 Nippes earthquake (<https://ayiti.unice.fr/ayiti-seismes/>; last accessed November 2021). These aftershocks were recorded by low-cost seismometers in the Ayiti-Seismes network between August 14 and August 23, 2021 and concentrated near the cities of Nippes (to the east) and Macaya (to the west).

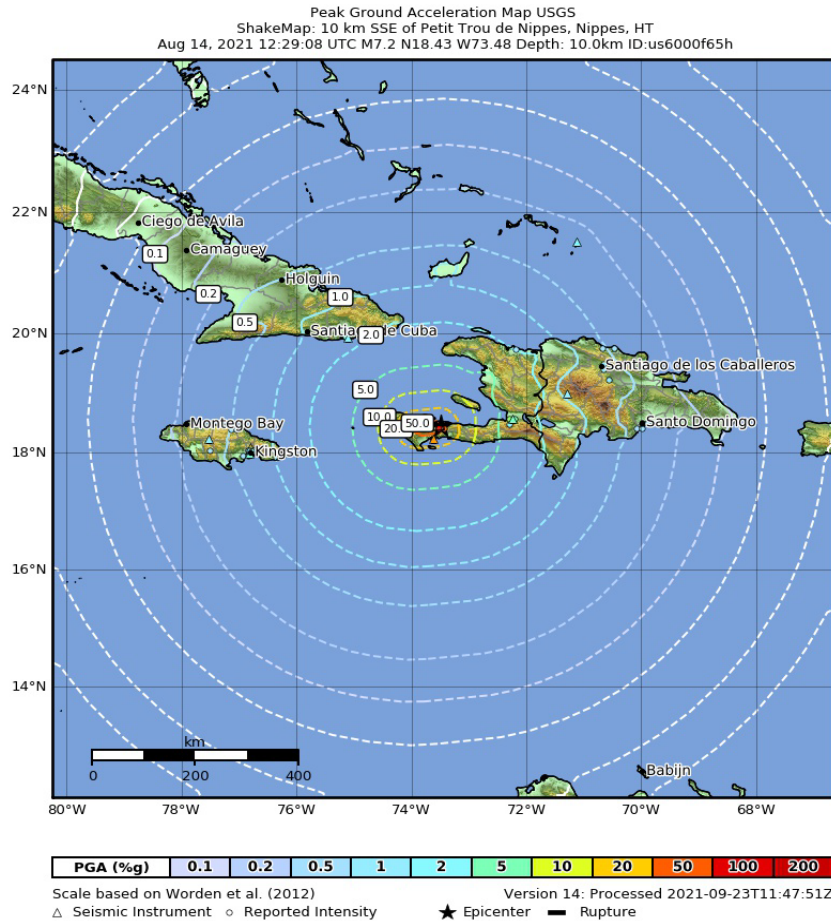


**Figure 5.6.** Peak ground acceleration ShakeMap in Haiti for the 2021 main event (USGS, last accessed October 2021).

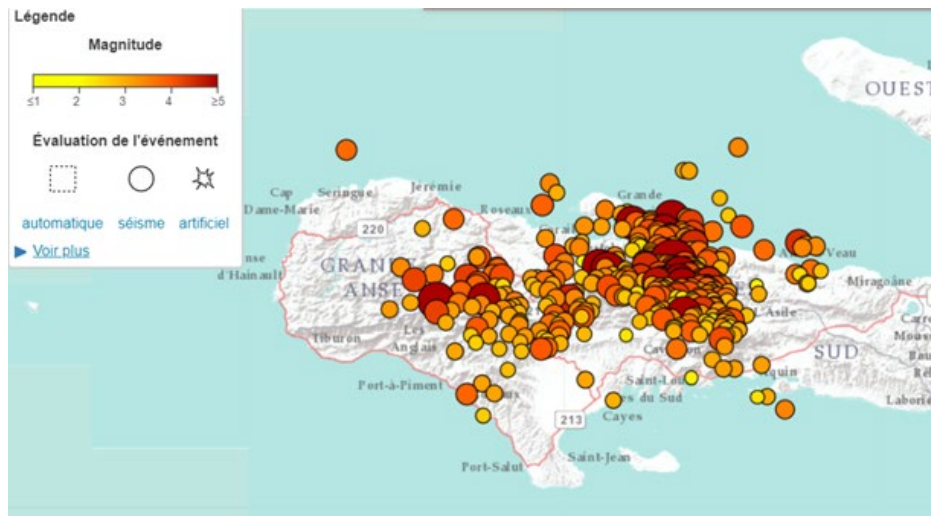


**Figure 5.7.** Magnitude and location of more than 400 aftershocks associated with the 2021 Nippes earthquake between August 14-23, 2021 (<https://ayiti.unice.fr/ayiti-seismes/>; last accessed November 2021).

### 5.3. Recorded Ground Motions from the 2021 Nippes Earthquake

Ground motions from the 2021 Nippes earthquake (mainshock) were processed with the USGS gmprocess software (Hearne et al. 2019), which is a python toolkit for automatic signal processing. Ground motions were screened so that only those recorded within 400 km, with three components (i.e., two horizontal and one vertical components). And minimum sampling frequency of 20 Hz were considered. The baseline was corrected and the instrument responses were removed with the USGS gmprocess protocol. Butterworth high-pass and low-pass filters with an order of 5 were subsequently applied to remove noise. A series of processed ground motion quality checks (e.g., signal-to-noise ratio check) were also applied afterwards.

Ten ground motion pairs passed the USGS gmprocess check (see Table 5.2), but only two correspond to seismic stations in Haiti: the AM.R50D4 operated by the Ayiti-Seismes, citizen science network (<https://ayiti.unice.fr/ayiti-seismes/>; last accessed November 2021), and AY.NQUSE operated by Haitian Seismic Network (AY). Table 5.2 presents ground motion characteristics of these records, namely, peak ground acceleration (PGA) corresponding to the median value of all rotated ground motions (i.e., PGARotD50), peak ground velocity (PGV) corresponding to the RotD50 definition (i.e., PGVRotD50), Arias Intensity (for the geometric mean of both horizontal components), and two metrics of significant duration for the geometric mean of the two horizontal components (i.e., D5-75, and D5-95). Epicentral distances in km and back azimuths in degrees are also provided in Table 5.2. The first two rows in Table 5.2 correspond to the only two seismic stations in Haiti that recorded the 2021 Nippes earthquake. Other seismic stations in Haiti also recorded the 2021 mainshock but the corresponding ground motion records did not pass the signal processing quality checks included in USGS gmprocess protocol (e.g., records from stations AM.RD4D8 failed the SNR check and station AM.RA08A did not record horizontal components). The acceleration time series corresponding to the recorded ground motions in seismic stations within Haiti are provided in Figures 5.8 and 5.9. Larger amplitudes are observed in the closest record to the epicenter (i.e., AM.R50D4 with a PGA of 0.35g corresponding to the NS horizontal component) as expected.

**Table 5.2.** Ground motion characteristics of the records corresponding to the 2021 Nippes earthquake.

Station	Back Azimuth (degree)	Epicentral Distance (km)	PGArotD50 (%g)	PGVrotD50 (cm/s)	Arias intensity (m/s); Geometric mean	Duration 5-75; Geometric mean (s)	Duration 5-95; Geometric mean (s)
AM.R50D4	35.7	24.9	30.6	37.5	2.3291	10.52	21.39
AY.NQUSE	262.6	130.74	2.78	4.88	0.0364	29.74	49.08
LO.LOBH	287.56	203.53	0.71	1.58	0.0034	35.21	62.83
LO.LODU1	271.97	211.58	1.25	3.06	0.0105	44.11	65.74
LO.LONE3	264.48	214.06	0.54	1.67	0.002	39.61	59.25
LO.LODA2	236.28	224.96	2.02	1.6	0.0214	38.84	53.38
LO.LOVI	287.16	233.05	0.84	1.67	0.0055	34.08	57.77
CU.SDDR	254.95	239.33	0.31	1.16	0.0009	52.01	79.08
CU.GTBY	134.07	240.54	0.95	1.9	0.0032	24.51	61.92
JM.STHB	83.56	354.5	11.1	16.2	0.1728	23.74	53.87

LO - refers to the Observatorio Sismologico Politecnico Loyola, a seismic network in Dominican Republic

CU - station in Cuba

JM - station in Jamaica

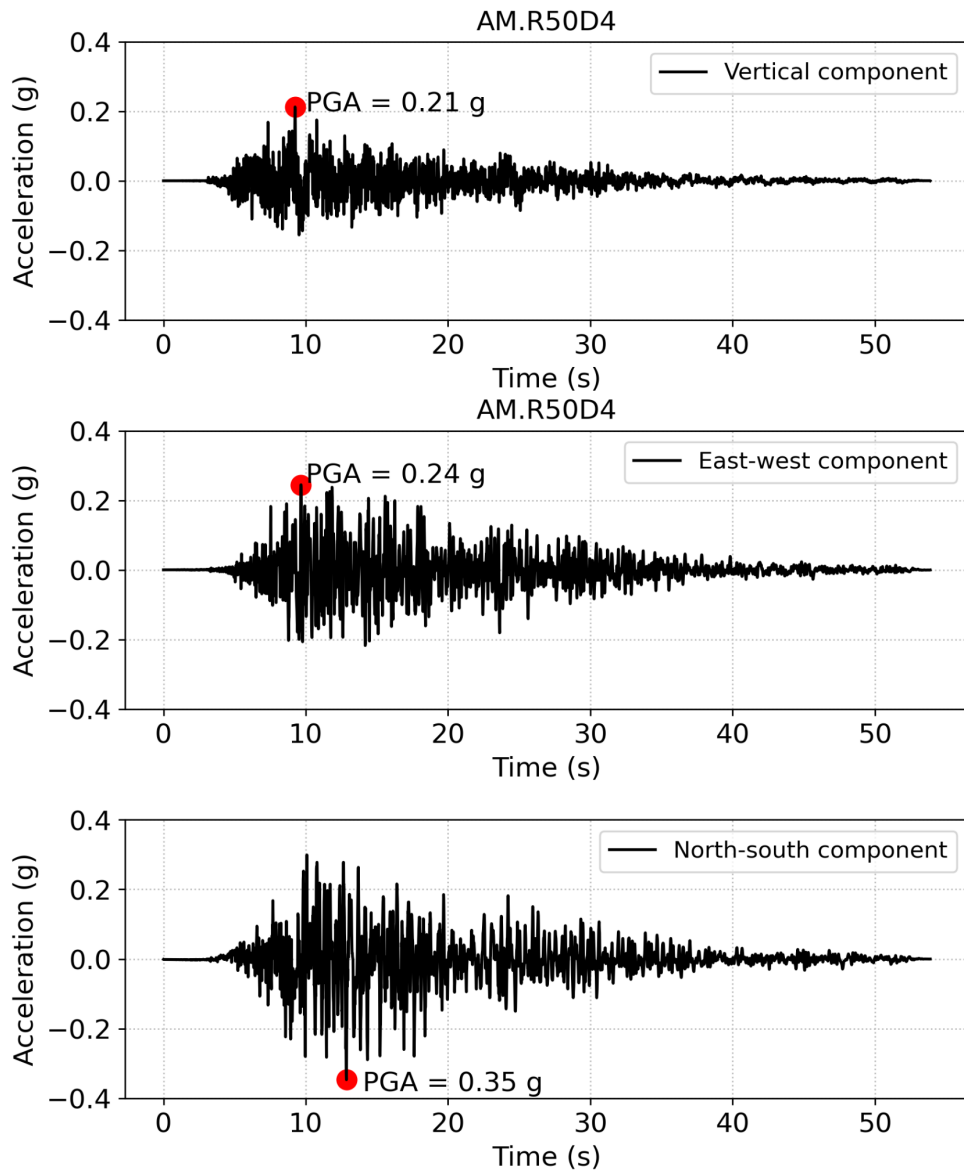


**Figure 5.8.** Acceleration time series observed at station AM.R50D4 during the 2021 Nippes Earthquake.

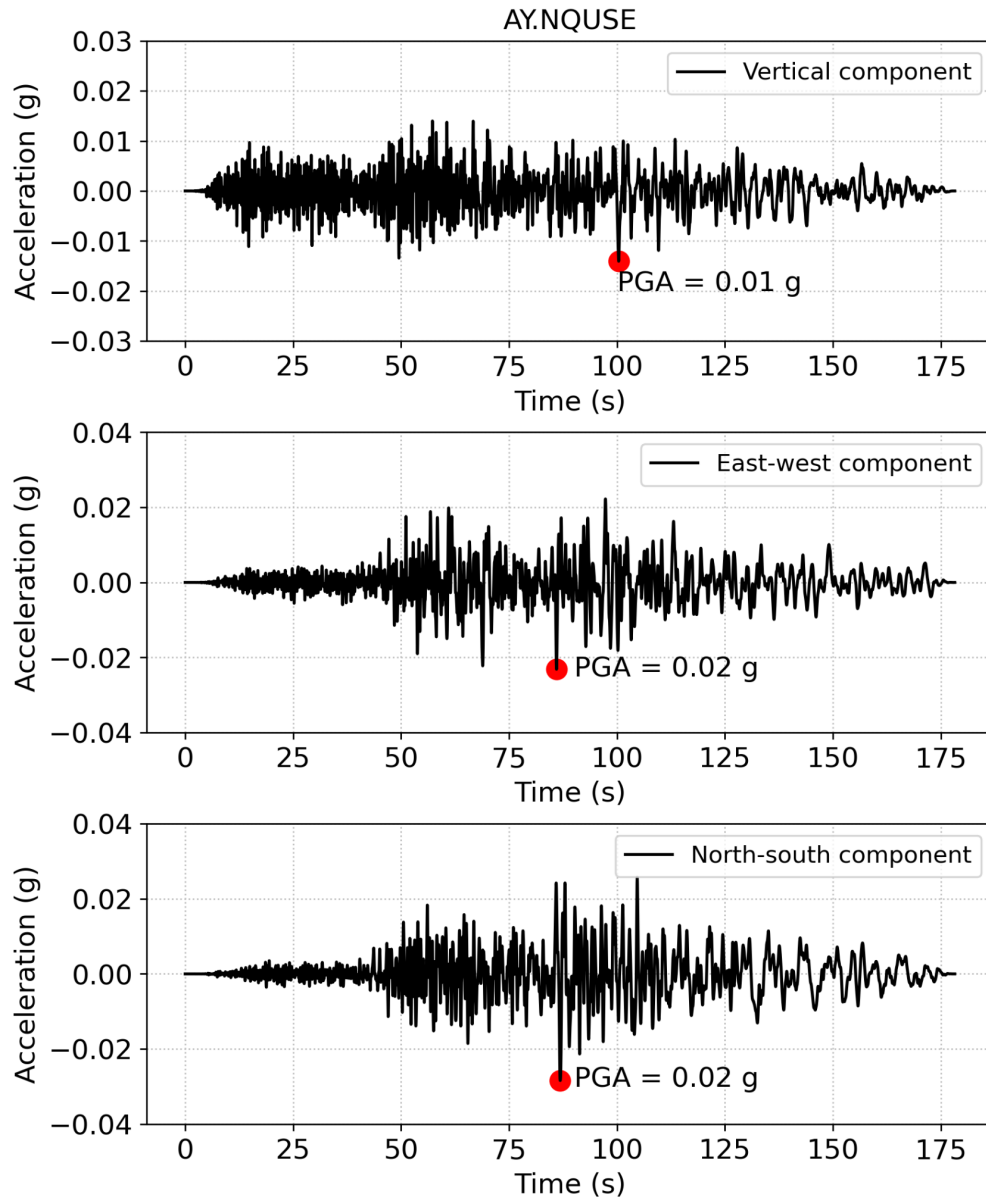


**Figure 5.9.** Acceleration time series observed at station AY.NQUSE during the 2021 Nippes Earthquake.

Velocity time series are also evaluated and a velocity pulse indicative of potential directivity effects is identified in the north-south horizontal component of the recording at AM.R50D4 (see Figure 5.10). The epicentral distance corresponding to this record is 24.9 km, which may be close enough to the source to be considered a near-source record. Additionally, the EPGF (a strike-slip fault) trace trends approximately east-west along the southern Haiti. The velocity pulse only becomes apparent in the fault-normal orientation (i.e., in the NS component as seen in Figure 5.10). Additional analyses are necessary to confirm directivity effects on this record.

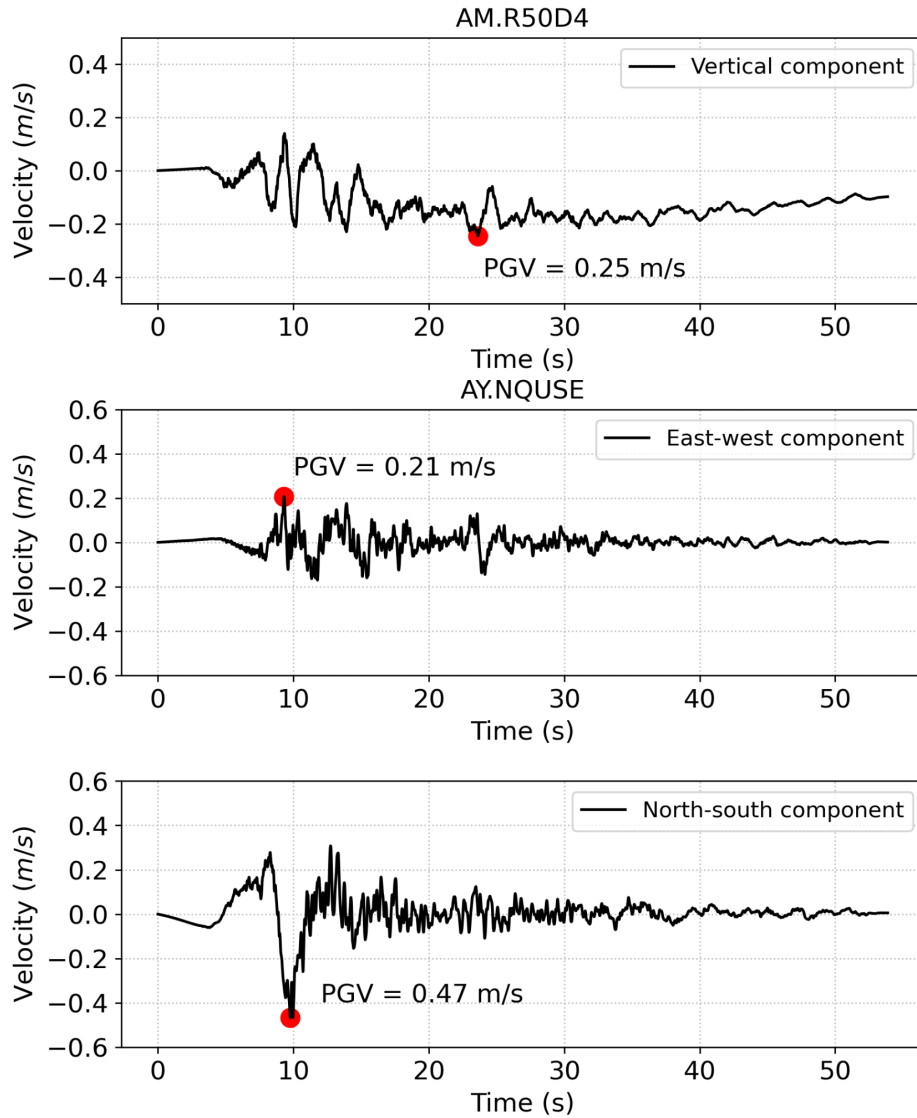


**Figure 5.10.** Velocity time series observed at station AM.R50D4 during the 2021 Nippes Earthquake.

Fourier amplitude spectra corresponding to the ground motion records at AM.R50D4 and AY.NQUSE are provided in Figure 5.11. Differences between horizontal components are more significant for the ground motion recorded at the closest epicentral distance by means of a Raspberry Shake low-cost seismometer. Response spectra for the aforementioned records at AM.R50D4 and AY.NQUSE are also shown in Figure 5.12 to provide a complete characterization of the observed ground motions in Haiti.

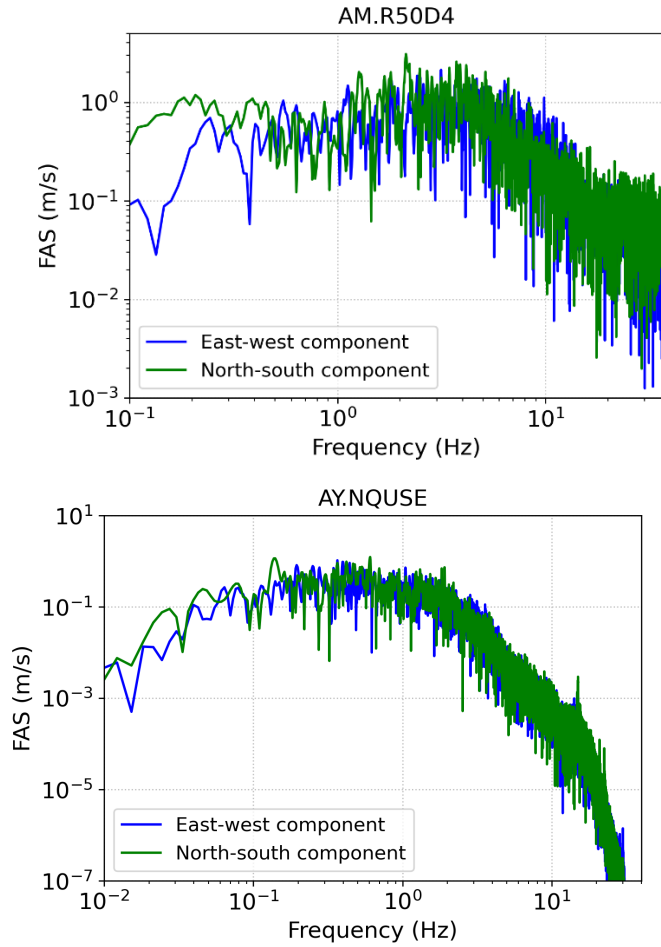


**Figure 5.11.** Comparison of the Fourier amplitude spectra in the two orthogonal horizontal directions observed at stations AM.R50D4 and AY.NQUSE. The AM.R50D4 may indicate potential directivity effects in the amplification of low-frequency motions in the north-south component.

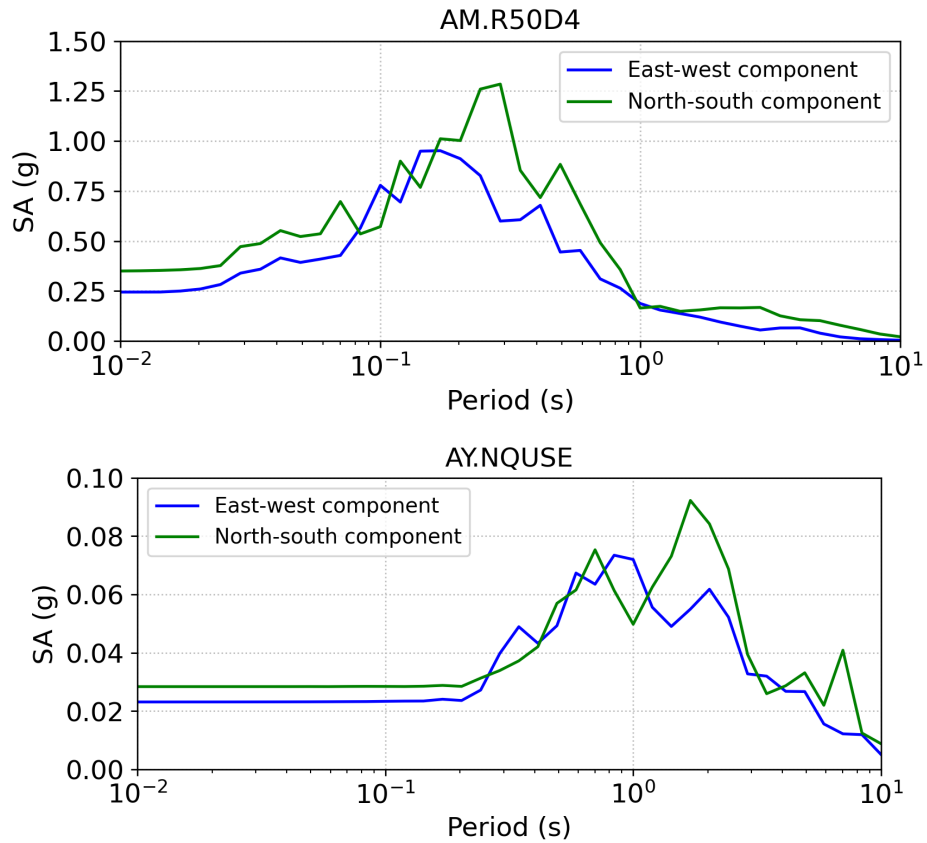


**Figure 5.12.** Comparison of the acceleration response spectra (5%-damped) in the two orthogonal horizontal directions observed at stations AM.R50D4 and AY.NQUSE. The AM.R50D4 may indicate potential directivity effects in the amplification of long-period motions in the north-south component.

## **6. SIMULTANEOUS HAZARDS AND CRISES IN HAITI AFFECTING VULNERABILITY**

### **6.1. Natural Hazards**

About 96% of Haiti's population are vulnerable to natural hazards (World Bank, 2021). Besides earthquakes, with 1,100 miles of coastline in the hurricane belt, the country is subject to severe storms during the hurricane season (June 1 to November 30). According to EM-DAT (2021), between 2010 and 2021, 233,562 Haitians lost their lives to disasters. Of these, 96.4% and 3% were associated with earthquakes and hurricanes, respectively. The remaining losses were due to such events as biological and technological disasters, floods, and droughts.

The Mw 7.0, 2010 earthquake was the most devastating catastrophic event that Haiti has faced recently. This earthquake was centered about 25 km south and west of Port-au-Prince, the capital city (DesRoches et al., 2011). It claimed an estimated 222,570 lives (EM-DAT, 2011) and destroyed about 80% of the city's infrastructure (Beaubien, 2013). It displaced more than 1.5 million individuals (World Bank, 2019) and affected over a third of the country's population (World Bank Group, 2015). The earthquake ended up costing \$7.8 billion in economic damages, corresponding to 120 percent of the country's GDP (World Bank, 2019). The ensuing cholera epidemic claimed 8,346 additional lives (PAHO, 2015), introducing new challenges for those who strove to recover from the earthquake.

Other catastrophic events that took place since the 2010 Haiti Earthquake include Hurricane Thomas in 2010, Isaac and Sandy in 2012, and Matthew in 2016. On average, 58% of the population in each of the country's ten departments have been impacted by natural hazards between 2014 and 2016. As shown in Figure 6.1, the top three departments with the most impact include Grand'Anse (Capital: Jérémie), Centre (Capital: Hinche), and Sud-East (Capital: Jacmel). While many Caribbean countries are prone to the natural hazards that affect Haiti, weak administrative capabilities, as detailed below, and a frail economy increase Haitians' vulnerabilities to respond to crises further (World Population Review, 2021). Widespread deforestation, environmental pollution, and lack of access to clean water and sanitation make matters worse for Haitians throughout the country.

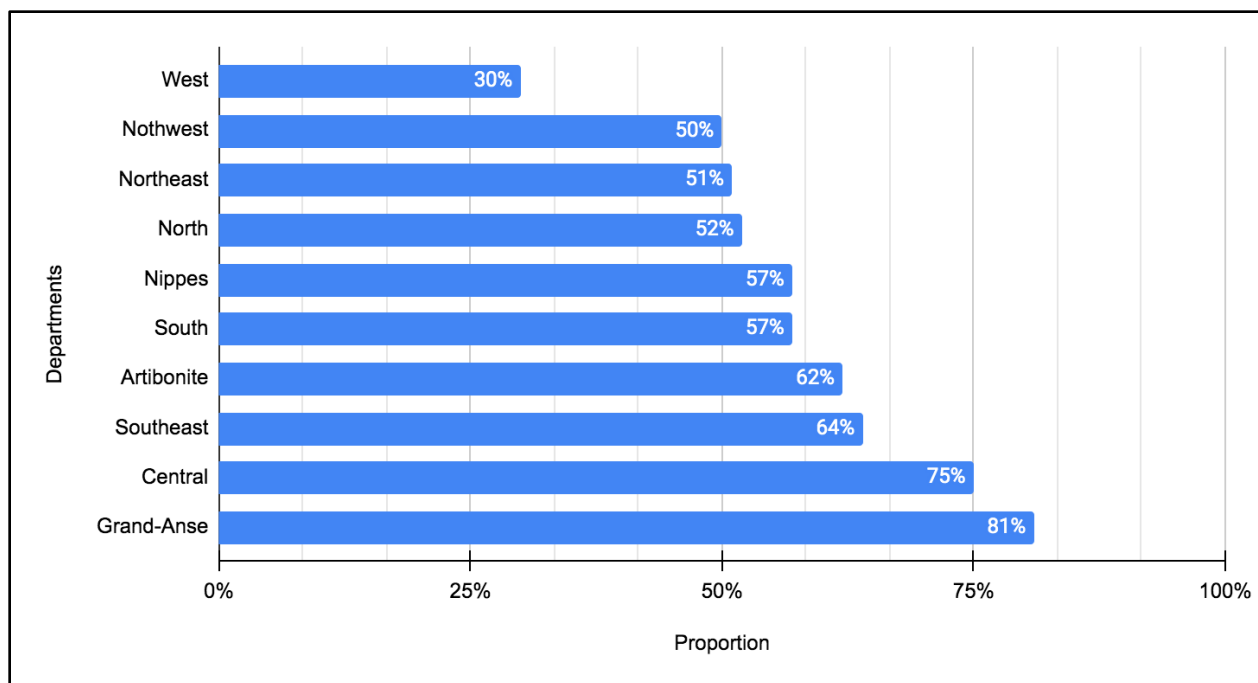


**Figure 6.1.** Percentage of Haitian population impacted by three or more events by department (region) between 2014-2016.

In terms of COVID-19, on September 16, 2021, the Haitian Ministry of Health (Ministère de Santé Publique de la Population) confirmed the Delta and Mu variants in the country and asked all citizens to apply protective measures to reduce their risk of exposure (Le Nouvelliste, 2021). Although the number of COVID-19 cases (21,453) and deaths (607) have remained low compared to that of other countries, those numbers nearly doubled between January and May 2021. Until July 15, 2021, Haiti was the only country in the Americas whose government had not administered a single dose of the covid-19 vaccine. Of the 500,000 covid-19 vaccine doses donated by the United States government, 61,204 have been administered between July 15 and September 21, 2021. From this donation, 18,987 individuals have been fully vaccinated (MSPP, 2021).

## 6.2. Governance Challenges

By conquering its independence from colonial France in the early 19<sup>th</sup> century, Haiti became the first ‘black republic’ and second independent nation in the Americas (Fanning, 2007). It is now referred to as a “fragile” or “failed” state, however. This is a term reserved for states that are unable to provide basic services to their people, including educational programs, health care services, clean water, and security (Collier, 2007; Pritchett et al., 2013; World Bank, 2011b). The reasons behind the fragility of Haitian state are complex, involving both domestic and international strategies “that promoted NGOs as substitutes for the state” (Zanotti 2010, p. 755).

To carry out its functions, the government of Haiti relies heavily on foreign donors and the nongovernmental organizations (NGOs) (Zanotti, 2010). The emergence of NGOs in Haiti dates back to 56 years after its independence, when the 1860 Concordat with the Catholic Church was

executed. This accord was accompanied by the Vatican recognizing Haiti's independence and allowing international faith-based organizations to access Haiti. The first wave of NGOs began to flock to Haiti in 1954, when Hurricane Hazel, a category 4 storm, hit the country. A response that intended to provide immediate humanitarian assistance at that time turned into a long-term development agenda. An agreement between former dictator, Francois Duvalier, and the U.S. government to support his succession of power to his son, Jean-Claude Duvalier, would allow U.S. Protestant churches (as well as factories) to install themselves in Haiti (Schuller, 2017).

Between 1957 and 1986, an estimated 86 NGOs were providing services in Haiti (Schuller, 2017). Before the 2010 earthquake, the number of NGOs in the country had soared up to an estimated 8,000 to 9,000 (Hallward, 2007). Former United States President Bill Clinton, as a United Nations Special Envoy to Haiti, indicated in 2009 that Haiti had ranked second in the world with the highest number of NGOs per capita, earning it the nickname the 'Republic of NGOs' (Kristoff & Panarelli, 2010; Bradley, 2012).

Many NGOs provide life-saving and life-sustaining care to Haitian people. At the same time, the nonprofit sector in general has been heavily criticized for undermining local government capacity (Edmonds, 2012), and putting their own interests before those of others (Sueliman, 2013). The 2010 Haiti earthquake has resurfaced similar concerns on NGO work and accountability in the country. Some also criticized the NGOs for their excessive operational costs (Kwok, 2016), their failures to deliver in the rebuilding process (Elliott & Sullivan, 2015; Sontag, 2012), and for their undermining of the Haitian Government because NGOs have more resources and funding to operate.

The social science team's own research conducted after the 2010 earthquake (Rahill, Ganapati, Clérismé, & Mukherji, 2014) has shown how inequalities involved in aid distribution led to increased tensions and conflicts between those who have access to aid and those who do not. A community leader from Port-au-Prince explained violent acts carried out by those who did not have access to shelter resources (e.g., tents) as follows (p. S88):

*People enter the camps and use knives and razor blades to slice your tent open out of selfishness. People have thrown dirty oil from their automobiles on my tent, just because I had one and they didn't.*

There were also concerns raised about the disconnect between international aid agencies, the Haitian government and the people. Another community leader stated,

*Our government is tricking both the people and the international aid organizations...who come to help the government. They [aid agencies] don't contact us; they deal with the government but the government knows nothing of the population's needs.*

Delivering humanitarian assistance on the ground in Haiti, however, is no easy task. As noted by the head of the International Committee of the Red Cross in Haiti after the 2010 earthquake,

“Given the scale of the needs, the task facing humanitarian organizations is daunting” (Xinhua, 2010). Despite being less deadly, the 2021 earthquake perhaps makes the work of NGOs even more daunting given the ongoing rebuilding needs associated with the massive earthquake that struck the country 11 years ago and the safety and security challenges the country is facing at the moment, which are detailed below.

### **6.3. Security Challenges**

Ensuring security has been a long-standing issue in Haiti, which also affected the ability of the GEER team to travel to Haiti in person. From 2004, the year President Bertrand Aristide departed Haiti for exile, to 2017, the United Nations (U.N.) Stabilization Mission in Haiti (MINUSTAH) provided security throughout the country. Following the 2010 Haiti earthquake, there was an increase in overall U.N. forces, mainly to support the extensive reconstruction needs and to ensure stability throughout the country. However, MINUSTAH was closed on October 15, 2017; and was replaced with a smaller, peacekeeping Mission. Despite international efforts to strengthen the rule-of-law institutions and the Haitian National police, the security situation continues to deteriorate in Haiti.

Last year has especially been turbulent, with increases in kidnappings, gang violence, civil unrest, and protests against the government, coupled with unemployment, food insecurity, fuel shortages and the COVID-19 pandemic (Human Rights Watch, 2020; Mérancourt & Faiola 2021). Mérancourt and Faiola (2021) reports that this year’s recorded kidnappings have increased sixfold compared to the same period (January to September) last year and that Haiti has now the highest per capita kidnapping rate in the world. The number of kidnappings in September was estimated at 117, with 119 cases reported for the first half of the month of October (Haiti Libre, 2021). A European executive expressed how he feels about living with the fear of being kidnapped every day as follows: “Every time you leave your door in Port-au-Prince, it’s like a game of Russian roulette” (Mérancourt & Faiola, 2021).

Haiti also faces a constitutional and political crisis. President Jovenel Moïse was murdered at his private residence on President Jovenel Moïse July 7, 2021, which was followed by the power struggle between two prime ministers and the head of the senate. Prior to his death, President Moïse had dissolved the parliament, ruled by decree, and aimed at expanding the powers of the executive branch. In September 2021, the country’s presidential and legislative elections were postponed indefinitely after the Prime Minister’s dismissal of the council that organizes elections (Reuters, 2021). Furthermore, according to Jean-Baptiste (2021, p.1), “The independence of the justice system is under attack in ways never before seen.” Many lawyers and judges face fear and intimidation and are forced to deal with political divisions and tensions between the executive and the judiciary.

Security challenges in the country further complicate response and recovery efforts in the earthquake affected area for several reasons. First, these challenges lead to some international aid agencies downsizing their operations in Haiti despite the immense need. Second, they make these agencies’ operations costlier due to added security costs the agencies need to budget both for their

foreign and local personnel. Third, security challenges make it more challenging to reach the affected area. In an interview, Laurent Duvillier, Regional Chief of Communication for UNICEF's Latin America and the Caribbean operation, also highlighted how security challenges makes the aid work more complicated as follows (NPR, 2021),

*Well, you know, there are a set of measures that we are constantly updating. And one of the difficult part is that it's extremely volatile security environment. And I was there three weeks ago, so I can tell you. I found myself in that situation that one road that you take to deliver aid in the morning is safe, and then there is a security incident with gang criminality and shooting in the street, and it becomes more dangerous. So you constantly need to adjust, and you constantly have a plan B, a plan C and a plan D. All this insecurity is making our humanitarian work much more costly and complicated.*

#### **6.4. Developmental Challenges**

Haiti's post-earthquake challenges are unprecedented not only because of its governance and security challenges but also because of its ongoing developmental challenges. Haiti's current Gross Domestic Product (GDP) per capita is estimated at US\$1,149.50, making it the poorest country in the Americas and one of the poorest countries in the world (World Bank, 2021). As indicated in Table 7.1, the country has experienced minimal annual GDP growth in 1990 and 2000, followed by negative annual GDP growth both in 2010 (-3.8%) and 2020 (-3.4%) (Table 6.1).

The roots of Haiti's developmental challenges date back to the 1800s after proclaiming its independence in 1804 and being one of the wealthiest French colonies making more money for France than all the other 13 French colonies (McKey, 2016). However, Haiti was obligated to pay reparations to France to maintain its independent status and gain immunity from French military invasion. Haiti took 122 years to pay this debt, estimated at \$21 billion, and finally settled in 1947. Subsequent multiple shocks have battered the country since, including foreign intervention, political instability, and disasters.

**Table 6.1.** Haiti’s Economic Profile.

Year	1990	2000	2010	2020
Economy				
GDP (current US\$) (billions)	3.1	6.87	11.66	13.42
GDP growth (annual %)	1	0.9	-3.8	-3.4
Inflation, GDP deflator (annual %)	12	92.9	6.6	15.1
Agriculture, forestry, and fishing, value added (% of GDP)	30	17	20	20
Industry (including construction), value added (% of GDP)	23	23	24	24
Exports of goods and services (% of GDP)	12	7	7	8
Imports of goods and services (% of GDP)	35	18	37	32

Haiti relies heavily on foreign aid and external remittance. Foreign aid accounts for over 20% of the Haitian government's annual budget, which was \$3.7 billion for 2020-2021 (Le Nouvelliste, 2021). As shown in Table 6.2, with \$696 million in aid, Haiti is one of the top foreign aid recipients in the Americas after Colombia (\$874 million) and Bolivia (\$708 million) (World Bank, 2021). Remittance sent to Haiti represents about 25% of the GDP (Pew Research Center, 2019), up from 8.42% of the country’s GDP in 2000 (World Bank, 2020). In 2020, out of 266 countries, Haiti ranked seven with the highest inflow of remittances as the percentage of the country’s GDP in the world, behind Somalia (35.28%), Kyrgyz Republic (28.44%), Tajikistan (26.69%), El Salvador (24.09%), Nepal (24.07%), and Honduras (23.40%). (World Bank, 2020).

**Table 6.2.** Largest Official Development Assistance Recipients in the Americas in 2019.

Category	Country	Net Disbursement in 2019 (USD million)
Top 10 ODA Recipients Total: \$8,805 million	Columbia	874 (10%)
	Bolivia	708 (8%)
	Haiti	696 (8%)
	Mexico	525 (6%)
	Ecuador	507 (6%)

	Cuba	498 (6%)
	Peru	459 (5%)
	Honduras	452 (5%)
	Guatemala	388 (4%)
	Nicaragua	388 (4%)
	Other Recipients	3,309 (38%)

In 2020, Haiti ranked 170 out of 189 countries in the United Nations Development Programme (UNDP) Human Development Index (HDI), down from 163 in 2015 (UNDP, 2015) and 149 in 2009 (UNDP, 2009). This index summarizes a country's achievements on population health and standard of living. Population health is measured by population life expectancy at birth and different dimensions of education. Standard of living is evaluated by gross national income per capita. The decline of HDI in Haiti is attributed to substantial inequalities in population health and standard of living (UNDP, 2010). According to the World Bank (2021), Haiti is one of the most unequal countries in the Americas. The richest 20 percent of Haiti's population holds more than 64 percent of the country's total income. In comparison, the bottom 20 percent holds less than 2 percent of the country's total income.

The poverty rate is nearly at 60% in Haiti, with two thirds of the poor living in rural areas (World Bank, 2021). About 38% lack access to acceptable water, and 76% live with inadequate access to sanitation (UNDP, 2020). Reports from international organizations estimate that 33% (4 million) of the population faces food insecurity. An estimated 25% of the population is illiterate (UNDP, 2020). About half of school-aged children are illiterate (HRW, 2020). The lack of affordable and good education, ongoing political unrest, and the COVID-19 pandemic have prevented four million (70%) of children from school during the 2019-2020 academic year alone.

## **6.5. Mental Health Challenges**

Prior studies have established a relationship between disasters and increased risks for psychological trauma including, panic disorder, generalized anxiety disorder, alcohol dependence, and abuse, to name a few (Galea, Nandi & Vlahov, 2005; Grubener et al., 2016; Makwana, 2019; Mao, Agyapong, 2021; Norris & Wind, 2012). In Haiti, concurrent disasters from natural hazards, political unrest, gang violence, and extreme poverty present levels of complexity on the long-term impact on the Haitian population. They leave the population in a survival state that requires

constant adaptation to the new normal. Social networks are disrupted, schooling interrupted, employment loss, loved ones gone, and home is no longer a steady place as individuals are forced to relocate to safer environments (Shultz et al., 2016).

Women are especially vulnerable as studies conducted in Haiti reveal a higher prevalence of mental health symptoms among women compared to men (Blanc et al., 2016; Joshi, Rahill, & Rhode, 2021), in addition to increased instances of sexual violence towards them (Kay Fanm, 2012; Willman & Marcelin, 2010; Rahill et al., 2015, 2020). It is estimated that about 50%-72% of women in a shantytown in Port-au-Prince, Cité Soleil, for instance, experienced sexual violence after the 2010 earthquake in Haiti (Kay Fanm, 2012; Willman & Marcelin, 2010). Children are vulnerable as well. Although conditions for children are concerning even without disasters, chaotic conditions and breakdown of social infrastructure, separation from parents or parental death, and displacement of families associated with disasters in Haiti further increased the vulnerability of an estimated 500,000 children (CDC & INURED, 2014).

## 7. GEOTECHNICAL HAZARDS

An on-the-ground GEER Team of five students from *Université d'État d'Haïti* (University of Haiti) documented geotechnical impacts of the 2021 Haiti earthquake on October 9th and 10th, 2021. Based on the remotely gathered data in the initial phase of this reconnaissance, the team took two routes of exploration shown in Figs. 7.1 and 7.2. Route 1 was along National Route 7 (RN7), a major highway connecting Les Cayes to Jeremie. The Route 1 team focused on documenting landslides, rockfalls, pavement damage, lateral spreads, and foundation damage. They first investigated Les Cayes, continued north to Pestle, and then backtracked south to Camp-Perrin. Route 2 was along National Route 2 (RN2) from Les Cayes to Cavaillon and then continuing along RN2 past Saint-Louis-du-Sud and Aquin to Route Communale 204-A (RC-204A). The Route 2 team then continued north/northwest along RC-204A past L'Asile, Balou, and Bonne Fin and then back to Cavaillon where they headed back to Les Cayes along RN2. The Route 2 team focused on landslides, rockfalls, lateral spreads, and surface fault rupture. These routes were determined based on preliminary information and reports from mainstream and social media as well as our partners at StEER, GeoHazards International, and *Université d'État d'Haïti*.

This chapter provides images of geotechnical impacts from the August 14 earthquake provided by the GEER Team in Haiti between October 9-10. This preliminary report does not provide extensive interpretation of the images beyond what is readily seen directly from the images. The images provided were gathered under limited time constraints. More detail is possible with additional reconnaissance time, resources, and measurement on the ground in Haiti in the future.

-  Epicenter
-  Ground motion station
-  Damage observations
-  Media reports of damage

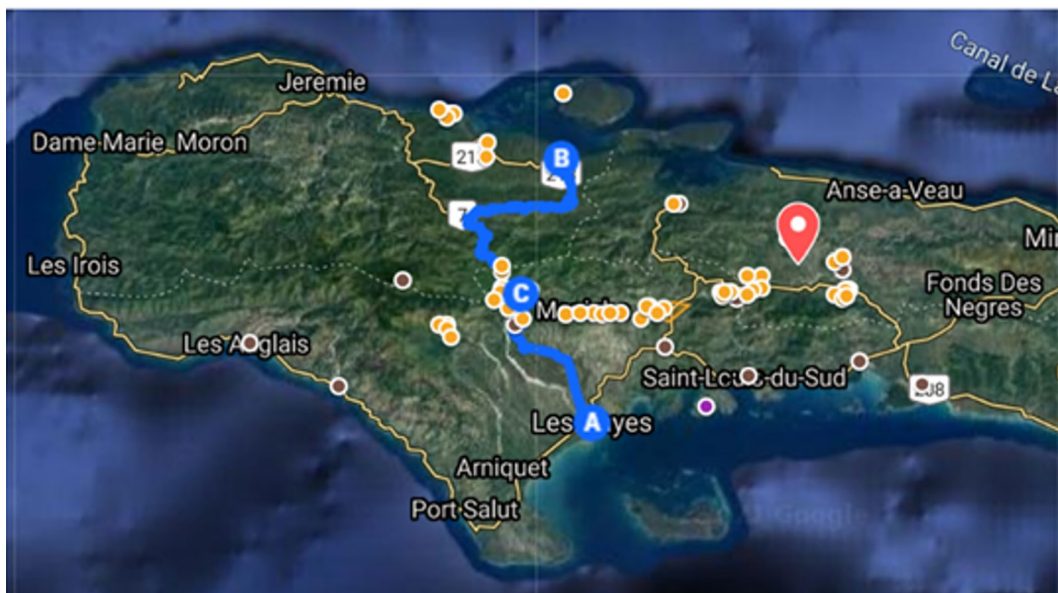


**Figure 7.1.** Route 1 taken by the October 9-10 GEER Team. Point A: Les Cayes. Point B: Pestle. Point C: Camp-Perrin.

- 📍 Epicenter
- Ground motion station
- Damage observations
- Media reports of damage

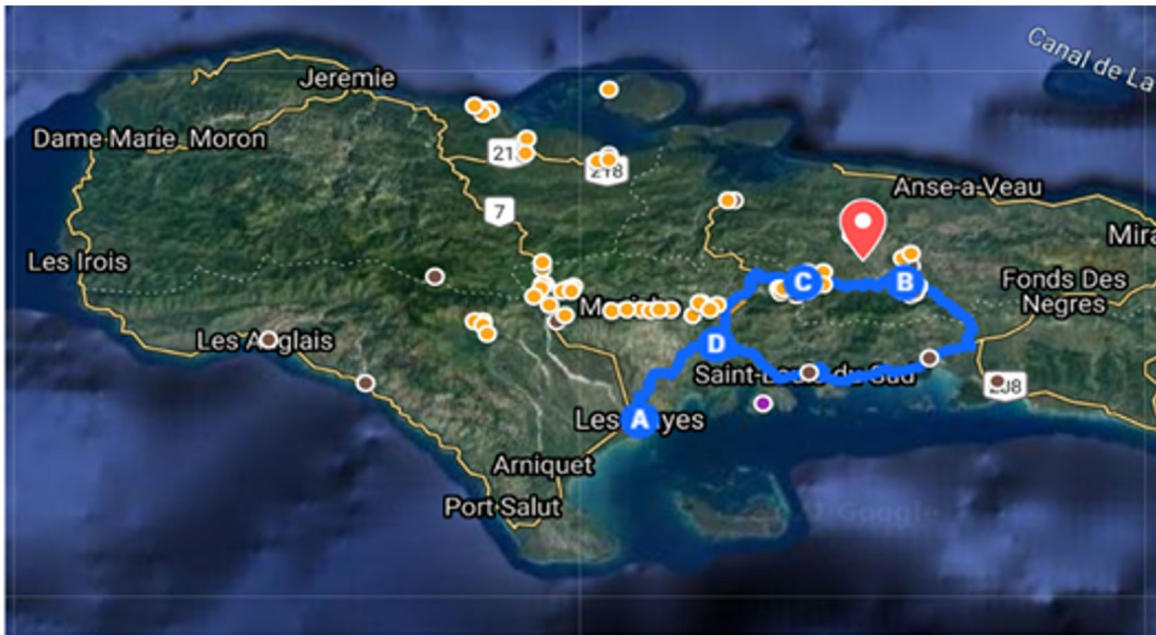


**Figure 7.2.** Route 2 taken by the October 9-10 GEER Team. Point A: Les Cayes. Point B: L’Asile. Point C: Balou. Point D: Cavaillon.

### 7.1. Ground Failure along the Fault

The GEER Team in Haiti identified several locations of ground failure along the Enriquillo-Plaintain Garden Fault (EPGF) between Bonne Fin and L’Asile. The locations of these near-fault observations are shown in Fig. 7.3. The types of near-fault ground failures include rockfalls, landslides, possible surface fault rupture, and lateral spreading caused either by soil liquefaction or cyclic softening in the underlying soil. In some cases, the exact mechanism of ground failure could not be identified with certainty, until further site investigation and measurement become feasible. In those cases, however, possible causes are hypothesized based on the existing evidence.



**Figure 7.3.** Locations of geotechnical observations nearest to the Enriquillo-Plaintain Garden Fault (courtesy of Google Earth). The Enriquillo-Plaintain Garden Fault is delineated in red by Saint Fleur et al. (2020). The pins correspond to the location of subsequent figures.

The GEER Team documented a rockfall adjacent to road RC-204 approximately 60 meters north of the EPGF in Balou, shown in Fig. 7.4. On the other side of the road is possible evidence of surface fault rupture shown in Fig. 7.5. Further investigation is required to determine if the ground failure in Fig. 7.5 is indeed surface fault rupture.



(a)



(b)

**Figure 7.4.** Rockfall next to road RC-204 (Lat: 18.37306, Lon: -73.53889).



(a)



(b)

**Figure 7.5.** Possible surface fault rupture next to road RC-204 (Lat: 18.37306, Lon: -73.53889).

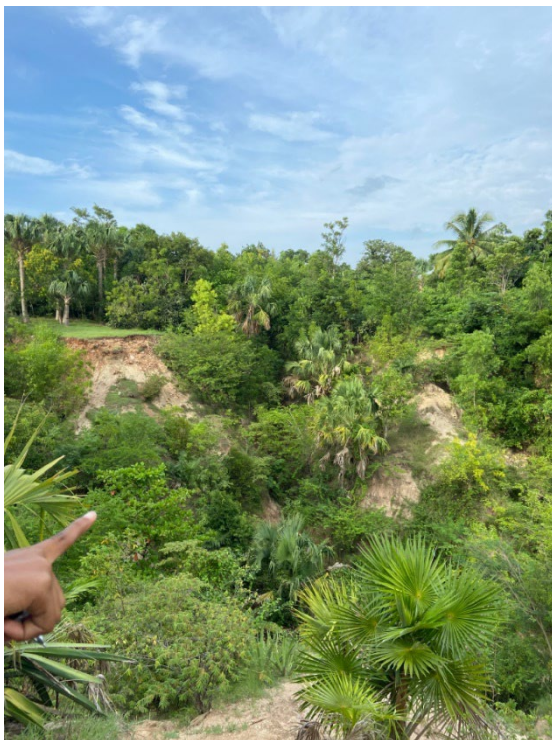
Further east along the EPGF and near RC-204A, the GEER Team documented a slope failure shown in Fig. 7.6 between Balou and L'Asile. This slope failure occurred approximately 0.4 km away from a river on a slope with an average gradient of approximately 14% between the river and RC-204 (as measured in Google Earth). Further east, the GEER Team documented a possible earthquake-induced landslide approximately 0.2 km north of the EPGF, shown in Fig. 7.7. The landslide shown in Fig. 7.7 occurred within a relatively narrow gulley with steep slopes on each side. The landslide appears to have fresh vegetation on the slope, as shown in Fig. 7.7a, including entire trees along the slope that appear to have come from the top of the hill, as shown in Fig. 7.7b and 7.7c.



(a) (b) (c)  
**Figure 7.6.** Slope failure near Balou (Lat: 18.37866, Lon: -73.51278).



(a)



(b)



(c)

**Figure 7.7.** Possible earthquake-induced landslide near RC-204A between L'Asile and Balou (Lat: 18.37528, Lon: -73.46333).

Significant ground failure occurred near the EPGF near L'Asile approximately 0.3 km north of the EPGF, shown in Figs. 7.8, 7.9, and 7.10. The images in Figs. 7.8-7.10 were obtained approximately 0.1 km upslope from a river on a slope with an average gradient of approximately 5% (estimated using Google Earth). Fig. 7.8 shows the upslope view of a scarp associated with

slope instability. The scarp shown in Fig. 7.8a,b is over 2 meters in height. The downslope view in Fig. 7.9 shows significantly disturbed ground directly in front of the scarp in Fig. 7.8. Further investigation is needed to determine with any certainty what were the causes of the failures shown in Figs. 7.8-7.10. If the cause was surface fault rupture resulting from close proximity to the EPGF, the downward movement of the ground in Fig. 7.8 would suggest that this is the hanging wall of a normal fault rupture. However, this would be inconsistent with the oblique reverse fault mechanism of the EPGF. The cause was possibly lateral spreading due to liquefaction of saturated granular soils or cyclic softening of plastic soils. The slope at this location supports that hypothesis, and the ground fissures shown in Fig. 7.10 are consistent with a lateral spread. Further investigation into the subsurface soil at this site would be required to determine if the ground failure at this site was related to liquefaction or cyclic softening. The exact depth of the cracks seen in Fig. 10 is unknown due to the fissures being filled with mud during the Tropical Storm Grace. The width of the cracks observed ranged from about 15 cm to 40 cm. Additional images of the ground failure at this site are shown in Fig. 7.11. Fig. 7.12 shows a foundation failure due to its proximity to the zone of ground failure. Fig. 7.12 shows that this foundation was directly atop the scarp. The purpose of the structure, whether it was a single-story dwelling or other structure, is unclear. A similar ground failure is also seen 30 meters east, shown in Fig. 7.13

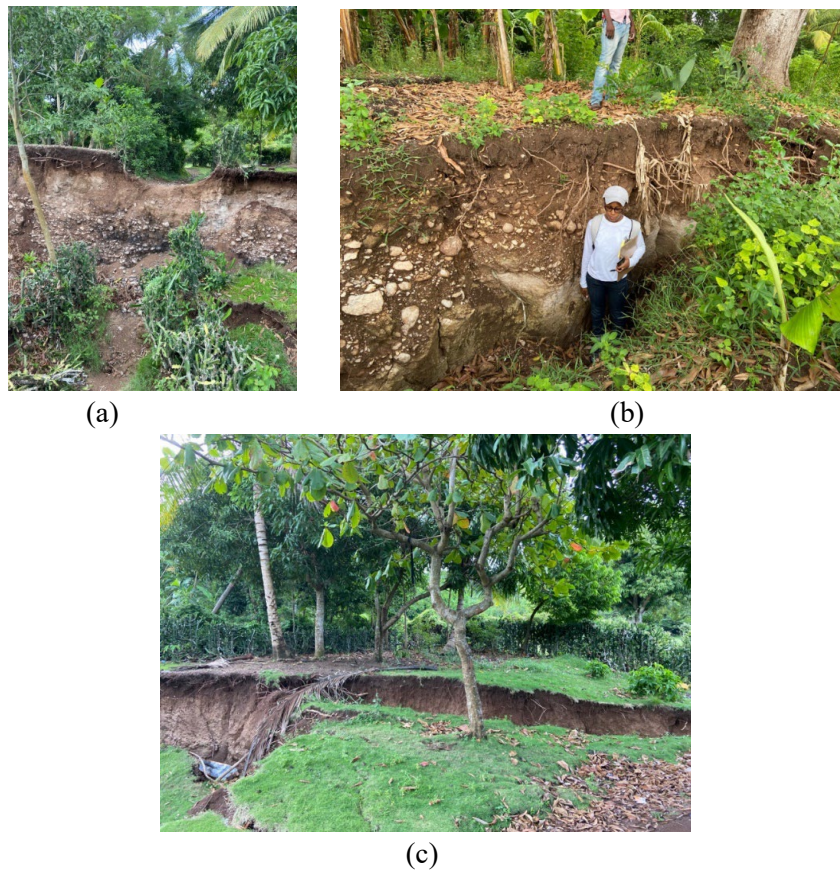


**Figure 7.8.** Upslope view of scarp associated with ground failure near L'Asile (Lat: 18.37444, Lon: -73.43278). For scale, person in (b) is 1.6 meters in height.



(a)



(b)



(c)



(d)



(e)



(f)



(g)

**Figure 7.9.** Downslope views of ground failure near L'Asile (Lat: 18.37444, Lon: -73.43278).



**Figure 7.10.** Ground cracking associated with ground failure near L'Asile shown in Figs. 7.8 and 7.9 (Lat: 18.37444, Lon: -73.43278).



(a)



(b)



(c)



(d)

**Figure 7.11.** Additional views of the ground failure shown in Figs. 7.8-7.10 (Lat: 18.37444, Lon: -73.43278).



(a)



(b)

**Figure 7.12.** Foundation damage associated with ground failure shown in Figs. 7.8-7.11 (Lat: 18.37444, Lon: -73.43278).



(a)



(b)

**Figure 7.13.** Ground failure scarp near L'Asile (Lat: 18.3744, Lon: -73.4325).

The ground failures shown in Figs. 7.8-7.13 occurred upslope of a riverside landslide, shown in Fig. 7.14. This landslide occurred adjacent to Rivière Mahot. Pre-earthquake satellite imagery does not show this landslide. Therefore, it was very likely triggered by the August 14 earthquake.

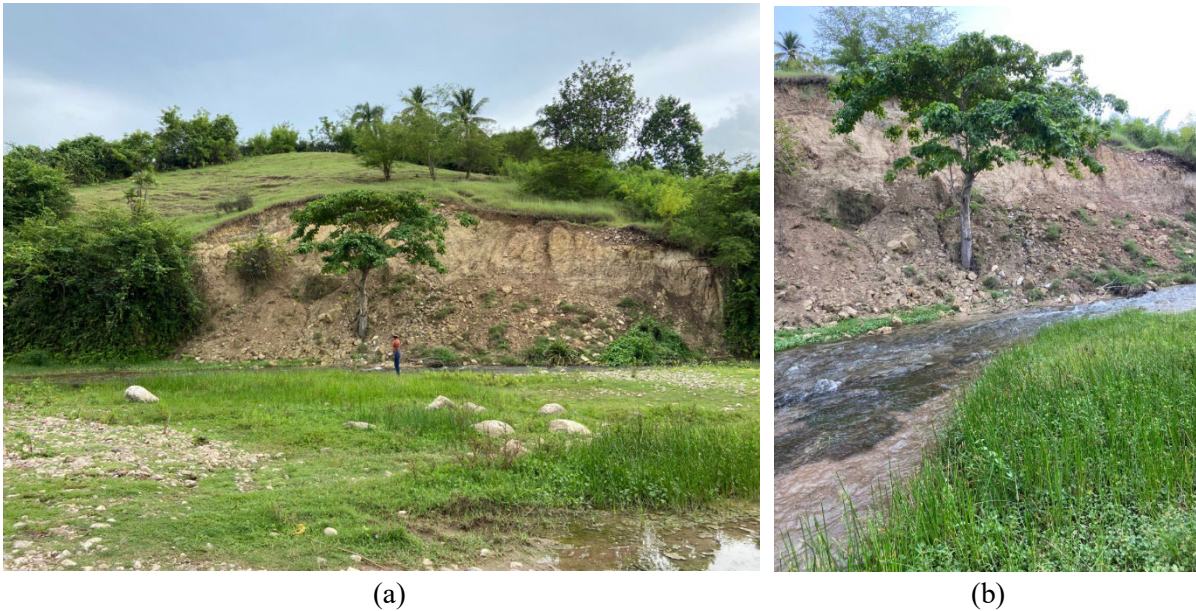


**Figure 7.14.** Landslide adjacent to river in Saint Ange (Lat: 18.37333, Lon: -73.43278)

The GEER Team documented a rockfall with debris containing meter-sized boulders along RC-204A between L'Asile and Mornes. This rockfall is shown in Fig. 7.15. Satellite imagery confirms that this rockfall was directly related to the August 14 earthquake.



(a)



(b)



(c)



(d)



(e)



(f)

**Figure 7.15.** Rockfall along RC-204a between L'Asile and Mornes (Lat: 18.36833, Lon: -73.39417).

Figs. 7.16 shows surface cracks approximately 1.5 km north of the EPGF near Bertrana. The grayish-brown sand surrounding the cracks is possibly sand ejecta and evidence of liquefaction at this site. Fig. 7.17 shows similar evidence of liquefaction west of RN7 adjacent to Riviere de Cavaillon and 0.2 km north of the EPGF. The source of the cracking and whether or not it is related to earthquake surface fault rupture is undetermined.



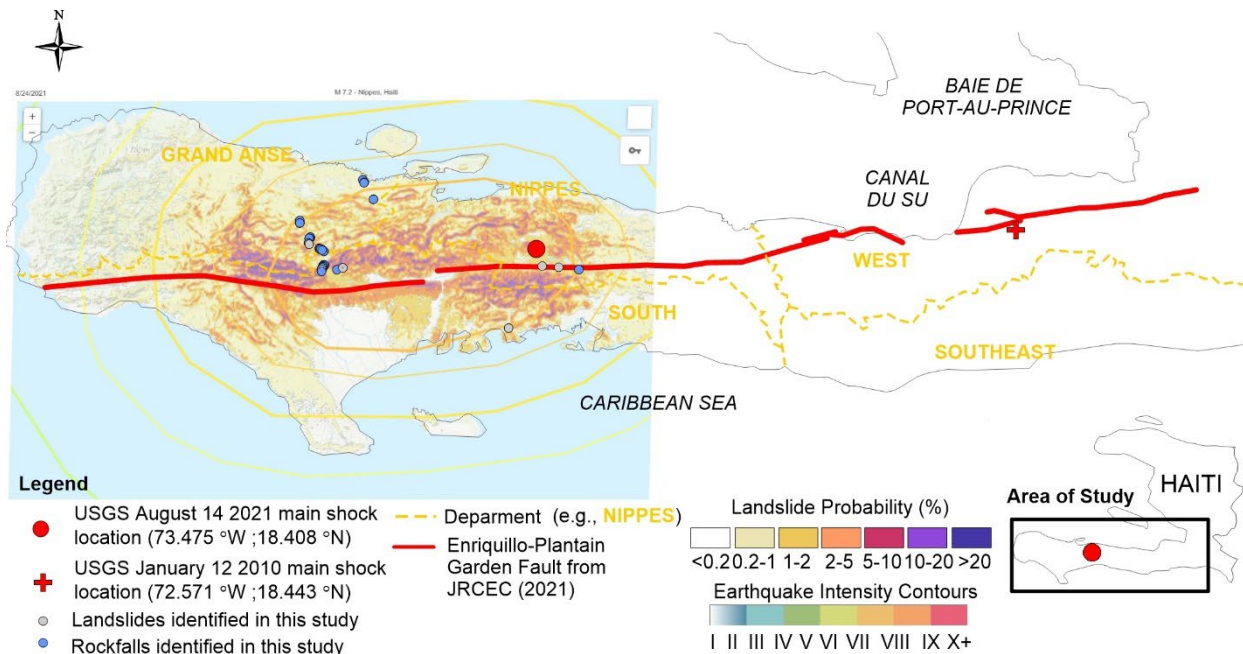
**Figure 7.16.** Surface cracks with evidence of sand ejecta immediately adjacent to the cracks (Lat: 18.38574, Lon: -73.41023). Photos taken on August 25, 2021, courtesy of Dr. Newdeskarl Saint Fleur.



**Figure 7.17.** Surface cracks with evidence of sand ejecta immediately adjacent to the cracks (Lat: 18.35, Lon: -73.70694). Photos taken on August 28, 2021, courtesy of Dr. Newdeskarl Saint Fleur.

## 7.2. Seismic Slope Stability and Landslides

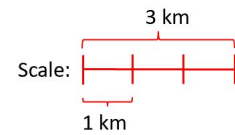
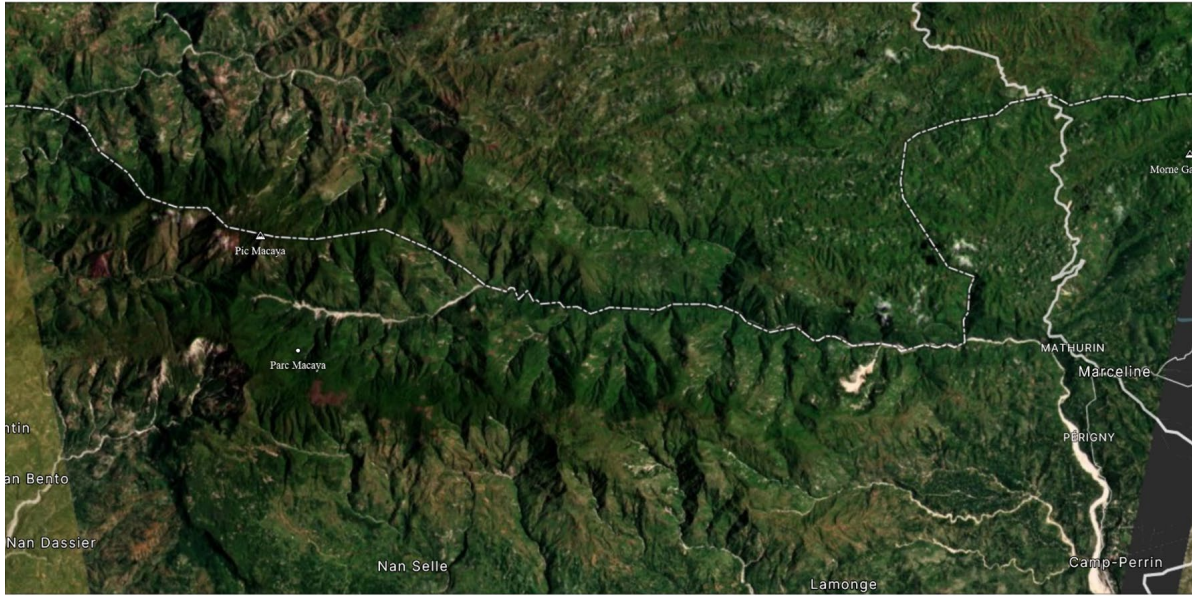
The mountainous terrain of southwest Haiti is prone to seismically induced landslides, particularly around Pic Macaya National Park. Fig. 7.18 shows regions of landslide susceptibility in the country. The August 14 earthquake triggered several landslides visible across the Pic Macaya National Park. Fig. 7.19 shows satellite views of the Pic Macaya National Park four days before the earthquake and two weeks after the earthquake. The landslides, interpreted as removed vegetation in Fig. 7.19b, may have been partially caused by Tropical Storm Grace two days after the earthquake. However, the impact of the storm on landslide activity is difficult to determine via satellite imagery due to widespread cloud cover during the storm.



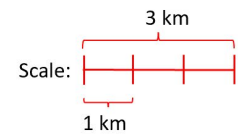
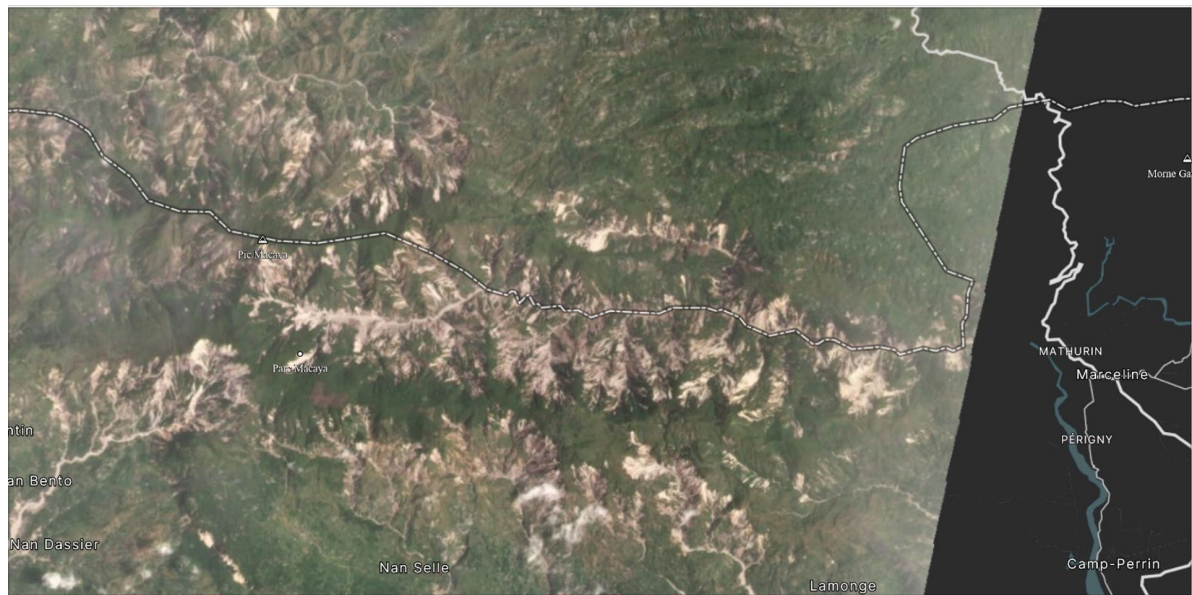
Source:

-Center National de l'Information GeoSpatiale (CNIGS), UNDAC, OpenStreetMap. Created by MAP Action on 22/09/2021. <https://mapaction.org>  
 -USGS ground failure maps. Last updated 19 August 2021 <https://earthquake.usgs.gov/earthquakes/eventpage/us6000f65h/ground-failure/summary>  
 -Joint Research Center European Commission. 2021. Mw 7.2 Earthquake and Tsunami in Haiti

**Figure 7.18.** Landslide susceptibility base map in Haiti (the sources are provided in the figure legend).



(a)



(b)

**Figure 7.19.** Satellite views of Pic Macaya National Park. (a) Imagery from August 10, 2021. (b) Imagery from August 29, 2021. Landslides are interpreted from the removed vegetation in the second image. Images courtesy of Planet Labs (planet.com).

The remote GEER Team on the ground identified several more slope failures, including landslides and rockfalls, at different locations shown in Fig. 7.20. Many of these locations were along RN7, and two of them occurred along the EPGF (as discussed previously in Section 7.1). An isolated landslide location is in Saint Georges adjacent to RN2 between Saint Louis du Sud and Meyance, shown in Fig. 7.21. As shown in Fig. 7.21a, this landslide was accompanied by rockfall. Whether or not this landslide ever crossed the road and was later cleared is not known at the time of this report.

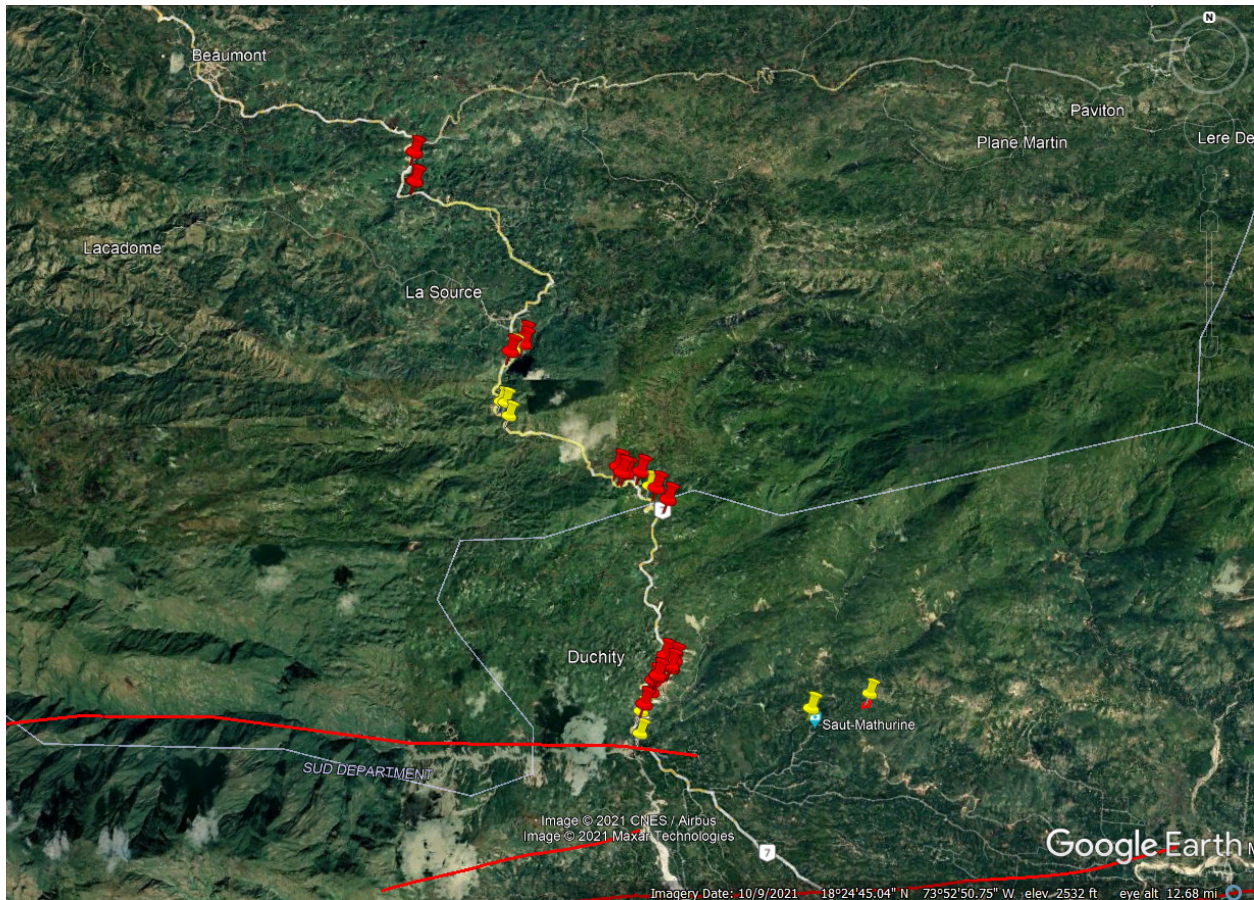


**Figure 7.20.** Locations of slope instabilities identified by the remote GEER Team between October 9-10 (courtesy of Google Earth). Red pins are locations of rockfalls. Yellow pins are locations of landslides. Fault traces are delineated in red by Saint Fleur et al. (2020).



**Figure 7.21.** Landslide along RN2 between Saint Louis du Sud and Meyance (Lat: 18.25861, Lon: -73.52694).

A landslide crossed a neighborhood road east of Champlois and Saut Mathurine approximately 4.5 km away from RN7, shown in Fig. 7.22. This landslide occurred on a slope with an average grade of 46% and ran a distance of 0.17 km from the scarp to the end tip of the debris (as measured in Google Earth). The landslide debris crossed a neighborhood road. The satellite imagery in Fig. 7.23 shows the full extent of this landslide. Google Earth provides a rough approximation of 8,800 m<sup>2</sup> for the area of the landslide outlined in red shown in Fig. 7.23.

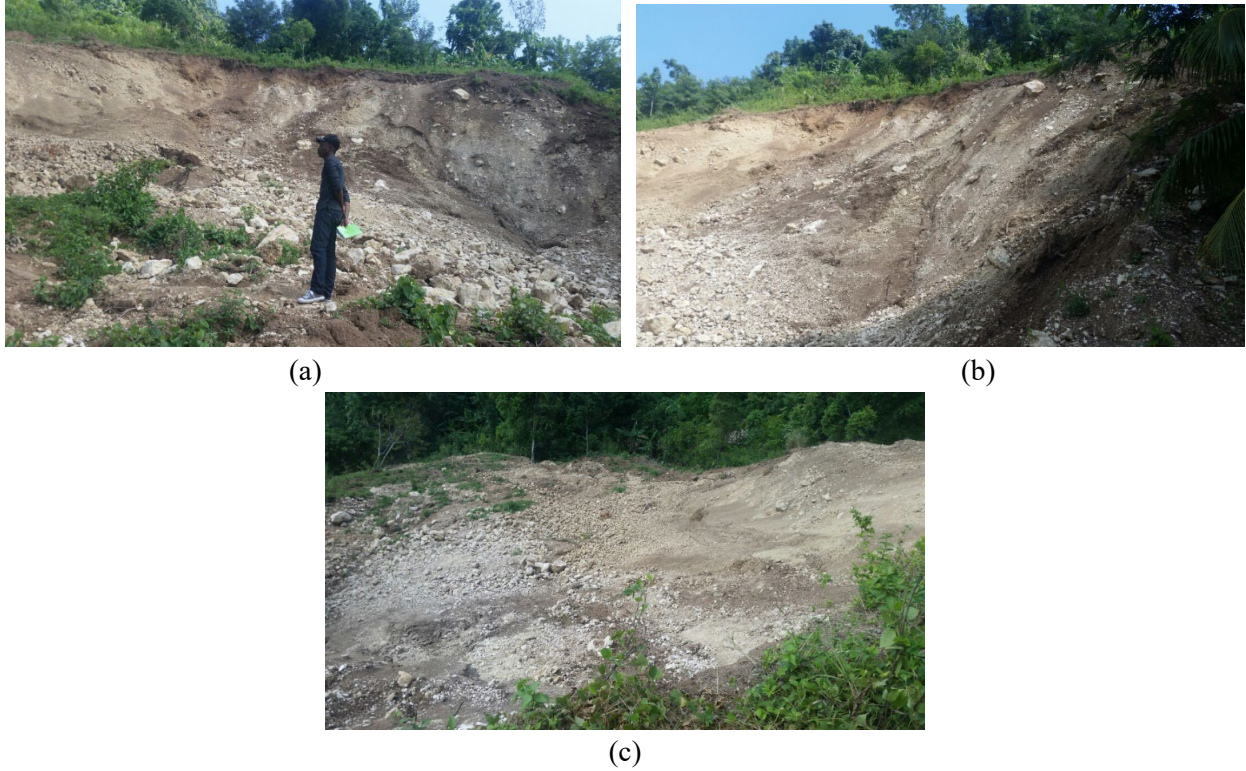


**Figure 7.22.** Landslide near Champlois (Lat: 18.3718016, Lon: -73.8393673).



**Figure 7.23.** Satellite imagery of Landslide (roughly outlined in red) shown in Fig. 7.22 (courtesy of Google Earth).

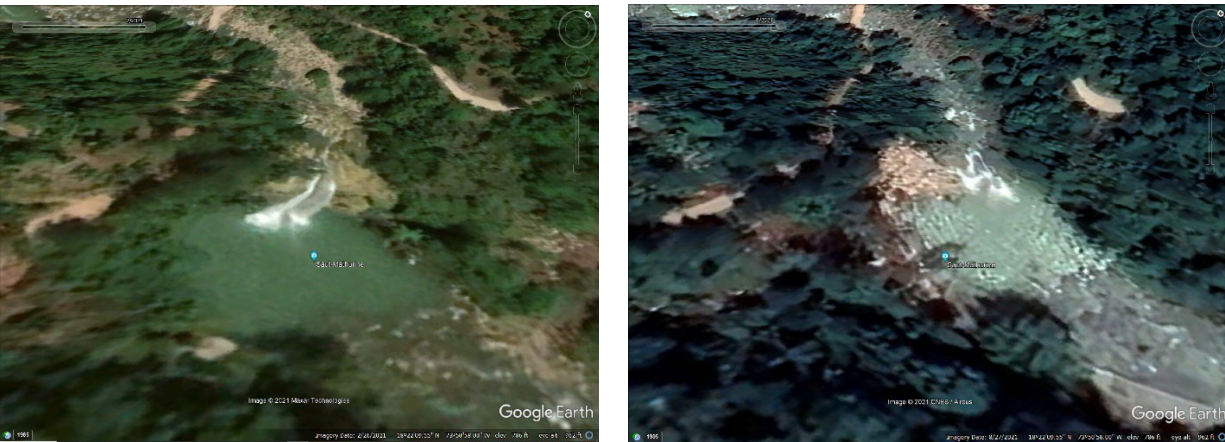
West of the landslide shown above, the August 14 earthquake triggered a landslide adjacent to the Saut-Mathurine waterfall. This waterfall is associated with the Rivière Cavaillon in Camp-Perrin. Fig. 7.24 shows that this landslide also includes significant amounts of rock and boulder debris. This landslide is reported to have displaced the path of the river and waterfall. Fig. 7.25 shows through satellite imagery the extent to which the landslide displaced the river and waterfall.



(a)

(b)

**Figure 7.24.** Landslide and rockfall adjacent to Saut-Mathurine (Lat: 18.3690876, Lon: -73.8495348).



(a)

(b)

**Figure 7.25.** Google Earth imagery of Saut Mathurine (a) before the earthquake on February 26, 2021, and (b) after the earthquake on August 27, 2021.

Several slope failures and rockfalls occurred near each other along RN7 between Marceline and Beaumont. The southernmost of these documented slope failures is shown in Fig. 7.26. Fig. 7.26a shows a water tank with foundation still intact at the top of this slope failure. Nearby this slope failure, a landslide occurred near a slope extending down to Ravine du Sud on an approximately 53% grade over a distance of 0.25 km (measured in Google Earth), as shown by the satellite imagery in Fig. 7.27.



**Figure 7.26.** Slope failure along RN7 with water tank at top of slope (Lat: 18.3652708, Lon: -73.8791013).



**Figure 7.27.** Pre-event and post-event satellite imagery of landsliding along RN7 west of Champlois (courtesy of Planet Labs, planet.com): (a) February 26, 2021. (b) August 27, 2021.

Additional landslides and rockfalls were observed along an approximately 1.6 km stretch of road with headscarps along the west side of the road. The locations of these slope instabilities are shown in Fig. 7.28. This stretch of slope instabilities lies east of Duchity and west of Champlois. Images from these slope instabilities are shown in Figs. 7.29 to 7.39. Fig. 7.40 shows an additional rockfall that covered one lane of RN7 slightly further up the road. A large landslide occurred above Rivière de Cavaillon as shown in Fig. 7.41. This landslide occurred on an average slope 47% over length of ~0.4 km, as measured in Google Earth

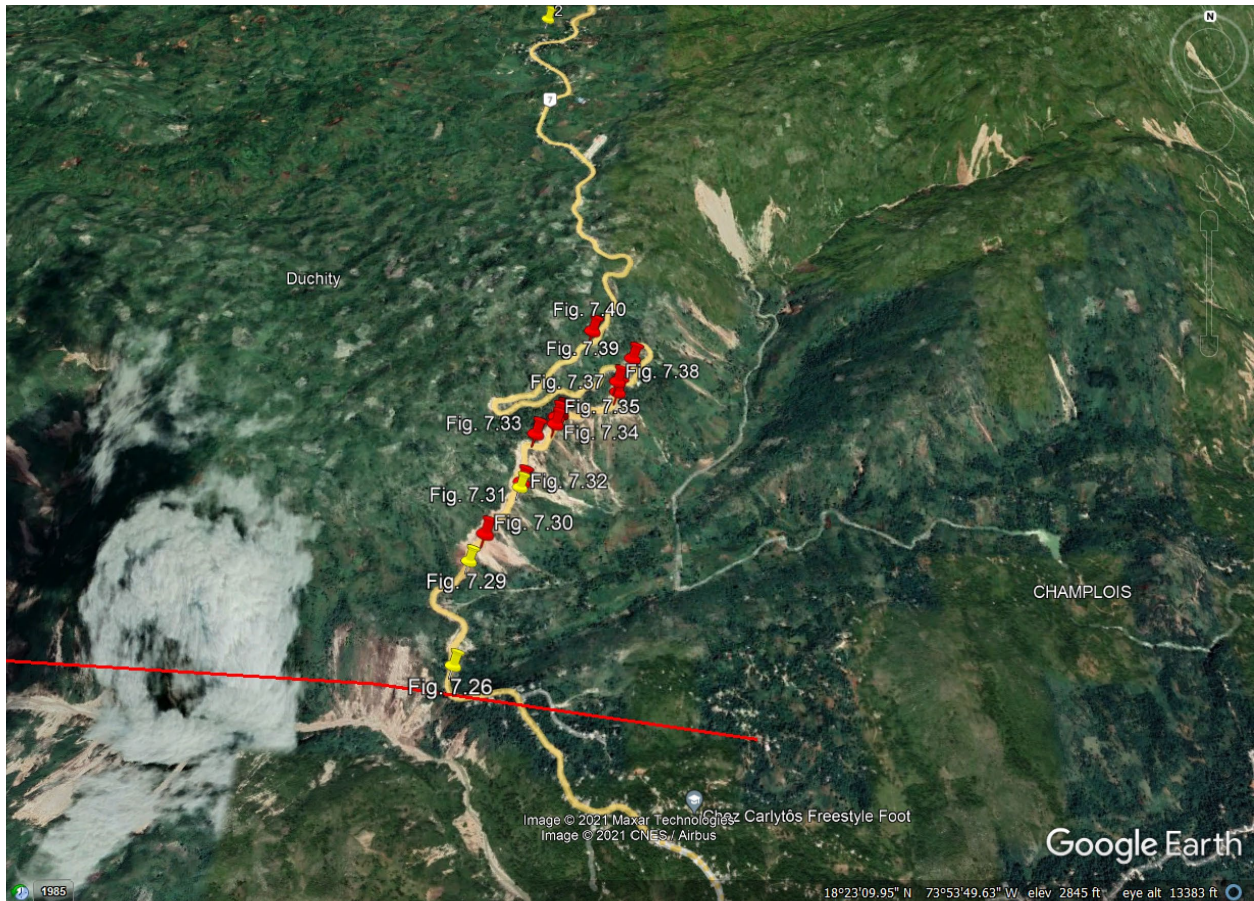


**Figure 7.28.** Locations of landslides and rockfalls observed along RN7 east of Duchity and West of Champlois. Mapped fault strand shown in red from Saint Fleur et al. (2020). Imagery date October 9, 2021.

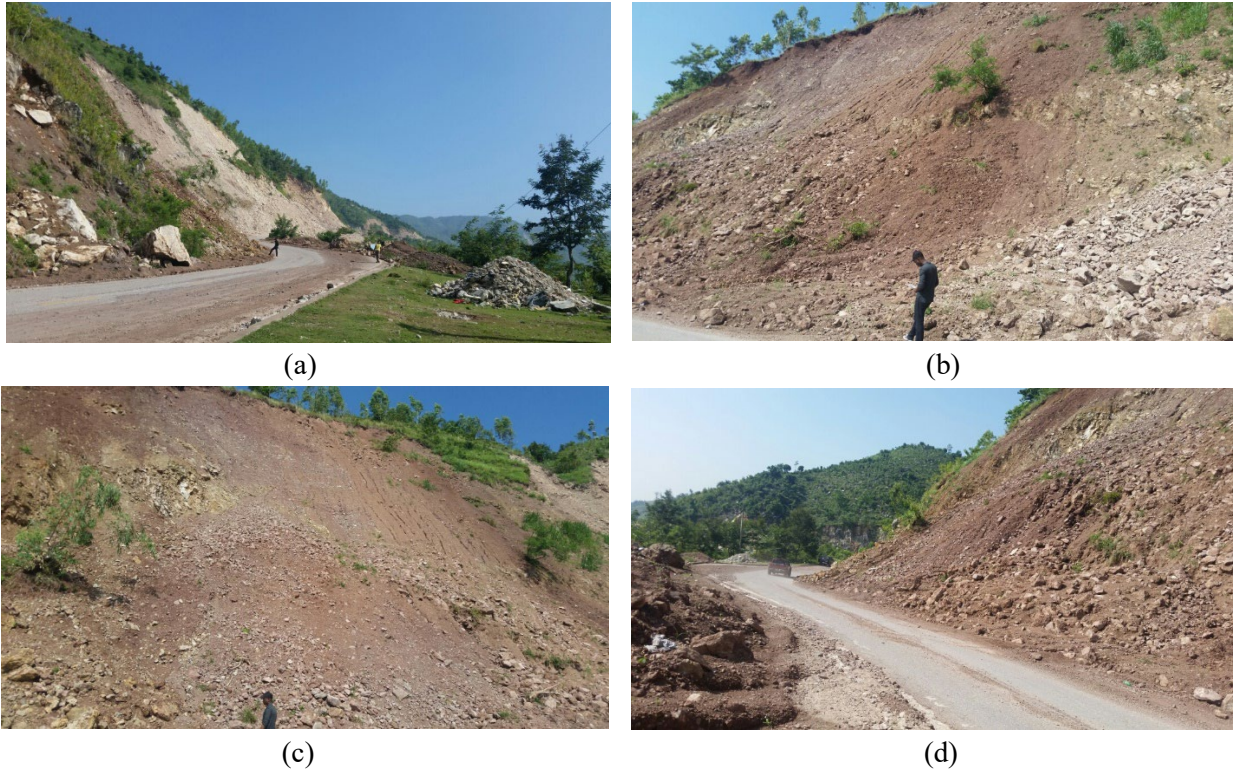


**Figure 7.29.** Slope failure along RN7 associated with 1.6 km stretch of landslide activity (Lat: 18.3688969905183, Lon: -73.8789592310786).



**Figure 7.30.** Rockfall along RN7 associated with 1.6 km stretch of landslide activity (Lat: 18.369867, Lon: -73.8784972). Photo taken September 27, 2021.



(a)



(b)



(c)



(d)

**Figure 7.31.** Slope failure along RN7 associated with 1.6 km stretch of landslide activity (Lat: 18.371743, Lon: -73.8773852).



(a)



(b)

**Figure 7.32.** Rockfall along RN7 (Lat: 18.3718874, Lon: -73.8773472).



(a) (b)  
**Figure 7.33.** Rockfall along RN7 (Lat: 18.3737682, Lon: -73.8769681).

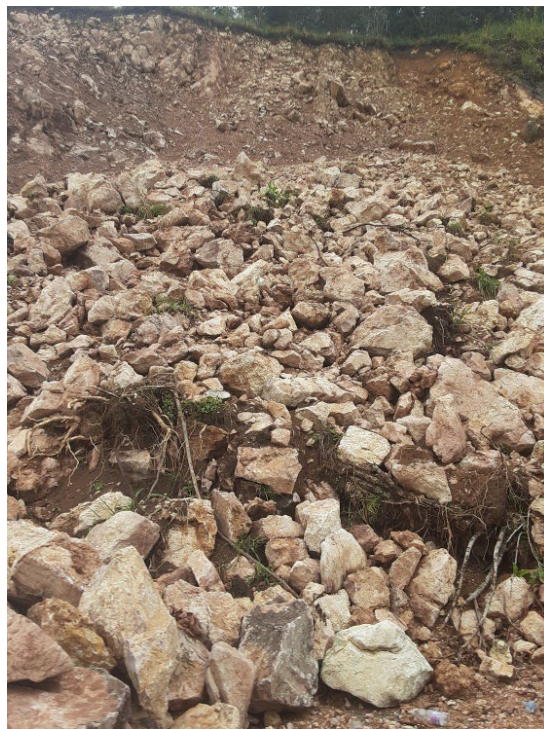


**Figure 7.34.** Rockfall along RN7 (Lat: 18.37430287, Lon: -73.87626537). Photo taken September 28, 2021.



**Figure 7.35.** Rockfall along RN7 (Lat: 18.3745397, Lon: -73.8762437). Photo taken September 28, 2021.



**Figure 7.36.** Rockfall along RN7 (Lat: 18.374679, Lon: -73.8760854).

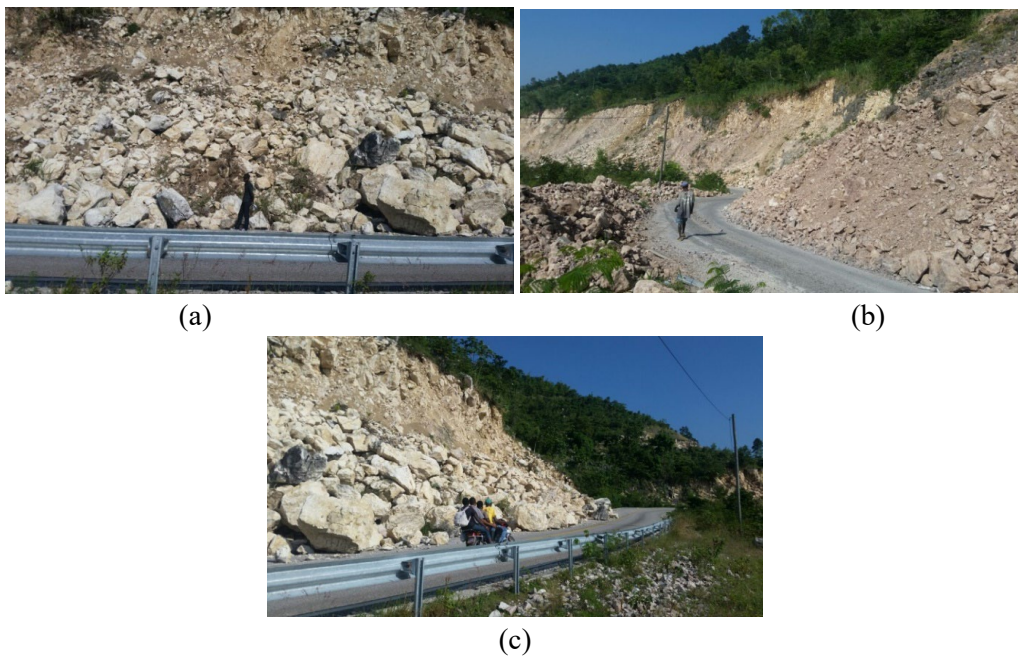


**Figure 7.37.** Rockfall along RN7 (Lat: 18.3757585, Lon: -73.8739482).



**Figure 7.38.** Rockfall along RN7 (Lat: 18.376124, Lon: -73.8739723). Photo taken September 28, 2021.



(a)



(b)

**Figure 7.39.** Rockfall along RN7 (Lat: 18.3771116, Lon: -73.8734214).



(a)



(b)

**Figure 7.40.** Rockfall along RN7 (Lat: 18.3777911, Lon: -73.8750105).



**Figure 7.41.** Landslide near RN7 with an average slope 47% over length of ~0.4 km as measured in Google Earth (18.385256, Lon: -73.869594). (a) February 26, 2021. (b) August 27, 2021.

Approximately 4 km north along RN7 was another stretch of slope failures along RN7. The locations of these slope failures are shown in Fig. 7.42. The rockfalls in Figs. 7.43-7.49 contain particularly large boulder debris. Fig. 7.43 shows how a large boulder of several meters in diameter damaged an approximately 1 meter-high retaining wall (Fig. 7.43a). Figs. 7.44, 7.47, and 7.49 show landslides containing notable amounts of boulder debris. Fig. 7.46b shows pavement damage that appears to have resulted from the impact of the rockfall, and Fig. 7.49b shows another possible impact-related road damage.



**Figure 7.42.** Locations of landslides (yellow pins) and rockfalls (red pins) observed along RN7 (courtesy of Google Earth). Imagery date October 9, 2021.



(a)

(b)



(c)

**Figure 7.43.** Rockfall along RN7 in Catiche (Lat: 18.4030031, Lon: -73.8747026).



(a)

(b)



(c)

**Figure 7.44.** Rockfall along RN7 in Catiche (Lat: 18.4048258, Lon: -73.8767197).

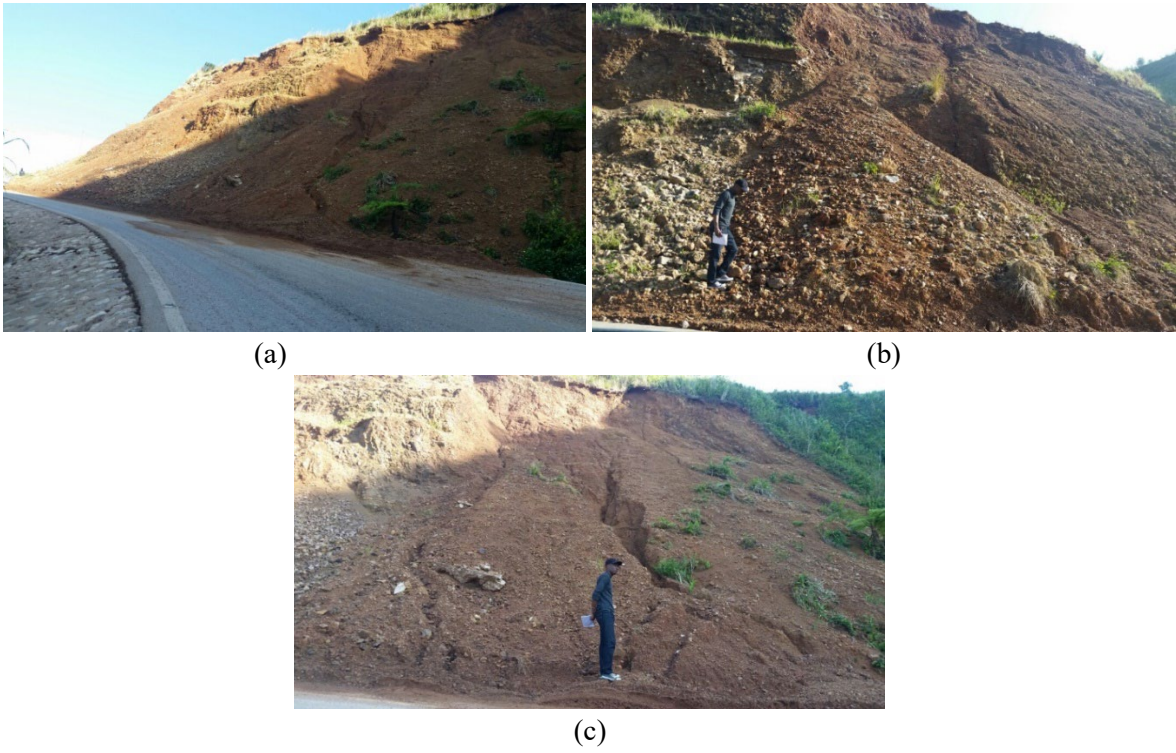


**Figure 7.45.** Landslide along RN7 (Lat: 18.4053372, Lon: -73.8777936).

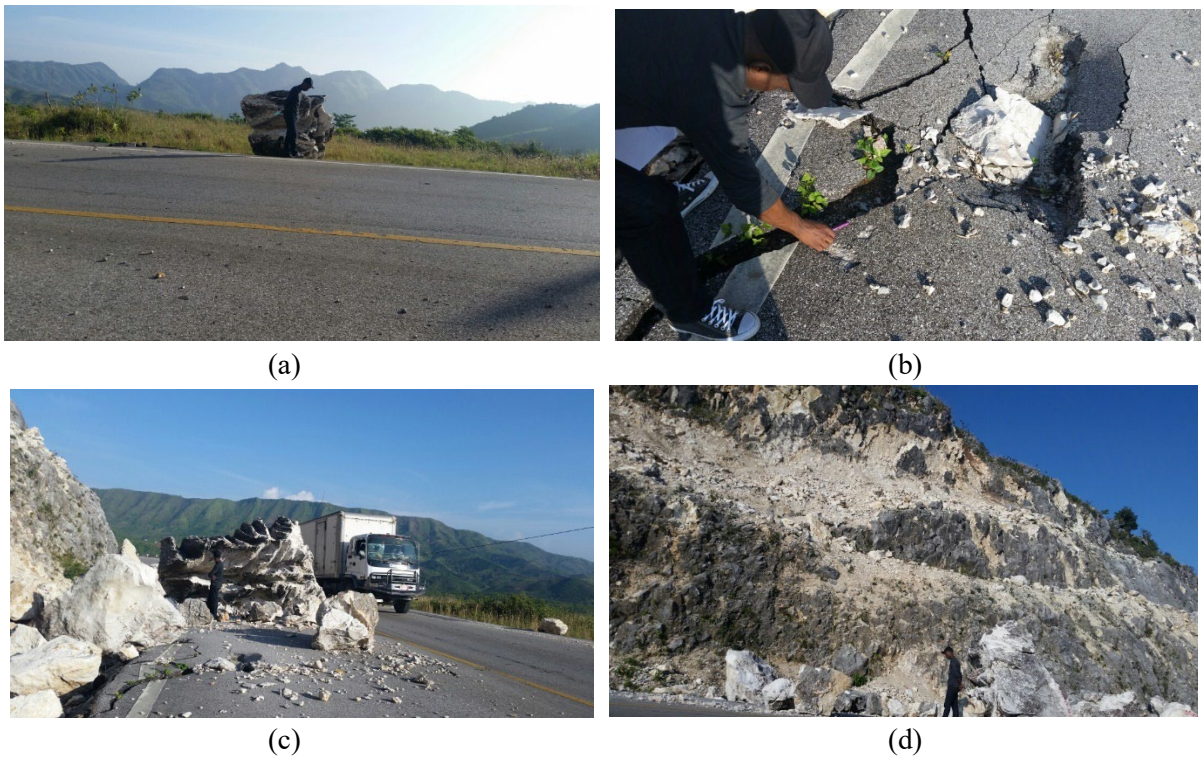


**Figure 7.46.** Rockfall along RN7 (Lat: 18.407487, Lon: -73.8794692).



**Figure 7.47.** Landslide with boulder debris along RN7 (Lat: 18.4072403, Lon: -73.8819915).



**Figure 7.48.** Rockfall along RN7 (Lat: 18.4073275, Lon: -73.8825593).



**Figure 7.49.** Rockfall along RN7 (Lat: 18.4082712, Lon: -73.8832756).

Fig. 7.50 shows the locations of additional landslides and rockfalls near Duchity. Other roadside slope failures containing notable amounts of boulder debris are shown in Figs. 7.51-7.53. These roadside slope failures are judged to be recent due to the fact that they intersected RN7. Fig. 7.54 shows a smaller rockfall occurring adjacent to RN7. Figs. 7.55 and 7.56 show a large slope failure above Riviere Glace near RN7. The debris from this slope was likely removed by the river by the time the GEER team arrived. The satellite imagery in Fig. 7.57 shows that this slope failure was non-existent prior to the August 14 earthquake.

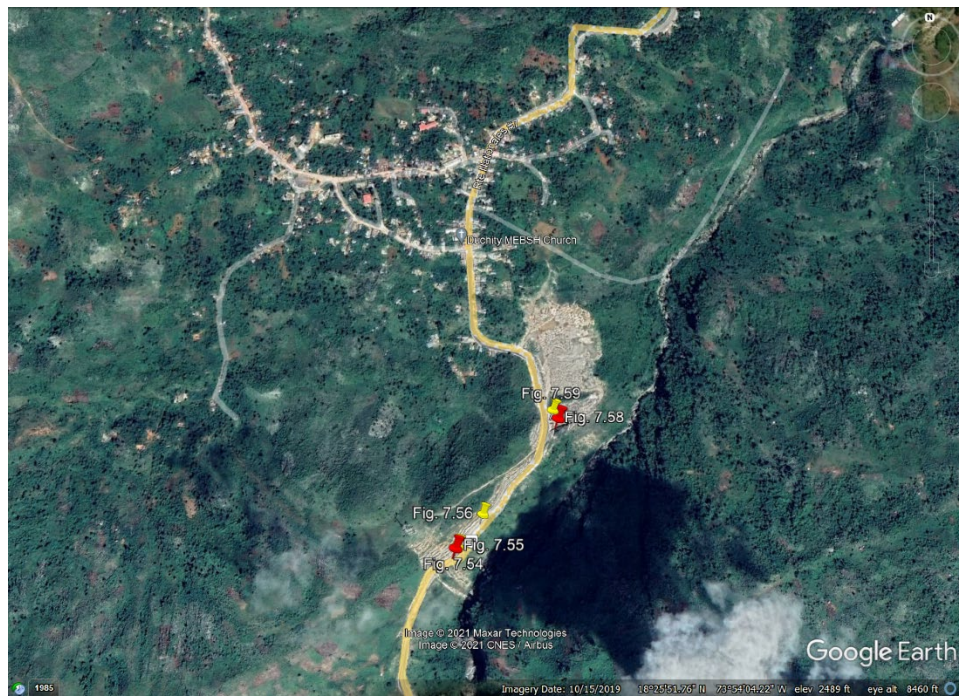


**Figure 7.50.** Locations of landslides and rockfalls along RN7 (courtesy of Google Earth). Imagery date October 15, 2019.



**Figure 7.51.** Slope failure along RN7 (Lat: 18.4166156, Lon: -73.9020873).

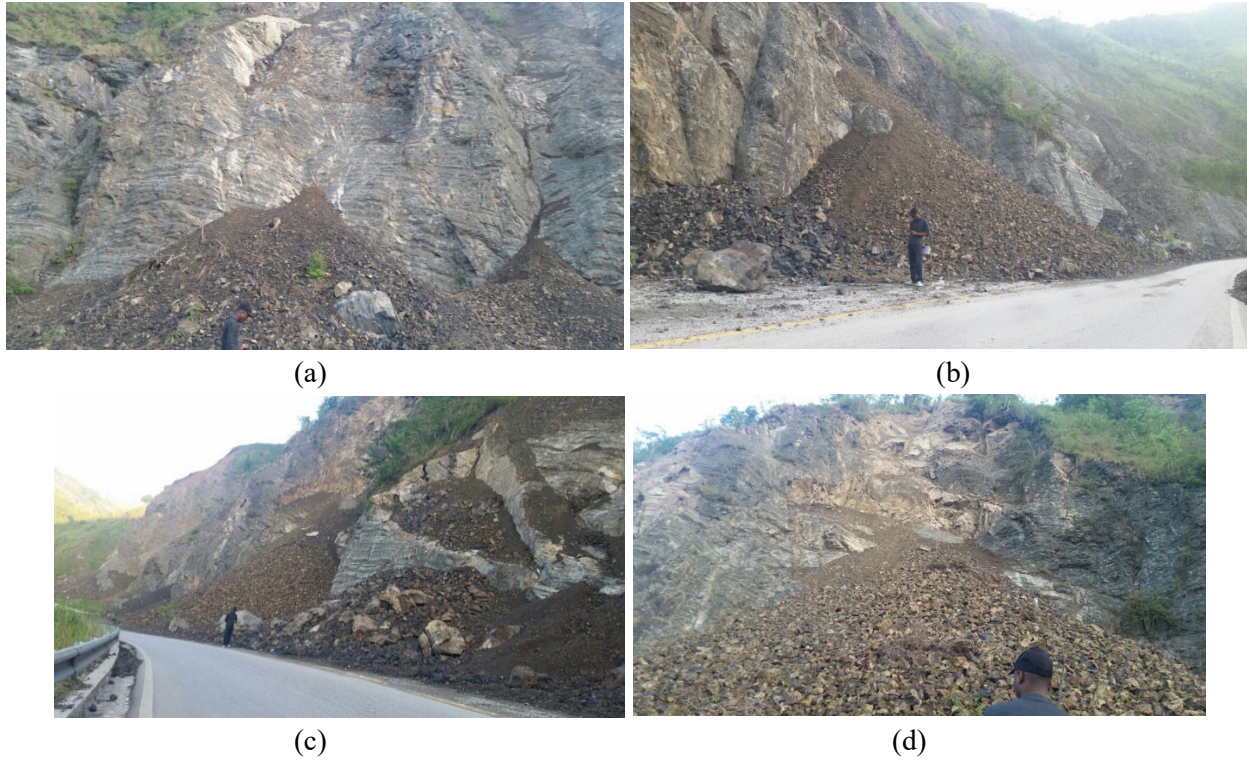


**Figure 7.52.** Slope failure along RN7 (Lat: 18.418817, Lon: -73.9027543).



**Figure 7.53.** Debris flow on RN7 (Lat: 18.4189306, Lon: -73.903528)



(a)

(b)

**Figure 7.54.** Smaller rockfall along RN7 (Lat: 18.427099, Lon: -73.9020971).



(a)

(b)

**Figure 7.55.** Landslide above Riviere Glace (Lat: 18.4271578, Lon: -73.9020508).



**Figure 7.56.** Landslide above Riviere Glace (Lat: 18.4277291, Lon: -73.9014994).

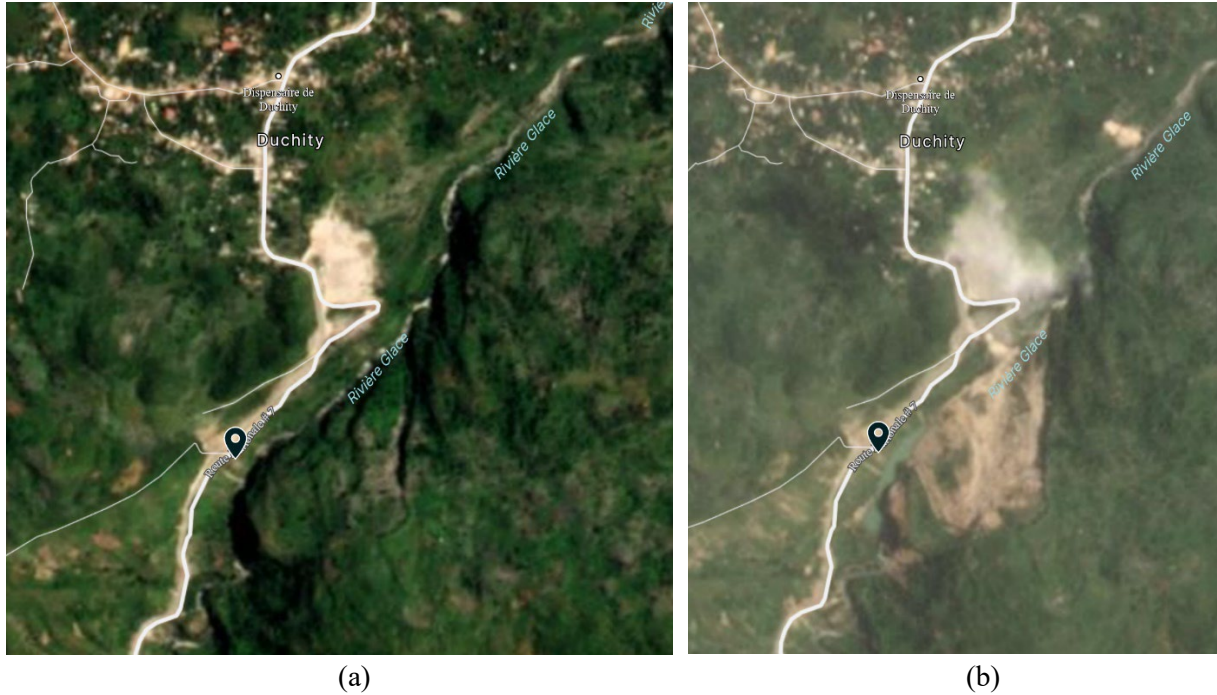


**Figure 7.57.** Satellite imagery for landslide shown in Figs. 7.29 and 7.30 (courtesy of Planet Labs, planet.com). Marker shown is where the photos in Fig. 7.29 were taken. (a) August 10, 2021. (b) August 30, 2021.

Further up RN7, a rock fall was observed as shown in Fig. 7.58. This rockfall is judged to be recent due to the exposure of un-weathered rock on a separate face from darker, weathered rock. The last landslide documented by the GEER team along RN7 is shown in Fig. 7.59. This landslide appears in satellite imagery taken before the August 14 earthquake, so it is deemed to not have resulted from the earthquake. Whether or not the August 14 reactivated this landslide is unclear. Three more rockfall locations were observed north of La Source, as shown in Fig. 7.60. Images of these rockfalls are shown in Figs. 7.61-7.63.



**Figure 7.58.** Possible failure of rockface along RN7 (Lat: 18.429466, Lon: -73.8998361).



**Figure 7.59.** Possible landslide with boulder debris that may have occurred sometime prior to the August 14 earthquake, judging based on satellite imagery (Lat: 18.429649, Lon: -73.899932).

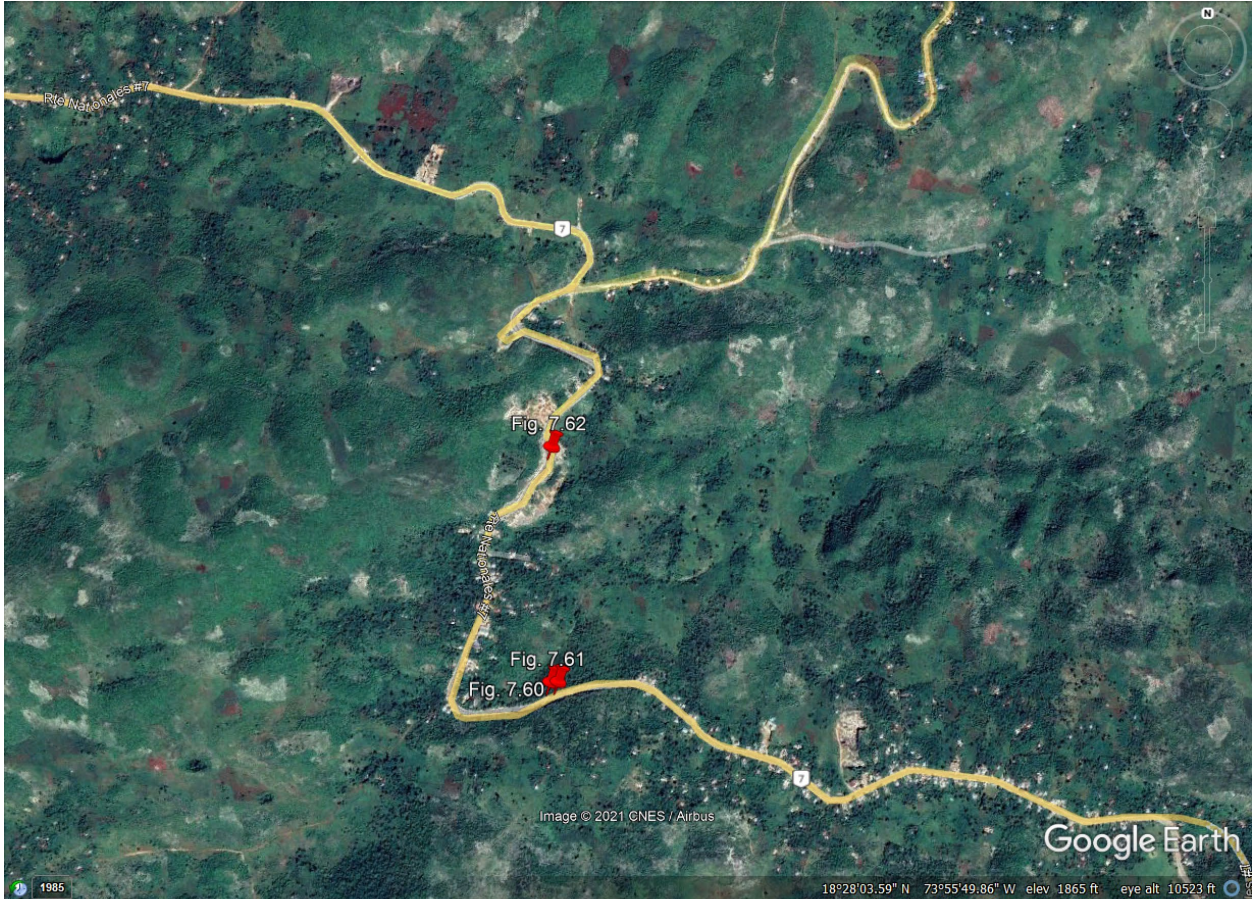


**Figure 7.60.** Locations of rockfalls observed along RN7 (courtesy of Google Earth). Imagery date October 15, 2019.



**Figure 7.61.** Rockslide along RN7 (Lat: 18.456184, Lon: -73.919748).



**Figure 7.62.** Rockslide along RN7 (Lat: 18.4561665, Lon: -73.9199208).



(a)



(b)



(c)

**Figure 7.63.** Rockfall along RN7 (Lat: 18.46123, Lon: -73.919987).

The locations of the northernmost documented rockfalls are shown in Fig. 7.64 between Joly Guirbert and Pestel. Figs. 7.65-7.68 show the images of these landslides. Figs. 7.66-7.68 all occur in close proximity to each other along Highway 218 in Pestel.

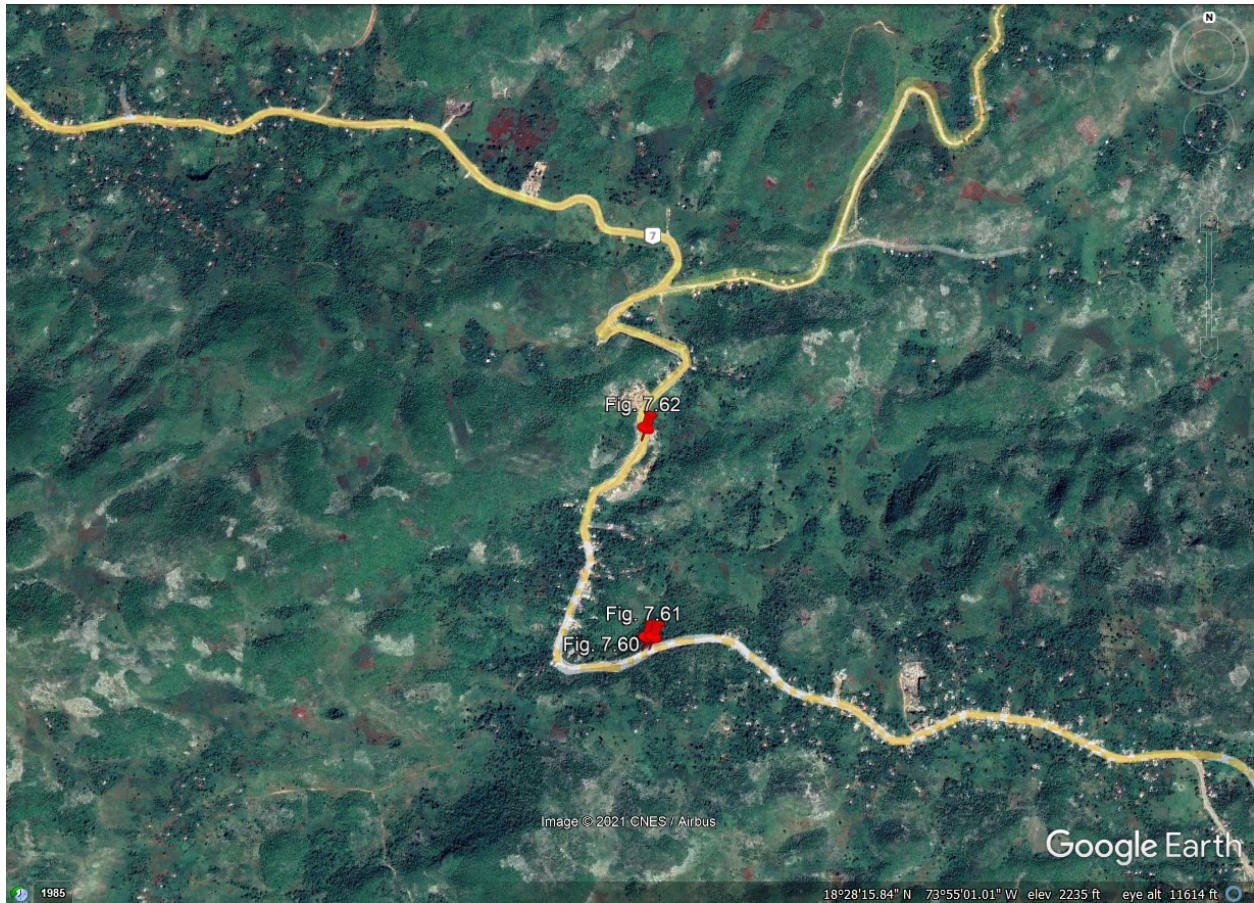


**Figure 7.64.** Northernmost locations of rockfalls documented by the GEER Team (courtesy of Google Earth). Imagery date October 15, 2019.



**Figure 7.65.** Rockfall between Joly Guirbert and Nan Dance (Lat: 18.5009437, Lon: -73.7815141).



**Figure 7.66.** Rockfall along Highway 218 near Pestel (Lat: 18.5323424, Lon: -73.7988606)



(a)



(b)

**Figure 7.67.** Rockfall along Highway 218 near Pestel (Lat: 18.5326725, Lon: -73.7988475).



(a)



(b)

**Figure 7.68.** Rockfall along Highway 218 near Pestel (Lat: 18.5371693, Lon: -73.8009462).

Additional GEER team members documented the slope failures shown in Figs. 7.70-7.72 on August 23, 2021. Fig. 7.69 shows the locations of these photos in Nippes.

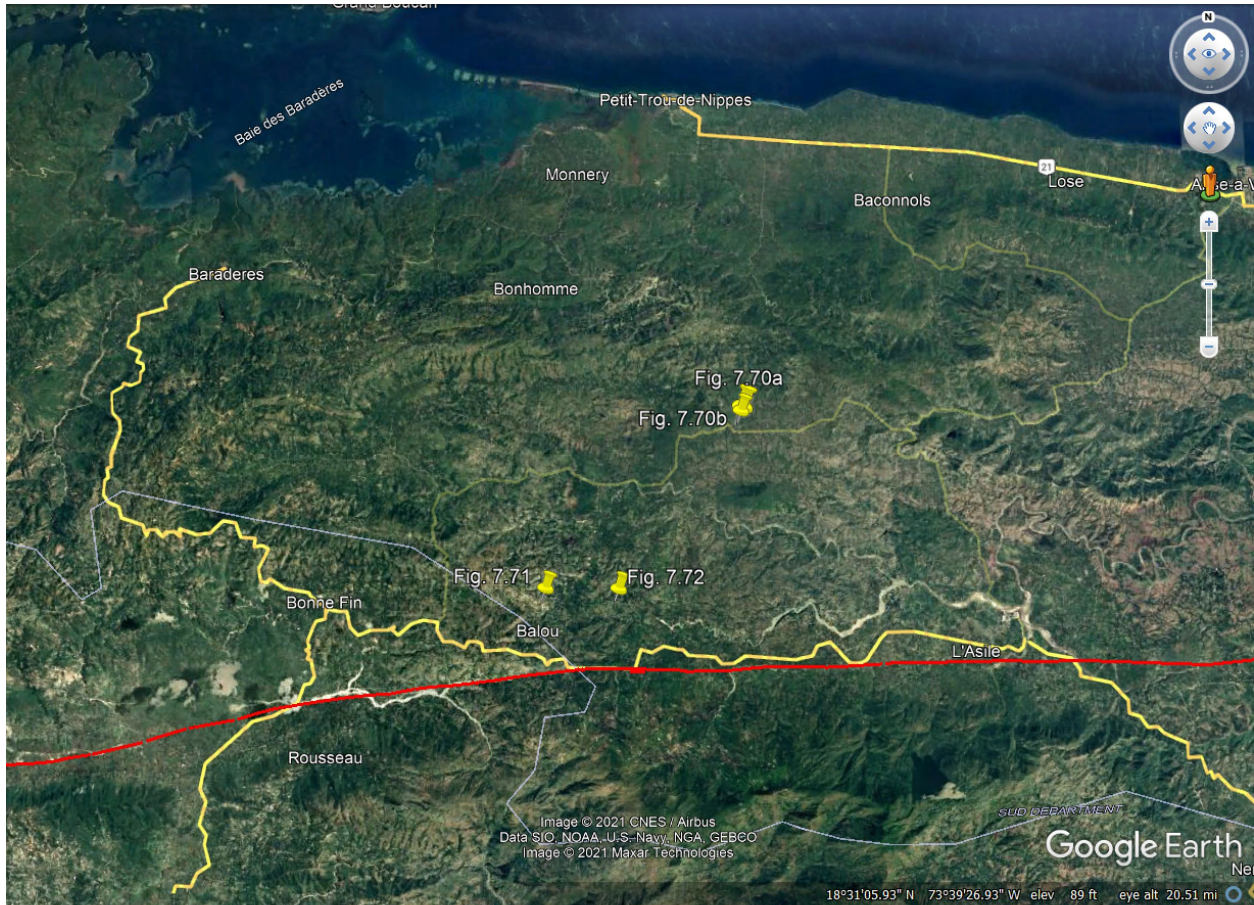


**Figure 7.69.** Locations of slope failures observed in Nippes on September 23, 2021. Courtesy of Google Earth.



**Figure 7.70.** Toppling slope failure in Nippes. (a) Lat: 18.43791138, Lon: -73.49213398. (b) Lat: 18.437773, Lon: -73.4922458. Photos taken September 23, 2021.



**Figure 7.71.** Slope failure in Nippes. (Lat: 18.39118189, Lon: -73.54879741). Photo taken September 23, 2021.

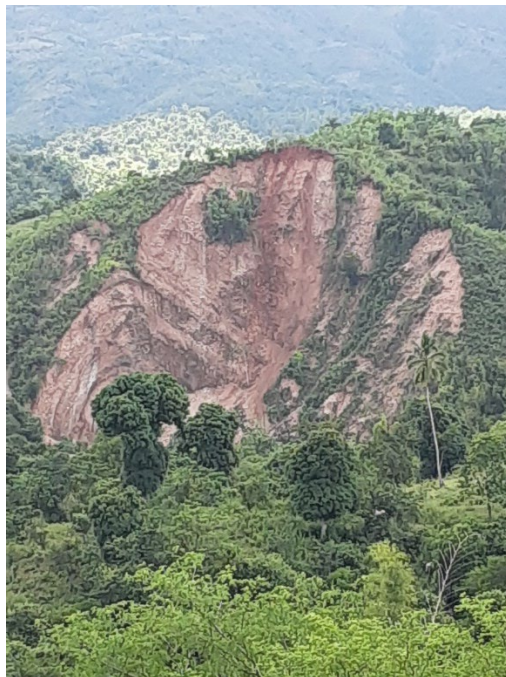


**Figure 7.72.** Slope failure in Nippes. (Lat: 18.3905122, Lon: -73.5280873). Photo taken September 23, 2021.

Dr. Newdeskarl Saint Fleur documented rockfalls along the northern coast of the southern peninsula of Haiti on September 29, 2021. The locations of images are shown in Fig. 7.73. Observations of rockfalls are shown in Figs. 7.74-79.

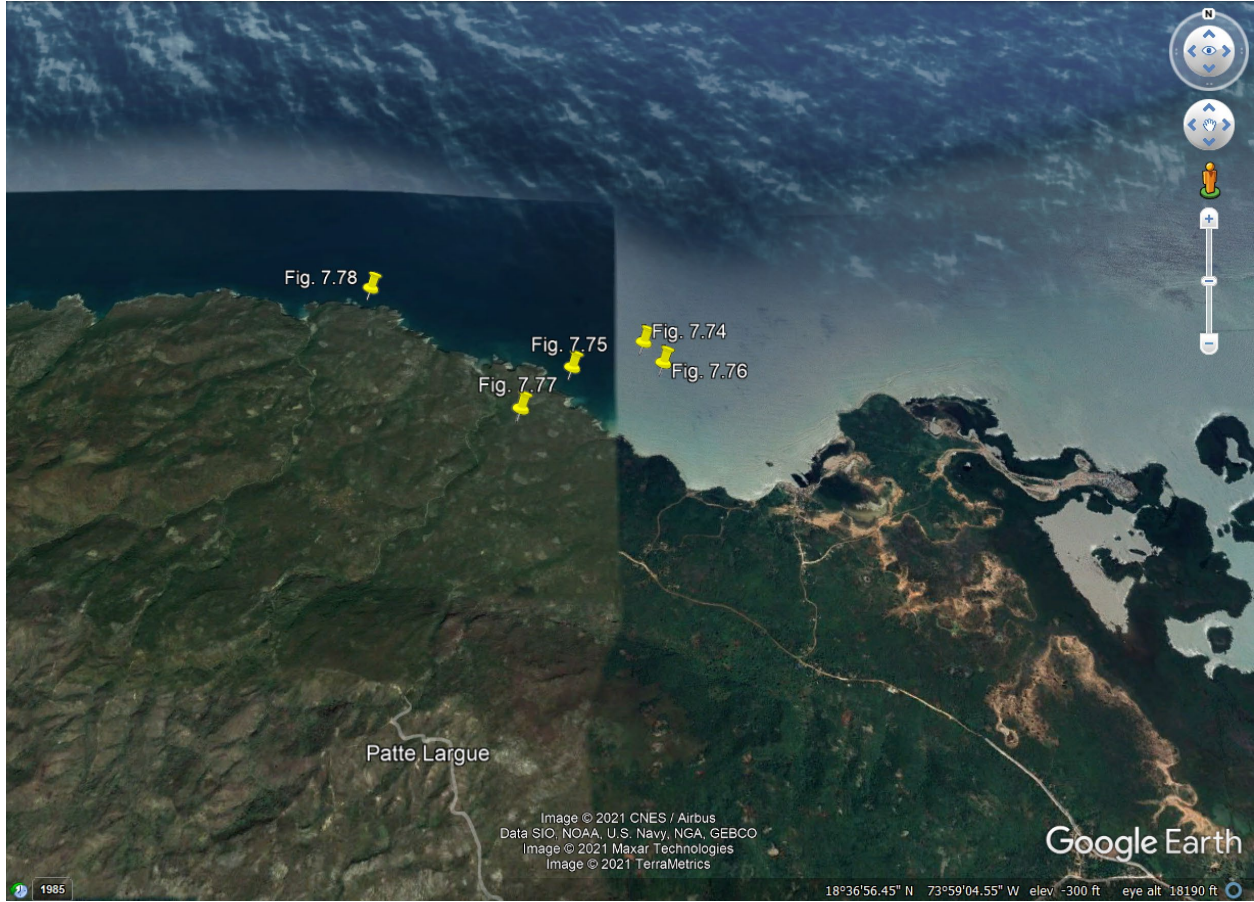


**Figure 7.73.** Locations of rockfalls observed along the northern coast of the southern peninsula of Haiti on September 29, 2021. Courtesy of Google Earth.



**Figure 7.74.** Rockfall along northern coast of southern peninsula of Haiti (Lat: 18.59722, Lon: -73.94528). Photo taken September 29, 2021 courtesy of Dr. Newdeskarl Saint Fleur.



**Figure 7.75.** Rockfall along northern coast of southern peninsula of Haiti (Lat: 18.59556, Lon: -73.94944). Photo taken September 29, 2021, courtesy of Dr. Newdeskarl Saint Fleur.



**Figure 7.76.** Rockfall along northern coast of southern peninsula of Haiti (Lat: 18.59583, Lon: -73.94417). Photo taken September 29, 2021, courtesy of Dr. Newdeskarl Saint Fleur.



**Figure 7.77.** Rockfall along northern coast of southern peninsula of Haiti (Lat: 18.5925, Lon: -73.95222). Photo taken September 29, 2021, courtesy of Dr. Newdeskarl Saint Fleur.



**Figure 7.78.** Rockfall along northern coast of southern peninsula of Haiti (Lat: 18.60111, Lon: -73.96167). Photo taken September 29, 2021, courtesy of Dr. Newdeskarl Saint Fleur.



**Figure 7.79.** Rockfall along northern coast of southern peninsula of Haiti (Lat: 18.62389, Lon: - 73.79583). Photo taken September 29, 2021, courtesy of Dr. Newdeskarl Saint Fleur.

### **7.3. Liquefaction and Cyclic Softening**

Evidence of liquefaction was difficult to document after the August 14<sup>th</sup> earthquake, because most of the evidence was likely erased by Tropical Storm Grace two days after the earthquake. Fig. 7.80 shows regions of high liquefaction susceptibility, which helped guide the GEER Team towards locations of interest. In particular, the GEER Team identified specific locations where liquefaction manifestation was likely based on reports of local residents in Pestel. These locations are shown in Fig. 7.81. It is possible that some of the slope failures discussed previously in Section 7.1 along the EPGF were also due to cyclic softening resulting in lateral spreading.

Fig. 7.82 shows images from a neighborhood in Pestel in which residents informed the GEER team that they saw water and mud rising through the cracks in the ground during the earthquake. Liquefaction is possible and likely in this region because the ground is saturated with water near the coast and the houses are built upon alluvium. The cracks also appeared to have been filled with alluvium after the earthquake.

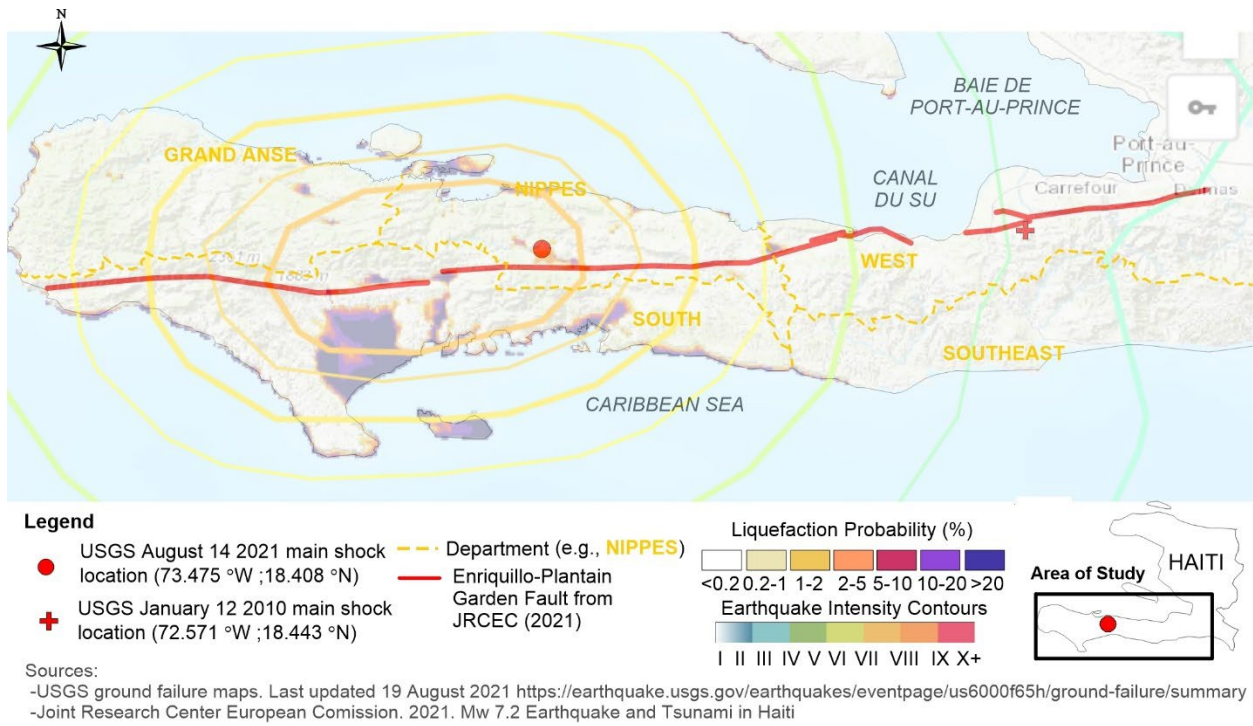


**Figure 7.80.** Liquefaction susceptibility base map.

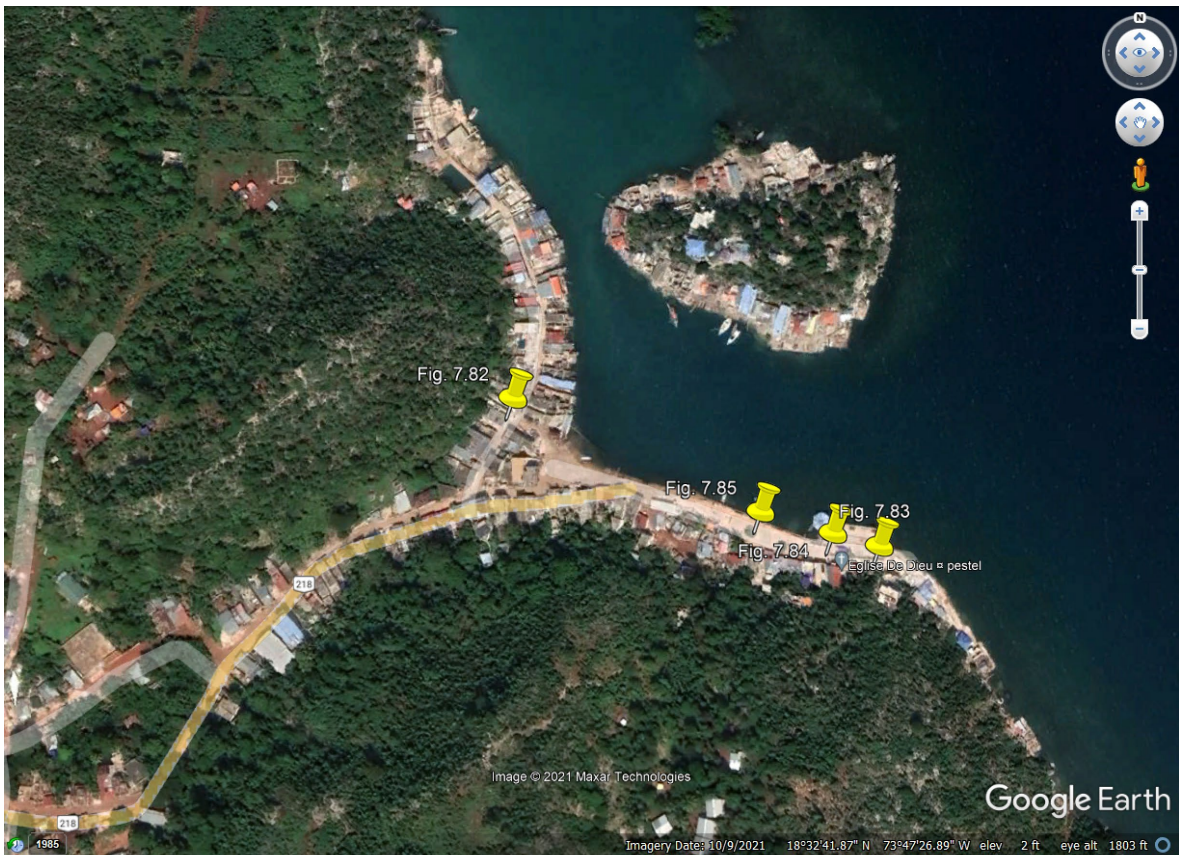


**Figure 7.81.** Locations of liquefaction observation by the in-ground GEER team.



**Figure 7.82.** Reported observations of liquefaction during the August 14<sup>th</sup> Nippes Earthquake (Lat: 18.5435502, Lon: -73.7921043).

Figs. 7.83 through 7.85 show cracking in concrete adjacent to the Pestel coast. The exact cause of this damage is unclear, but from the images it appears similar to damage to port facilities due to liquefaction and lateral spreading in Port-au-Prince from the 2010 Haiti earthquake.



**Figure 7.83.** Ground cracking near the coast in Pestel (Lat: 18.5422912, Lon: -73.7904188).



**Figure 7.84.** Ground cracking near the coast in Pestel (Lat: 18.5423509, Lon: -73.7906552).



**Figure 7.85.** Ground cracking near the coast in Pestel (Lat: 18.5424493, Lon: -73.7910169).

Additional observations of possible liquefaction-related damage were made via drone imagery (courtesy of Kate Allstadt, USGS). Fig. 7.86 shows the locations of possible liquefaction-induced damage in Les Cayes, and Figs. 7.87-7.96 show the associated drone imagery. As seen in Fig. 7.80, Les Cayes is a region of very high liquefaction susceptibility, most likely due to it being a coastal city situated on an alluvial plain. Fig. 7.97 shows an additional observation of possible lateral spreading further northeast in Cavaillon.



**Figure 7.86.** Drone observations of liquefaction in Les Cayes (courtesy of Google Earth).



**Figure 7.87.** Coast and slope damage near south Les Cayes: (a) before the earthquake; (b) after the earthquake. Coordinates: 18.181111, -73.758611. Images courtesy of OpenstreetMap (Pierre Béland, <https://pierzen.dev.openstreetmap.org/>).



**Figure 7.88.** Coastal damage and possible evidence of liquefaction-induced lateral spreading in south Les Cayes. Coordinates: 18.189722, -73.748333. Images courtesy of OpenstreetMap (Pierre Béland, <https://pierzen.dev.openstreetmap.org/>).

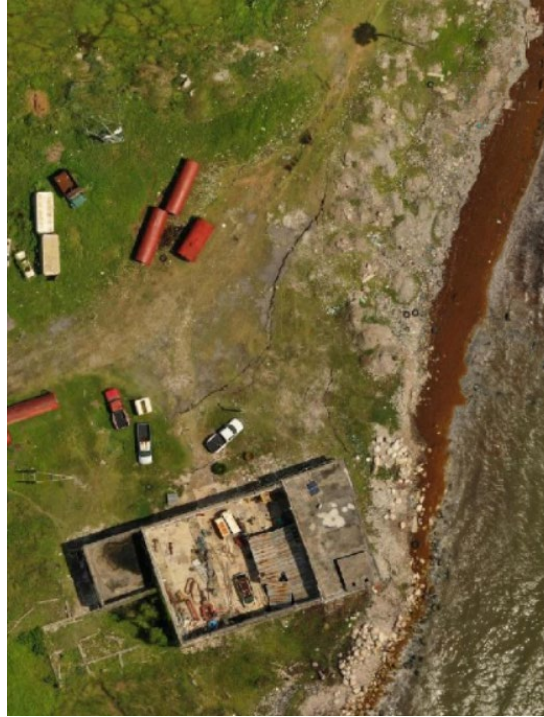


**Figure 7.89.** Coastal damage and possible evidence of liquefaction-induced lateral spreading in south Les Cayes. Coordinates: 18.188056, -73.750556. Images courtesy of OpenstreetMap (Pierre Béland, <https://pierzen.dev.openstreetmap.org/>).



**Figure 7.90.** Possible lateral spreading in Les Cayes. Coordinates: 18.198611, -73.745833. Images courtesy of OpenstreetMap (Pierre Béland, <https://pierzen.dev.openstreetmap.org/>).



**Figure 7.91.** Damage and possible evidence of liquefaction-induced lateral spreading near river (Ravine du Sud) in Les Cayes. Coordinates: 18.195556, -73.759722. Images courtesy of OpenstreetMap (Pierre Béland, <https://pierzen.dev.openstreetmap.org/>).

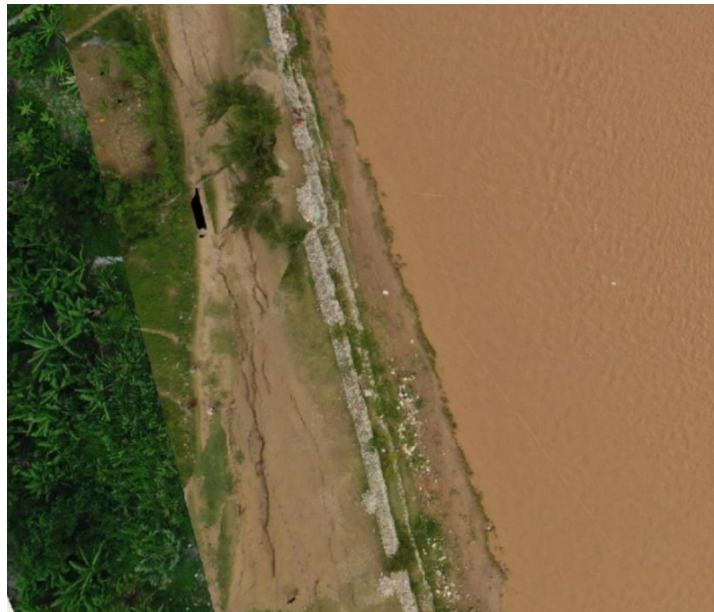


**Figure 7.92.** Damage and possible lateral spreading near river (Ravine du Sud) in Les Cayes. Coordinates: 18.195 -73.760278. Images courtesy of OpenstreetMap (Pierre Béland, <https://pierzen.dev.openstreetmap.org/>).



**Figure 7.93.** Damage and possible lateral spreading near river (Ravine du Sud) in Les Cayes. Coordinates: 18.195 -73.760278. Images courtesy of OpenstreetMap (Pierre Béland, <https://pierzen.dev.openstreetmap.org/>).



**Figure 7.94.** Damage and possible lateral spreading near river (Ravine du Sud) in Les Cayes. Coordinates: 18.196389, -73.760833. Images courtesy of OpenstreetMap (Pierre Béland, <https://pierzen.dev.openstreetmap.org/>).



**Figure 7.95.** Damage and possible lateral spreading near river (Madan Samdi) in Les Cayes. Coordinates: 18.218333, -73.759444. Images courtesy of OpenstreetMap (Pierre Béland, <https://pierzen.dev.openstreetmap.org/>).



**Figure 7.96.** Possible damage of water facility near river (Riviere L'Islet) in Les Cayes. Coordinates: 18.215278, -73.745833. Images courtesy of OpenstreetMap (Pierre Béland, <https://pierzen.dev.openstreetmap.org/>).



**Figure 7.97.** Damage and possible lateral spreading near river (Riviere de Cavaillon) in Cavaillon. Coordinates: 18.299167, -73.655833. Images courtesy of OpenstreetMap (Pierre Béland, <https://pierzen.dev.openstreetmap.org/>).

#### **7.4. Performance of Roads, Bridges, Retaining Structures, and other Infrastructure**

The GEER team documented locations of damage to retaining structures and pavement along RN7. The locations of damage observations are shown in Fig. 7.98. Figs. 7.99-7.101 show retaining wall damage on RN7. The common observation at each of these locations is that the retaining walls were impacted by boulder debris from rockfalls. This occurrence was also observed in Fig. 7.43. Fig. 7.102 shows another retaining wall failure in Bonne Fin, approximately 2.7 km north of the EPGF.

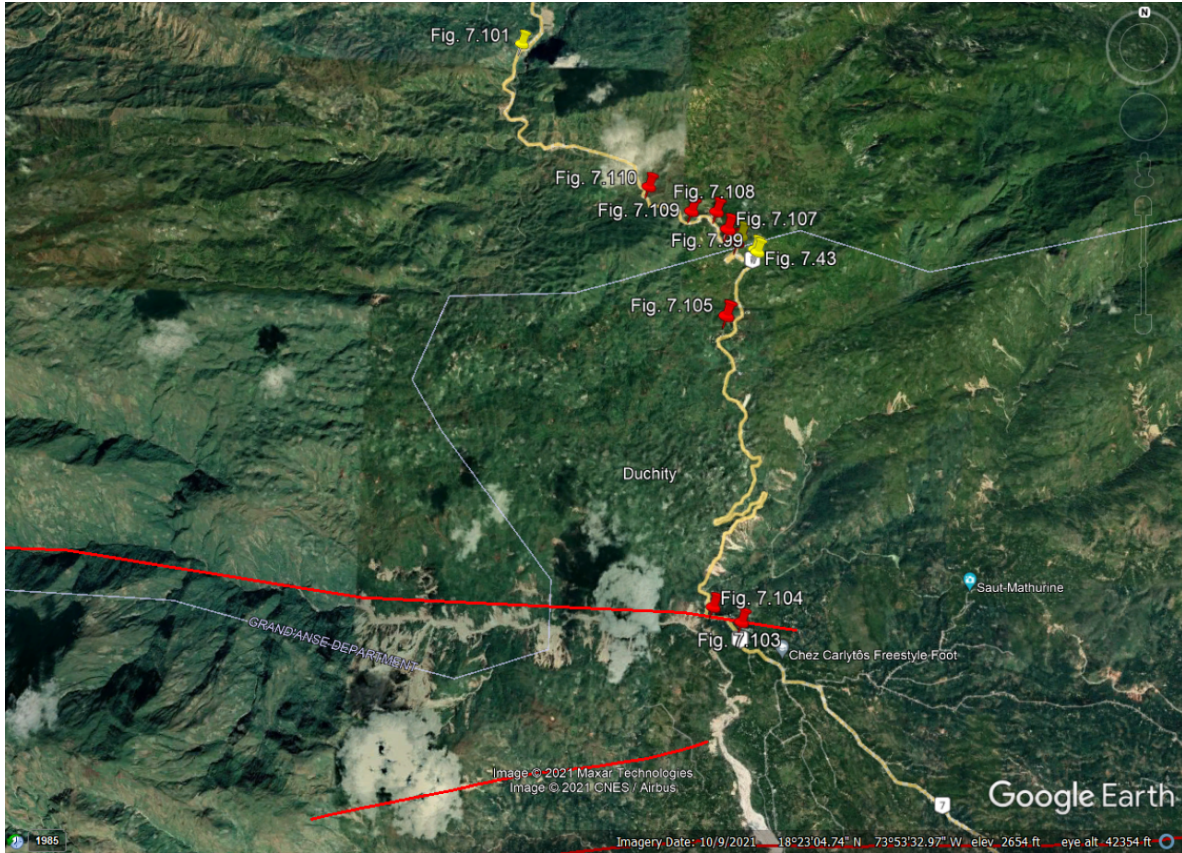


**Figure 7.98.** Locations of damage to roads and highways (red pins) and retaining structures (yellow pins). Courtesy of Google Earth.



**Figure 7.99.** Retaining wall damage along RN7 (Lat: 18.403283, Lon: -73.8750032).



(a)

(b)



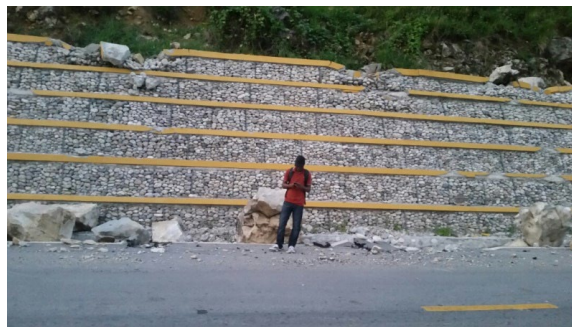
(c)

**Figure 7.100.** Retaining wall damage along RN7 (Lat: 18.4046922, Lon: -73.8766514).



(a)

(b)



(c)

**Figure 7.101.** Retaining wall damage along RN7 (Lat: 18.4262836, Lon: -73.9027722).



**Figure 7.102.** Retaining wall damage 2 km north of Enriquillo-Plaintain Garden Fault in Bonne Fin (Lat: 18.38944, Lon: -73.61028).

Damage to the highway pavement of RN7 is shown in Figs. 7.103 -7.110. Much of the cracking in the pavement appears to have been caused by slope instability, given that the cracking appears skewed towards the downslope side of the highway. The cracks in the slope shown in Fig. 7.109 provide further evidence of slope failure. Fig. 7.110 shows that impact from rock debris was another source of damage to RN7.



(a)

(b)



(c)

**Figure 7.103.** Pavement damage on RN7. (Lat: 18.3631332, Lon: -73.8753663).



(a)



(b)



(c)



(d)



(e)



(f)



(g)



(h)



(i)



(j)



(k)

**Figure 7.104.** Pavement damage on RN7 (Lat: 18.3646397, Lon: -73.8785984).



**Figure 7.105.** Pavement damage on RN7 (Lat: 18.39580833, Lon: -73.87810833). Photo taken September 29, 2021.

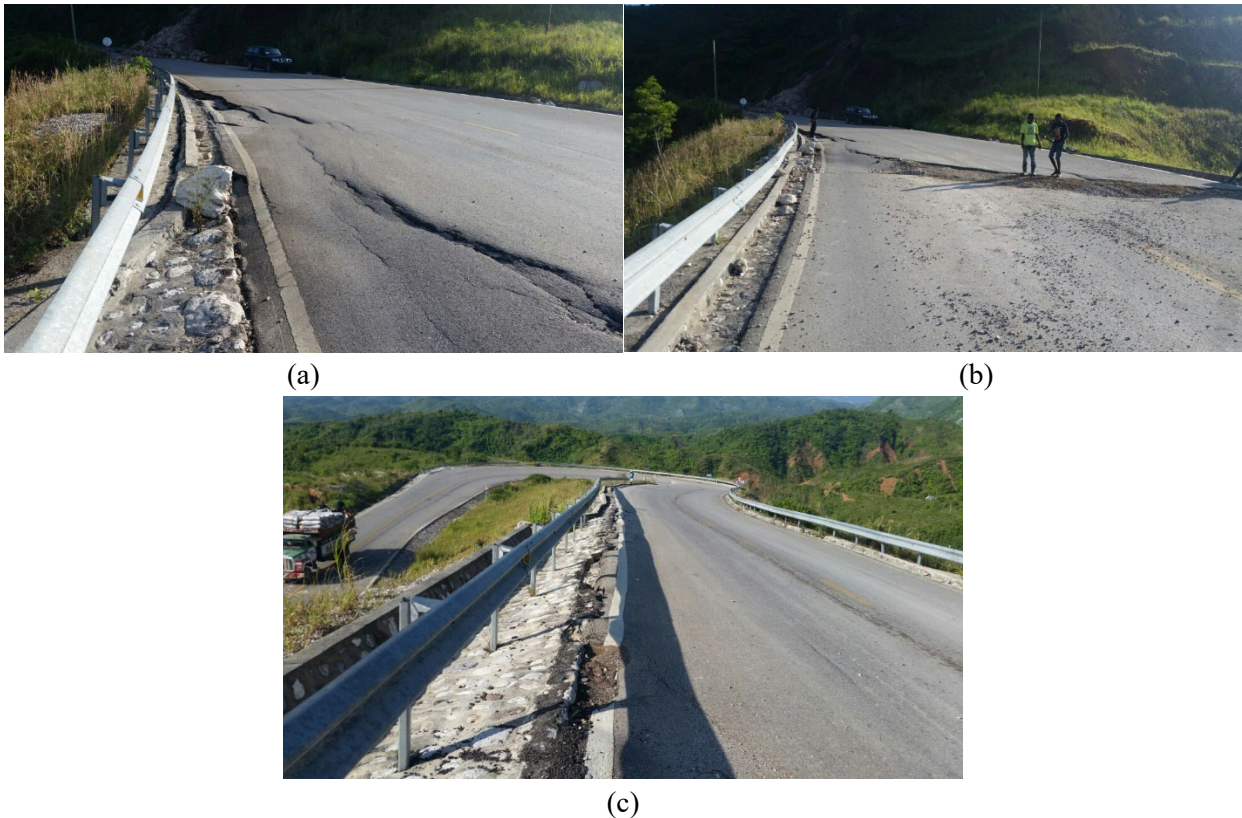


**Figure 7.106.** Pavement damage on RN7 (Lat: 18.4039901, Lon: -73.8770421).



**Figure 7.107.** Pavement damage on RN7 (Lat: 18.40532455, Lon: -73.87818961). Photo taken September 29, 2021.



(a)



(b)



(c)



(d)



(e)

**Figure 7.108.** Pavement damage on RN7 (Lat: 18.4073805, Lon: -73.8794886).



(a)



(b)



(c)



(d)



(e)

**Figure 7.109.** Road embankment damage on RN7 (Lat: 18.4073147, Lon: -73.8823895).

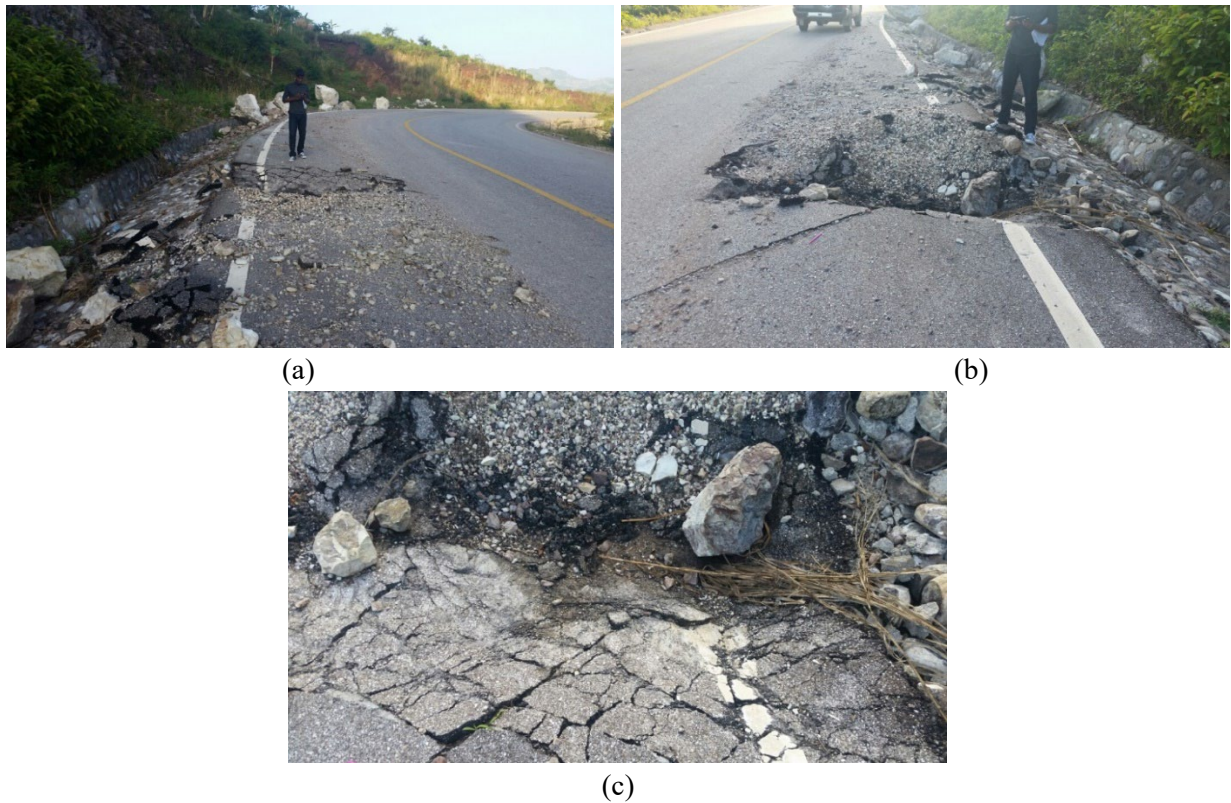


**Figure 7.110.** Pavement damage on RN7 (Lat: 18.410061, Lon: -73.8873537).

### **7.5. Damage to Building Structures due to Geotechnical Effects**

The GEER team documented two damaged 3-story buildings in Les Cayes, as shown in Figs. 7.111 and 7.112. The 3-story buildings were directly adjacent to single story shanty structures that appeared to have collapsed or were damaged, likely from the Nippes Earthquake and likely affected by structure-soil-structure interaction with such short spacings. More extensive structural damage has been identified and documented by StEER and others (e.g., Geo Hazards International) across the affected regions.



**Figure 7.111.** Damaged building in Les Cayes (Lat: 18.1944, Lon: -73.7456).



**Figure 7.112.** Damaged building in Les Cayes (Lat: 18.1956, Lon: -73.7456).

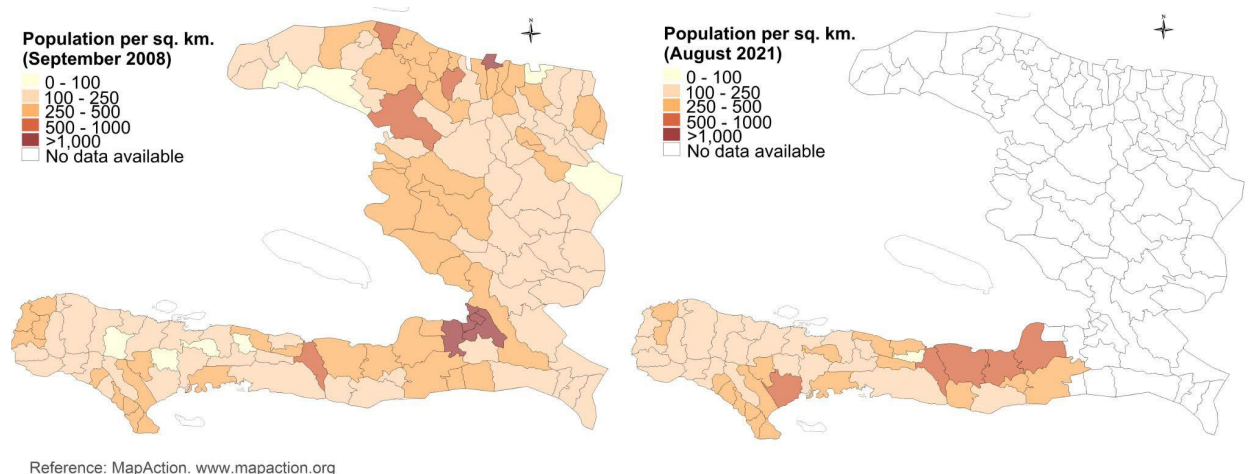
## **8 INTERSECTION OF SOCIAL AND ENGINEERING OBSERVATIONS**

In this chapter, we explore the intersection of different crises in Haiti since 2010, the social-political-economical effects of these crises, and a few specific engineering hazards from the 2021 Nippes earthquake (e.g., in terms of shaking intensity or the liquefaction hazard). The intersectional maps explored here depict the impact of pre-earthquake conditions on vulnerability of different populations and the resulting impact of the 2021 earthquake on their livelihood. In this preliminary investigation, we explore the following areas: Sud, Grand’Anse, and Nippes.

### **8.1. Pre-Earthquake Conditions**

The challenges that characterize Haiti as a fragile state have amplified in recent years. For instance, as previously detailed in the chapter on “developmental challenges”, nearly 33,000 victims of the 2010 earthquake still live in displacement camps, and over 300,000 have not received government assistance to resettle. Also, over 140,000 families displaced by Hurricane Matthew in 2016 have not secured a decent shelter to date. More currently, from January to August 2020, an estimated 944 intentional homicides, 124 kidnappings, and 159 deaths resulting from gang violence have been reported by the United Nations Integrated Office in Haiti (BINUH). At least 12,000 displacements that same year are attributed to gang violence and Hurricane Isaias.

The widespread deforestation, environmental pollution, and lack of access to clean water and sanitation have increased the risks for the most vulnerable communities. Reports from international organizations estimate that 33% (4 million) of the population faces food insecurity. The lack of affordable and good education, ongoing political unrest, and the covid-19 pandemic have prevented 70% of children from school during the 2019-2020 academic year. About half of school-age children are illiterate (HRW, 2020). Therefore, natural hazards and conflicts have both contributed to internal displacements in Haiti. The Internal Displacement Monitoring Centre (IDMC), established in 1998 as part of the Norwegian Refugee Council (NRC), reported an estimated 2.03 million new displacements linked to disasters in Haiti from 2008 to 2020 (IDMC, n.d.). According to the MapAction, the population density has increased since 2008, particularly in Les Cayes, Petit-Goave, Grand-Goave, and Leogane (Figure 8.1). The IDMC also reported an estimated 10,000 new displacements from conflict for 2019 and 2020 (Figure 8.2). These changes are expected to influence the population’s vulnerability to earthquake-induced failure of infrastructure, such as those induced by ground failure or other geotechnical and structural hazards.



Reference: MapAction. [www.mapaction.org](http://www.mapaction.org)  
**Figure 8.1.** Population density per commune in 2008 and 2021 in Haiti (source: Map Action, [www.mapaction.org](http://www.mapaction.org)).

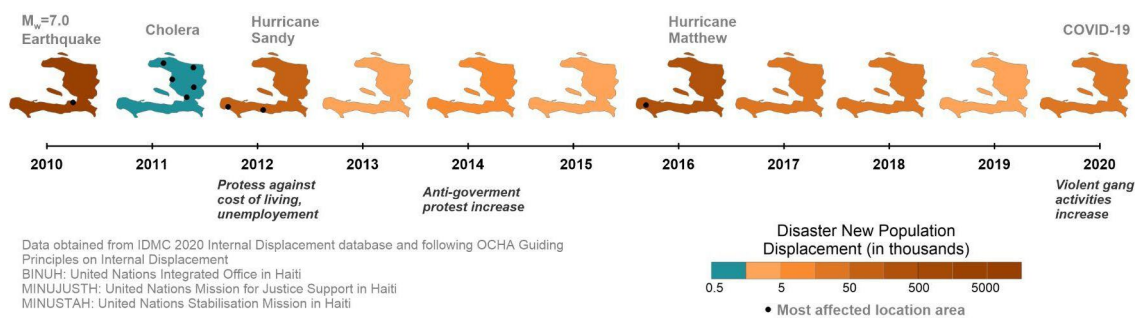


**Figure 8.2.** Social-political crises and natural disasters in Haiti since 2010, including the disaster new population displacements (sources noted in the legend).

## 8.2. Population Displacement following the Mw7.0, 2010 Earthquake

A few days after the January, 2010 earthquake in Haiti, the death toll reported by the government exceeded 230,000. The USAID reported more than 1,200,000 people displaced and about 3,000,000 affected (USAID 2010a). Nearly a month after the disaster, the United States Agency for International Development (USAID) estimated that over 500,000 had left Port-au Prince to other provinces within Haiti (USAID 2010b). The Grand'Anse and Southern regions were the second and third most popular destinations for many Haitians. Figure 8.3 shows the population movement following the 2010 earthquake and its intensity contours, which made a greater population exposed to the geotechnical and structural hazards of the 2021 earthquake, in view of proximity to the Nippes Earthquake epicenter, locations of surface fault rupture, greater shaking intensities, landslides, and liquefaction-prone coastal regions.

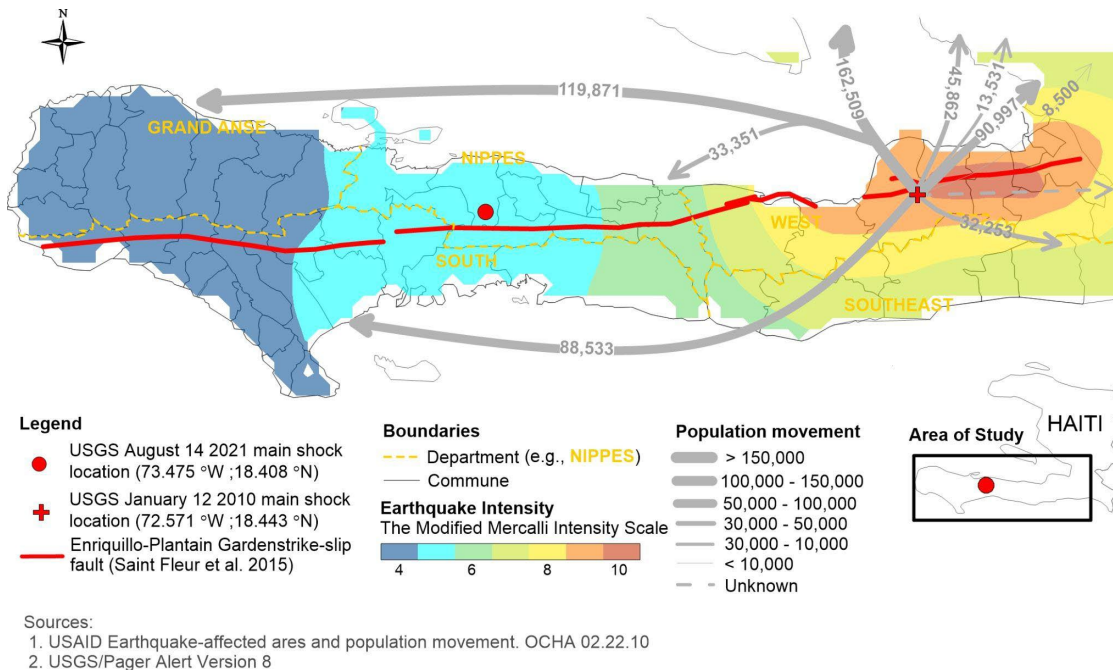


**Figure 8.3.** Map of population movements following the 2010 earthquake in Haiti (sources noted in the legend).

### 8.3. The 2012 Hurricane Sandy

Hurricane Sandy hit Haiti in October 2012. Heavy rains, strong winds, and flooding caused the death of 54 people and damage of thousands of houses and critical infrastructure (USAID 2013). Figure 8.4 shows the most flooded areas during the 2012 Hurricane Sandy (including some landslide areas and locations of maximum deaths). The majority of the damaged areas were identified in the four southern departments of Grand’Anse, Nippes, South, and Southeast (USAID 2013). The hurricane-induced damage to crops exceeded 67,000 hectares in southern departments, notably increasing food and economic insecurity. In addition, the hurricane-induced hazards (e.g., flooding, strong winds, and heavy rains) also resulted in great loss of livestock and fishing industries (USAID 2013). Most Haitian households in these regions were identified as the group with the lowest average annual income in 2015 (USAID 2015). The net outcome of these adverse impacts led to a displacement by about 19,000 people (USAID 2013).

The area flooded after Hurricane Sandy, particularly in Les Cayes, Mountain Pic Macaya, and L’Asile, typically experiencing a high flow period during May to October, according to the surface water map in Figure 4.7. In general, the high groundwater table may cause soil softening during seismic events, leading to possible earthquake-induced hazards associated with liquefaction of granular soils, cyclic softening of plastic soils, excessive lateral spread, and slope instability. Therefore, by looking at the flooded areas from prior case histories (e.g., Hurricane Sandy), we could identify those regions that are, in general, more prone to multiple hazards (e.g., hurricane and earthquake) in Haiti. This was particularly evident after the 2021 Nippes Earthquake. Most of

the damage from the 2021 earthquake (and partially the tropical storm that followed) related to soil liquefaction, lateral spreading, landslides, and rockfalls was reported from the three southern departments of South (Sud), Grand’Anse, and Nippes.

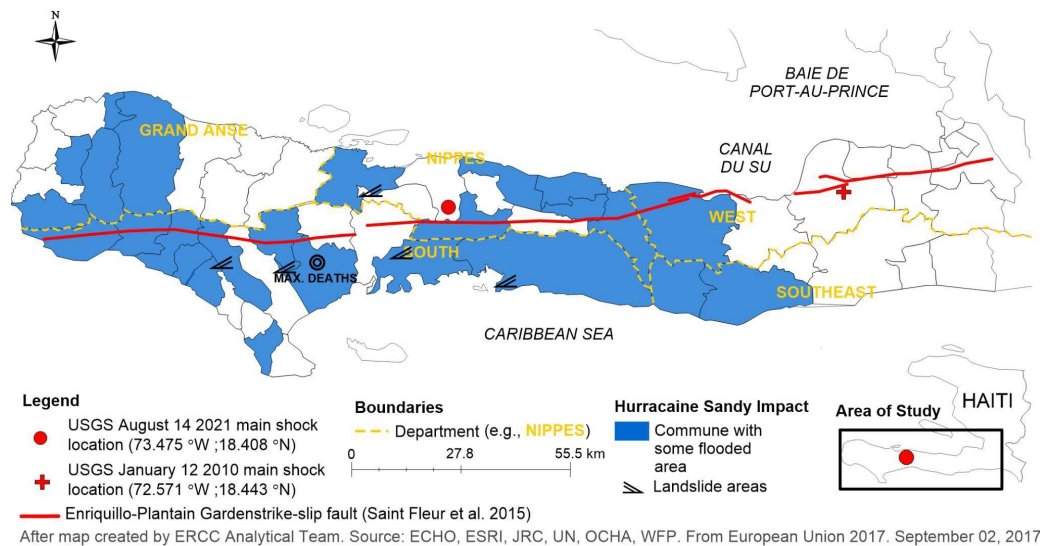


**Figure 8.4.** Map of flooded areas during the 2012 Hurricane Sandy, including some landslide areas and locations of maximum human casualty (sources noted in the legend).

#### 8.4. The 2016 Hurricane Matthew

Hurricane Matthew was the worst storm to strike Haiti in more than 50 years, bringing vast flooding and destruction in southern Haiti. Heavy rainfall, strong wind, and dangerous storm surge caused the death of 546 people (USAID 2017). More than 2.1 million people were affected, while approximately 925,000 people in Haiti required immediate food assistance (USAID 2017). Figure 9.5 shows the intersection map of the most affected areas during the 2016 Hurricane Matthew. This hurricane adversely affected crops and livestock, worsening household economic and nutrition security. The majority of the damaged area was identified in the three southern departments of Grand’Anse, Nippes, and Sud (USAID 2017), similar to the damaged areas during Hurricane Sandy. The hurricane-affected households in these departments were categorized as the group with the lowest average annual income in 2015 (USAID 2015).

Haiti is a high seismicity region that experiences landslides and hurricanes with heavy rainfall. Wdowinski and Tsukanov (2011) suggested that earthquakes in the tropical high seismic region were possibly triggered by rapid erosion induced by heavy rainfall due to typhoons or hurricanes. For example, in 2010, a magnitude 7.0 earthquake devastated Haiti only 18 months after four tropical cyclones (i.e., Fay, Gustav, Hanna, and Ike) hit Haiti. A similar observation was found in Taiwan. A subtropical island in a high seismicity area also experienced landslides and a large amount of precipitation. After Typhoon Morakot struck Taiwan in August 2009, Taiwan experienced the 2009, M=6.2, Nantou and 2010, M=6.4, Kaohsiung earthquakes in 3 and 7 months,

respectively. Wdowinski and Tsukanov (2011) used remote sensing observations, meshfree finite element modeling, and Coulomb failure stress analysis to identify the earthquake triggering process in high seismicity areas that experienced significant rainfall. Their results showed that the erosion induced by heavy rainfall (due to either typhoon or hurricane) reduced the stresses at the hypocentral depth, which eventually initiated rupture propagation, and hence the likelihood of earthquakes.

Similarly, the 2012 Hurricane Sandy and 2016 Hurricane Matthew were followed by the 2021 Nippes earthquake in the very same area (as shown in Figures 8.4 and 8.5) in Haiti. These observations may suggest a physical relationship between hurricane and earthquake in terms of timing and spatial distribution. Further research is needed to identify and support the general pattern of the interaction between earthquake and hurricane, to guide the mitigation of natural hazards in high seismicity regions like Haiti.

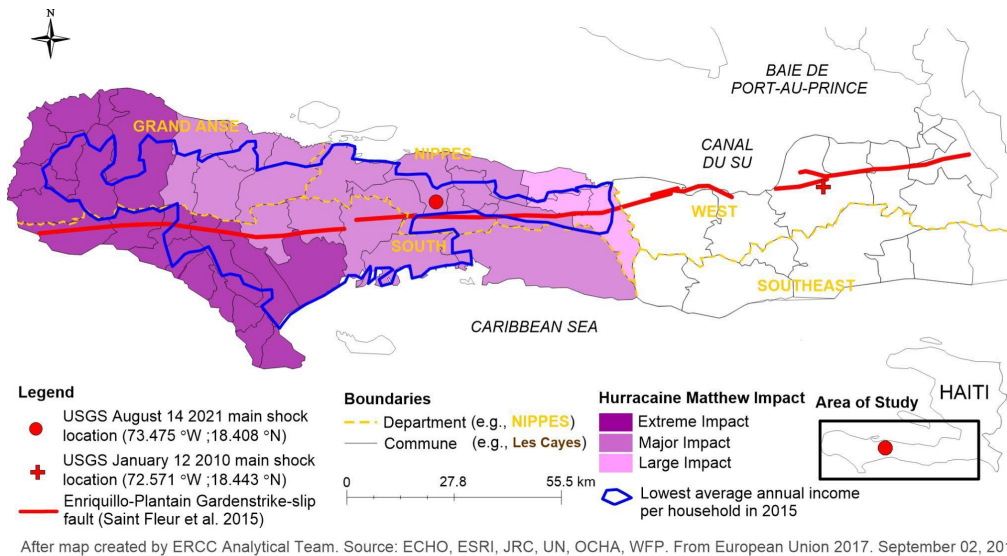


**Figure 8.5.** Map of affected areas during the 2016 Hurricane Matthew and the lowest average annual income from 2015 in the study region (sources noted in the legend).

### 8.5. The 2021 Mw7.2 Nippes Earthquake

Figure 8.6 shows the total population density per commune, the area with the lowest average annual income within the study region and the USGS liquefaction hazard map together with the 2021 earthquake intensity contours. The highest population density, the lowest income level, and the highest risk of soil liquefaction are shown to overlap in the South region, compromising the most vulnerable urban areas (e.g., Les Cayes). Notably the urban area of Les Cayes has been identified as the area most notably affected by the 2021 event, which has also been the victim of previous natural disasters, while simultaneously experiencing a population inflow since 2010. Similarly, Figure 8.7 shows the intersection between the landslide hazard maps and the lowest annual income. The USGS is rating the landslide risk as “orange” to indicate a significant area affected and significant population exposed.

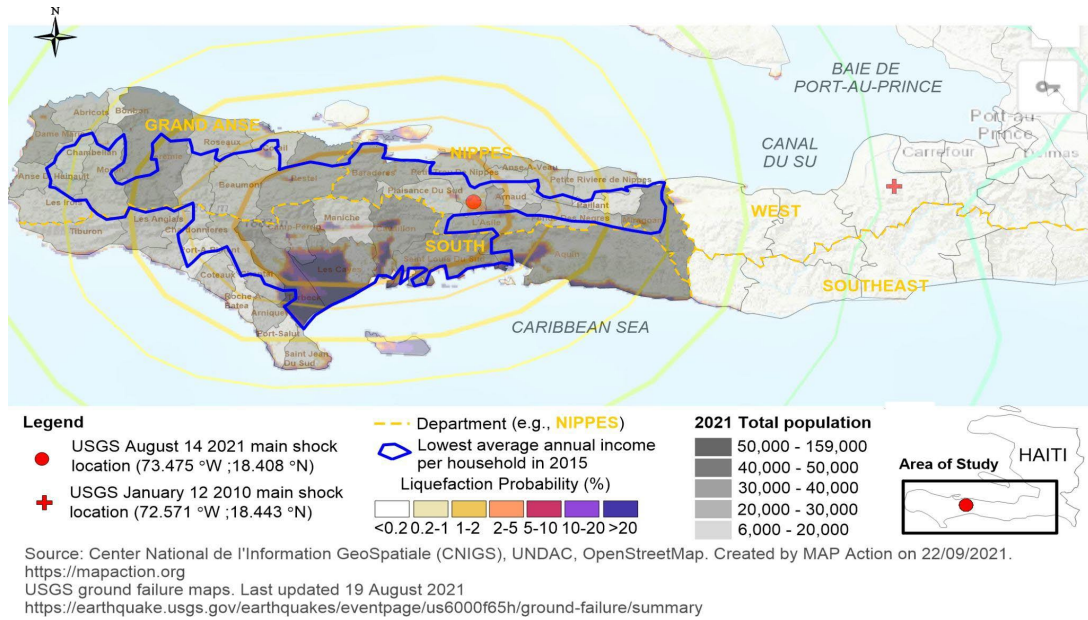


**Figure 8.6.** The USGS Liquefaction probability map and shaking intensity contours of the 2021 Nippes earthquake overlaid on the 2021 population map with the boundary of lowest average annual income within the study region in Haiti (sources noted in the legend).

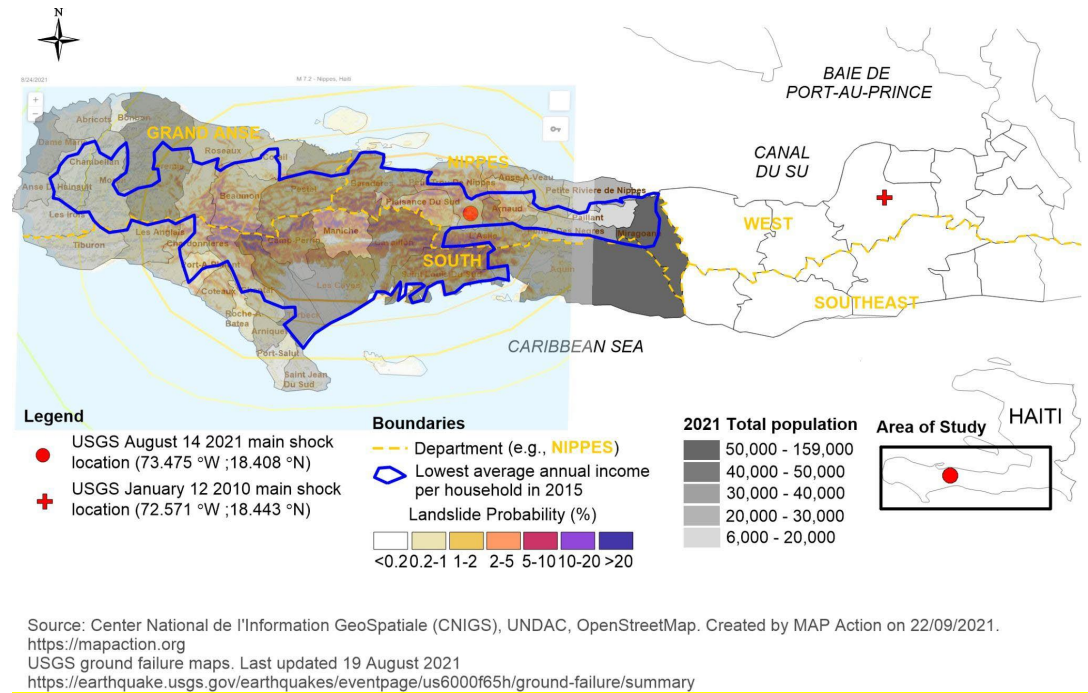


**Figure 8.7.** The USGS Landslide probability map and shaking intensity contours of the 2021 Nippes earthquake overlaid on the 2021 population map with the boundary of lowest average annual income within the study region in Haiti (sources noted in the legend).

## **9. FUTURE RESEARCH AGENDA AND RECOMMENDATIONS**

### **9.1. Engineering**

Future engineering research is anticipated to benefit greatly from access to in-situ sampling and testing capabilities; drones for larger scale documentation of landslide, fault rupture, lateral spread, and other forms of liquefaction induced damage; as well as additional installation of citizen based seismic stations. Soil sampling and testing is particularly important for determining the source of failures associated with landslide and lateral spread. Both engineering and social science endeavors explored in this report will strongly benefit from collaborations established between Haitian and U.S. researchers through this reconnaissance. In addition, the intersection of geotechnical, geological, and structural hazards with social/economical/political circumstances and crises in Haiti need to be further explored and evaluated in future studies, involving a transdisciplinary team and methodology.

### **9.2. Social Science**

Moving forward, it is important to consider directions for future research related to the contextual and social-political themes identified in this report. Some examples of potential options for future social science research include:

- Understanding how political, economic, and social-cultural factors are impacting response and recovery efforts.
- Establishing guiding principles for managing appropriate response and recovery in the midst of political instability and the COVID-19 pandemic.
- Assessing specific response and recovery activities undertaken and by various actors (governments, non-profit organizations, local community organizations, etc.).
- Assessing specific response and recovery activities undertaken in different recovery sectors (housing, infrastructure, health and social services, economic development, etc.).
- Exploring lessons learned in response and recovery since the 2010 earthquake.
- Addressing similarities and differences in approaches taken towards response and recovery activities between the 2010 and 2021 earthquakes.
- Understanding the impacts of cascading and intersecting hazards on resilience-building efforts in Haiti.
- Exploring the ways in which engagement, equity, and justice concerns are taken into account in response and recovery efforts.
- Examining how the public could be better prepared for future disasters despite the governance, security and developmental challenges faced.
- Detailing best practices for engaging in ethical data collection efforts in light of the complex political and social environment on the ground in Haiti.

## 10. GUIDING PRINCIPLES FOR POST-DISASTER RESPONSE, RECOVERY, AND MITIGATION IN HAITI

We conclude our report with a summary of key principles that should guide disaster response and recovery efforts in Haiti. These principles are based on our past research on Haiti and preliminary research on the 2021 Nippes earthquake.

*Local involvement and inclusiveness:* Marcelin et al. (2016) highlight the importance of community-based assets (e.g., family networks, solidarity) in meeting the public's basic needs following Hurricane Matthew. Hence, future efforts by international aid agencies and the Haitian government need to build on and integrate these assets while preparing for, responding to and recovering from disaster events. Care should be taken to actively involve all community members in the recovery and disaster risk reduction processes without excluding any person or groups based on gender, race/ethnicity, age, religion, language, social position or economic status (NDRF, 2016).

*Whole Community Recovery:* Beyond physical needs, thought should be given to acknowledging the linkages between individuals, families, social networks, and communities (NDRF, 2016). Attention should be given to preserving cultural identity and promoting a return to normalcy, such as the reopening of schools and religious or civic centers (Sovacool, 2017). As efforts are made toward providing food, shelter, and livelihoods, the psychological and emotional needs of the community should also be addressed in the form of crisis counseling and mental health support customized for each traumatic event (Shultz et al., 2011). Dehumanizing perceptions attributed to a lack of empathy or inclination to help victims (Andrighetto et al., 2014) should be evaluated as a factor that may impact the speed of recovery.

*Resilience and Sustainability:* After a disaster, the recovery phase is a window of opportunity for communities to become more resilient and more sustainable. Those involved in the recovery should identify and address the root causes of current and future vulnerabilities, and use the crisis as a starting point for development and risk reduction (Adger, 2006). This includes community planning, land use decisions, construction and infrastructure design, and addressing environmental concerns, among others.

*Pre-Disaster Mitigation and Recovery Planning:* After a disaster, governments, nongovernmental organizations (NGOs), private sector stakeholders and other community partners (e.g., civic or faith based groups, schools) should engage in pre-disaster and mitigation planning as part of the recovery process. The concurrent hazards and socio-political conflicts in 2021 are an example of the ripple adverse effects on several sectors: education, healthcare, transportation (Rivers, 2021). In Haiti, pre-disaster planning should be integrated into the recovery process in an effort to reduce the impacts of disasters in the future or cascading impacts that occur as a result of the primary crisis.

*Issues of equity and justice:* Response and recovery programs need to address issues of equity and justice to prevent additional tensions and conflicts between those with and without access to aid provided by international and Haitian agencies. Also needed are programs that challenge existing gender inequities and address the mental health and sexual violence impacts of disasters on women. Studies have shown that violence against women and children exponentially increase in the aftermath of disasters in Haiti (CDC & INURED, 2014; Marcelin & Cela, 2017). Prevention of violence against women and child victimization following a disaster must remain one of the paramount objectives of institutions involved in recovery and reconstruction in Haiti.

## 11. REFERENCES

- Adger, W. N. (2006). Vulnerability. *Global Environmental Change*, 16(3), 268–281. 902 doi:10.1016/j.gloenvcha.2006.02.006
- Aljazeera (2021). Haiti elections postponed indefinitely amid political crisis. Accessed on October 22, 2021, from <https://www.aljazeera.com/news/2021/9/28/haiti-elections-postponed-indefinitely-amid-crisis>
- Alphonse, R. (2020). L'administration Moïse/Jouthe se donne un budget de 254 milliards de gourdes. *Le Nouvelliste*. Accessed on September 15, 2021, from <https://lenouvelliste.com/article/221547/ladministration-moisejouthe-se-donne-un-budget-de-254-milliards-de-gourdes>.
- BBC News (2019). Haiti Profile - Timeline. Accessed on September 15, 2021, from <https://www.bbc.com/news/world-latin-america-19548814>
- Beaubien, J. (2013). What Happened To The Aid Meant To Rebuild Haiti? Accessed on September 24, 2021, from <http://www.npr.org/blogs/health/2013/02/28/172875646/what-happened-to-the-aid-meant-to-rebuild-haiti>
- Boulanger, R. W., & Idriss, I. M. (2014). CPT and SPT based liquefaction triggering procedures. *Report No. UCD/CGM.-14, 1*.
- Bradley, M. (2012). Notes from the Field: Haiti-Displacement and Development in the “Republic of NGOs”. Brookings. Accessed on September 23, 2021, from <https://www.brookings.edu/blog/up-front/2012/10/11/notes-from-the-field-haiti-displacement-and-development-in-the-republic-of-ngos/>
- Barchi, F., Singleton, M. K. & Jon F. Merz (2014). Fostering IRB Collaboration for Review of International Research. *The American Journal of Bioethics*, 14(50), 3-8.
- Browne, K., Peek, L. (2014). Beyond the IRB: An ethical toolkit for long-term disaster research. *International Journal of Mass Emergencies and Disasters*, 32(10), 82-120.
- Blanc, J., Rahill, G. J., Laconi, S., & Mouchenik, Y. (2016). Religious beliefs, PTSD, depression and resilience in survivors of the 2010 Haiti earthquake. *Journal of affective disorders*, 190, 697-703.
- Butterlin, J. (1960). *GÉOLOGIE GÉNÉRALE ET RÉGIONALE DE LA RÉPUBLIQUE D'HAÏTI* (Éditions de l'IHEAL ed.). OpenEdition Books. 10.4000/books.iheal.5606
- BUREAU DES MINES ET DE L'ÉNERGIE D'HAÏTI. (1986). Retrieved from <http://www.bme.gouv.ht/carte/index.htm>
- Bent, A. L., Cassidy, J., Prépetit, C., Lamontagne, M., & Ulysse, S. (2018). Real-time seismic monitoring in Haiti and some applications. *Seismological Research Letters*, 89(2A), 407-415.
- BSSC (2003). Building Seismic Safety Council, NEHRP recommended provisions for seismic regulations for new buildings and other structures. Report FEMA-450 (Provisions), Federal Emergency Management Agency (FEMA), Washington.
- CDC & INURED (2014). Violence against Children in Haiti: Findings from a National Survey, 2012. Port-au-Prince, Haiti: Centers for Disease Control and Prevention, 2014. Accessed on November 22, 2021, from [http://www.inured.org/uploads/2/5/2/6/25266591/cdc\\_final\\_haiti\\_05\\_22\\_2014.pdf](http://www.inured.org/uploads/2/5/2/6/25266591/cdc_final_haiti_05_22_2014.pdf)
- Coming Home After Disaster: Multiple Dimensions of Housing Recovery, Boca Raton, FL: CRC Press, Taylor and Francis Group.

- Calais, E., Boisson, D., Symithe, S., Prépetit, C., Pierre, B., Ulyse, S., ... & Clouard, V. (2020). A socio-seismology experiment in Haiti. *Frontiers in Earth Science*, 426.
- Chen, Y. Y., & Koenig, H. G. (2006). Traumatic stress and religion: Is there a relationship? a review of empirical findings. *Journal of Religion and Health*, 45(3), 371-381.
- Collier, P. (2007). *The bottom billion: Why the poorest countries are failing and what can be done about it*: Oxford University Press. New York:, pp. Xiii. Contreras, S. (2019). Using Arnstein's ladder as an evaluative framework for the assessment of participatory work in Postdisaster Haiti. *Journal of the American Planning Association*, 85(3), 219-235.
- Cox, B. R., Bachhuber, J., Rathje, E., Wood, C. M., Dulberg, R., Kottke, A., Green, R.A., & Olson, S. M. (2011). Shear wave velocity and geology-based seismic microzonation of Port-au-Prince, Haiti. *Earthquake Spectra*, 27, 67-92.
- Contreras, S. (2019). Using Arnstein's ladder as an evaluative framework for the assessment of participatory work in Postdisaster Haiti. *Journal of the American Planning Association*, 85(3), 219-235.
- de Utrera, F. C. (1995), Santo Domingo: Dilucidaciones históricas, I-II, 1st ed., 1191 pp., Secr. de Estado de Educ. Bellas Artes y Cultos, Santo Domingo, Dominican Republic.
- DesRoches, R., Comerio, M., Eberhard, M., Mooney, W., & Rix, G. J. (2011). Overview of the 2010 Haiti earthquake. *Earthquake Spectra*, 27(1\_suppl1), 1-21.
- Edmonds, K. (2012). Beyond Good Intentions: The Structural Limitations of NGOs in Haiti. *Critical Sociology*, 39(3), 439-452.
- Elliott, J. & Sullivan, L. (2015). How the Red Cross Raised Half a Billion Dollars for Haiti -and Built Six Homes. ProPublica and NPR. Accessed on September 23, 2021, from <https://www.propublica.org/article/how-the-red-cross-raised-half-a-billion-dollars-for-haiti-i-and-built-6-homes>
- i-and-built-6-homes
- EM-DAT (2011). The International Disaster Database.
- EM-DAT (2021). The International Disaster Database. Accessed on October 23, 2021, from <https://www.emdat.be>
- Eberhard, M. O., Baldrige, S., Marshall, J., Mooney, W., Rix, G. J. (2010a). The mw 7.0 Haiti earthquake of January 12, 2010: USGS/EERI advance reconnaissance team report. US Geological Survey Open-File Report, 1048(2013), 64.
- Fanning, S.C. (2007). The Roots of Early Black Nationalism: Northern African Americans' Invocations of Haiti in the Early Nineteenth Century. *Slavery & Abolition*, 28(1), 61-85.
- Fanm, K. (2012). Appel à la mobilisation citoyenne et à la solidarité en faveur de la construction nationale (Call for citizen mobilization and solidarity in favor of national construction). Port-au-Prince, Haiti: Kay Fanm, 1639.
- Flores, C.F., ten Brink, U.S., and Bakun, W.H., 2012, Accounts of damage from historical earthquakes in the northeastern Caribbean to aid in the determination of their location and intensity magnitudes: U.S. Geological Survey, Open-File Report 2011-1133, 237 p., at <https://pubs.usgs.gov/of/2011/1133>.
- Frankel, A., Harmsen, S., Mueller, C., Calais, E., & Haase, J. (2011). Seismic hazard maps for Haiti. *Earthquake Spectra*, 27(1\_suppl1), 23-41.

- Geomatrix (2007). Seismicity Update for U.S. Department of State New Embassy Compound in Santo Domingo, Dominican Republic. Report, San Francisco.
- Green, R. A., Olson, S. M., Cox, B. R., Rix, G. J., Rathje, E., Bachhuber, J., French, J., Lasley, S., & Martin, N. (2011). Geotechnical aspects of failures at Port-au-Prince seaport during the 12 January 2010 Haiti earthquake. *Earthquake Spectra*, 27, 43-65.
- Ganapati, N. E., & Rahill, G. J. (2017). In Sapat, A. and A. M. Esnard (Eds). *Early Post-Disaster shelter Recovery in Fragile States: A Case of the 12 January 2010 Haiti Earthquake* (pp. 161-174).
- Galea, S., Nandi, A., & Vlahov, D. (2005). The epidemiology of post-traumatic stress disorder after disasters. *Epidemiologic reviews*, 27(1), 78-91.
- Ganapati, N. E., & Mukjerji, A. (2019). In Edwards, F. (Ed.). 'House Keeping': Managing Post-Disaster Housing Recovery Long Term (pp. 167-192). *Housing Recovery After Disaster*. Boulder, CO, Lexington Books.
- Gruebner, O., Lowe, S. R., Tracy, M., Cerdá, M., Joshi, S., Norris, F. H., & Galea, S. (2016). The geography of mental health and general wellness in Galveston bay after hurricane Ike: a spatial epidemiologic study with longitudinal data. *Disaster Medicine and Public Health Preparedness*, 10(2), 261-273.
- Gaillard, J. C., Peek, L. (2019). Disaster-zone research needs a code of conduct. *Nature*. Accessed on November 3, 2021, from [https://www.nature.com/articles/d41586-019-03534z?fbclid=IwAR1Jjp579\\_awGJl2mTkpcmuNrr8WXfXK\\_lne5wCycQ8hIDW7tj\\_-kdO47r0](https://www.nature.com/articles/d41586-019-03534z?fbclid=IwAR1Jjp579_awGJl2mTkpcmuNrr8WXfXK_lne5wCycQ8hIDW7tj_-kdO47r0)
- GEER Association Report No. GEER 021, [http://www.geerassociation.org/GEER\\_Post%20EQ%20Reports/Haiti\\_2010/Cover\\_Haiti10.html](http://www.geerassociation.org/GEER_Post%20EQ%20Reports/Haiti_2010/Cover_Haiti10.html).
- Remington, C. L., & Ganapati, N. E. (2017). Recovery worker skills in post-earthquake Haiti: the disconnect between employer and employee perspectives. *Natural Hazards*, 87(3), 1673-1690.
- Green, R. A., Olson, S. M., Cox, B. R., Rix, G. J., Rathje, E., Bachhuber, J., French, J., Lasley, S., & Martin, N. (2011). Geotechnical aspects of failures at Port-au-Prince seaport during the 12 January 2010 Haiti earthquake. *Earthquake Spectra*, 27, 43-65.
- Guy, M.R., Patton, J.M., Fee, J., Hearne, M., Martinez, E.M., Ketchum, D.C., Worden, C.B., Quitoriano, V., Hunter, E.J., Smoczyk, G.M. and Schwarz, S.: National Earth-quake Information Center systems overview and integration. US Department of the Interior, US Geological Survey (2015). N3. (Last accessed 06 Sep 2021)
- Hearne, M., E. M. Thompson, H. Schovanec, J. Rekoske, B. T. Aagaard, and C. B. Worden (2019). USGS automated ground motion processing software, USGS Software Release, doi: 10.5066/P9ANQXN3. (Last accessed 06 Sep 2021)
- Hough, S. E., Yong, A., Altidor, J. R., Anglade, D., Given, D., & Mildor, S. L. (2011). Site characterization and site response in Port-au-Prince, Haiti. *Earthquake Spectra*, 27, 137-155.
- Hough, S. E., Yong, A., Altidor, J. R., Anglade, D., Given, D., & Mildor, S. L. (2011). Site characterization and site response in Port-au-Prince, Haiti. *Earthquake Spectra*, 27, 137-155.
- Hearne, M., E. M. Thompson, H. Schovanec, J. Rekoske, B. T. Aagaard, and C. B. Worden (2019). USGS automated ground motion processing software, USGS Software Release, doi: 10.5066/P9ANQXN3.
- Haiti Libre (2021). Haiti - Security : Already 119 kidnapping this month ! Accessed on October 20, 2021, from <https://www.haitilibre.com/en/news-35048-haiti-security-already-119-kidnapping-this-month.html>
- Hallward, P. (2007). *Damming the flood: Haiti, Aristide, and the politics of containment*. Verso.

Human Rights Watch (2020). World Report 2021: Haiti. Accessed on September 16, 2021, from <https://www.hrw.org/world-report/2021/country-chapters/haiti>

Hough, S. E., Yong, A., Altidor, J. R., Anglade, D., Given, D., & Mildor, S. L. (2011). Site characterization and site response in Port-au-Prince, Haiti. *Earthquake Spectra*, 27, 137-155.

Iwasaki T, Tatsuoka F, Tokida KI, and Yasuda S. (1978). A practical method for assessing soil liquefaction potential based on case studies at various sites in Japan. *In: Proceedings of the second international conference on Microzonation*; 2

Internal Displacement Monitoring Centre (n.d.). Country Information. Accessed on September 29, 2021, from <https://www.internal-displacement.org/countries/haiti>

International Organization of Migration (2021). Earthquake 14 August 2021 - SITREP 1. Accessed on September 29, 2021, from [https://displacement.iom.int/system/tdf/reports/IOM\\_DTM\\_EARTHQUAKE%2014%20AUGUST%2021\\_SITREP%201%5B18%5D.pdf?file=1&type=node&id=12212](https://displacement.iom.int/system/tdf/reports/IOM_DTM_EARTHQUAKE%2014%20AUGUST%2021_SITREP%201%5B18%5D.pdf?file=1&type=node&id=12212)

International Organization of Migration (2021). Flow Monitoring on 20 Border Crossing Points between Haiti and the Dominican Republic. The United Nations Migration Agency. Accessed on September 24, 2021, from [https://haiti.iom.int/sites/haiti/files/documents\\_files/IOM\\_Flow%20Monitoring\\_Weekly%20Sit\\_Rep\\_SPECIAL%20EDITION\\_ENG%281%29.pdf](https://haiti.iom.int/sites/haiti/files/documents_files/IOM_Flow%20Monitoring_Weekly%20Sit_Rep_SPECIAL%20EDITION_ENG%281%29.pdf)

Judy, B., KARRAY, M. and PAULTRE, P., 2014. Microzonage sismique de la ville des cayes (haïti) (Doctoral dissertation, Université de Sherbrooke).

Joint Research Centre (JRC), 2021. Mw 7.2 Earthquake and Tsunami in Haiti.

Jean-Baptiste, M. C. (2021). Haiti: The Rule of Law in Peril. ILAC Report. Accessed on October 26, 2021, from <https://ilacnet.org/publications/haiti-the-rule-of-law-in-peril/>

Joseph, C., Symithe, S., Cazeau, H., & Dornevil, W. (2017). Country document for disaster risk reduction: Haiti, 2016. United Nations Office for Disaster Risk Reduction – Regional Office for the Americas and the Caribbean Haiti - Government. Accessed on October 19, 2021, from <https://www.undrr.org/publication/country-document-disaster-risk-reduction-haiti-2016>

Joshi, M., Rahill, G. J., & Rhode, S. (2021). Comparison of Trauma Symptoms Among Nonpartner Sexual Violence Victims and Nonvictims in Urban Haiti's Cité Soleil Neighborhood. *Journal of Black psychology*, 0095798421997217.

Knowles R., Markley B., Buckalew J., Waite L. (1999), L'évaluation des ressources en eau d'Haïti, United States Southern command, Corps d'Ingénieurs

Kristoff, M. & Panarelli, L. (2010). Haiti: A Republic of NGOs? United States Institute of Peace: Peace Brief. Accessed on September 23, 2021, from <https://www.usip.org/sites/default/files/PB%2023%20Haiti%20a%20Republic%20of%20NGOs.pdf>

Kroll, A., Remington, C. L., Awasthi, P., & Ganapati, N. E. (2021). Mitigating the negative effects of emotional labor: A study of disaster response and recovery workers after the 2010 Haiti earthquake. *Governance*, 34(1), 87-106.

Kwok, T.C. (2016). Continued Challenges in Rebuilding Haiti. Accessed on September 24, 2021, from <https://www.e-ir.info/2016/03/11/continued-challenges-in-rebuilding-haiti/>

Le Nouvelliste (2021). Covid-19 : Les variants Delta et MU présents en Haïti, selon le MSPP. Accessed on September 24, 2021, from <https://lenouvelliste.com/alamminute/19727/covid-19-les-variants-delta-et-mu-presents-en-haiti-selon-le-mspp>

London, L. (2002). Ethical oversight of public health research: Can rules and IRBs make a difference in developing countries? *American Journal of Public Health*, 92(7): 1079–1084.

Louis-Charles, H. M., Howard, R., Remy, L., Nibbs, F., & Turner, G. (2020). Ethical Considerations for Postdisaster Fieldwork and Data Collection in the Caribbean. *American Behavioral Scientist*, 64(8), 1129–1144.

Lerner, A. B. (2019). Theorizing collective trauma in international political economy. *International Studies Review*, 21(4), 549-571.

Makwana, N. (2019). Disaster and its impact on mental health: A narrative review. *Journal of family medicine and primary care*, 8(10), 3090-3095.

Mao, W., & Agyapong, V. I. (2021). The Role of Social Determinants in Mental Health and Resilience After Disasters: Implications for Public Health Policy and Practice. *Frontiers in Public Health*, 9.

Marcelin, L. H., Cela, T., & Shultz, J. M. (2016). Haiti and the politics of governance and community responses to Hurricane Matthew. *Disaster health*, 3(4), 151-161.

McKey, C. (2016). Doctoral Dissertation. The Economic Consequences of the Haitian Revolution. University of Oregon.

Mann, P., Schubert, C., & Burke, K. (1990). Review of Caribbean neotectonics. IN: The geology of North America. Vol. H-The Caribbean region. Boulder, 1990, 307-338.

Mann, P., Taylor, F. W., Edwards, R. L., & Ku, T. L. (1995). Actively evolving microplate formation by oblique collision and sideways motion along strike-slip faults: An example from the northeastern Caribbean plate margin. *Tectonophysics*, 246(1-3), 1-69.

Mérancourt, W., & Faiola, A. (2021). Abductions by the busload: Haitians are being held hostage by a surge in kidnappings. *Washington Post*. Accessed on October 9, 2021, from <https://www.washingtonpost.com/world/2021/10/09/haiti-kidnapping/>

Ministère de Santé publique de la Population (2021). Bilan Vaksinasyon Kont Covid-19. Accessed on September 24, 2021, from <https://www.mspp.gouv.ht/wp-content/uploads/BILAN-VAKSINASYON-COVID-nan-dat-18-a-21-septanm-2021.pdf>

MapAction website: <https://storymaps.arcgis.com/stories/455b4d68f08148b2bc7bbc8492749f55>

MapAction, 2021. Aid item distribution in the shelter sector (as 22 September 2021) <https://reliefweb.int/map/haiti/haiti-aid-item-distribution-shelter-sector-22-sept-2021>

MapAction, 2008. Population Density by Commune (19 September 2008). Haiti: Population density by Commune (19 Sep 08) - Datasets - MapAction

Moloney, Anastasia (2020). A decade after U.N.-linked cholera outbreak, Haitians demand justice. *Reuters*. Accessed on October 22, 2021, from <https://www.reuters.com/article/us-haiti-cholera-un-feature-trfn/a-decade-after-u-n-linked-cholera-outbreak-haitians-demand-justice-idUSKBN2772RM>

Mukherji, A., Ganapati, N. E., & Rahill, G. (2014). Expecting the unexpected: field research in post-disaster settings. *Natural hazards*, 73(2), 805-828.

National Public Radio (2021). Delivering humanitarian aid to the people of Haiti has never been more dangerous. Accessed on October 26, 2021, from <https://www.npr.org/2021/10/23/1048646275/delivering-humanitarian-aid-to-the-people-of-haiti-has-never-been-more-dangerous>

Norris, F. H., & Wind, L. H. (2012). The experience of disaster: Trauma, loss, adversities, and community effects.

National Disaster Recovery Framework. (NDRF) | Federal Emergency Management Agency (2016) Retrieved from <https://www.fema.gov/emergency-managers/national-preparedness/frameworks/recovery>

O'Grady, K. A., Rollison, D. G., Hanna, T. S., Schreiber-Pan, H., & Ruiz, M. A. (2012). Earthquake in Haiti: Relationship with the sacred in times of trauma. *Journal of Psychology and theology*, 40(4), 289-301.

Olson, S. M., Green, R. A., Lasley, S., Martin, N., Cox, B. R., Rathje, E., Bachhuber, J., & French, J. (2011). Documenting liquefaction and lateral spreading triggered by the 12 January 2010 Haiti earthquake. *Earthquake Spectra*, 27, 93-116.

Organisation for Economic Co-operation and Development (2021). ODA to America - Summary. Accessed on September 28, from <https://www.oecd.org/countries/haiti/aid-at-a-glance.htm#recipients>

Olson, S. M., Green, R. A., Lasley, S., Martin, N., Cox, B. R., Rathje, E., Bachhuber, J., & French, J. (2011). Documenting liquefaction and lateral spreading triggered by the 12 January 2010 Haiti earthquake. *Earthquake Spectra*, 27, 93-116.

O'Loughlin, K.F., and Lander, J.F., 2003, Caribbean tsunamis, a 500-year history from 1498-1998: Kluwer Academic Publishers, The Netherlands, 263 p.

OpenstreetMap, <https://pierzen.dev.openstreetmap.org/>

Pan American Health Organization (2015). Epidemiological Updates: Cholera. Accessed on October 23, 2021, from <https://www.paho.org/hq/dmdocuments/2015/2015-dec-23-cha-cholera-epi-update.pdf>

Pew Research Center (2019). Remittance flows worldwide in 2017. Accessed on September 14, 2021, from <https://www.pewresearch.org/global/interactives/remittance-flows-by-country/>.

Pritchett, L., Woolcock, M., & Andrews, M. (2013). Looking like a state: techniques of persistent failure in state capability for implementation. *The Journal of Development Studies*, 49(1), 1-18.

Rahill, G. J., Joshi, M., Galea, J., & Ollis, J. (2020). Experiences of sexual and gender minorities in an urban enclave of Haiti: Despised, beaten, stoned, stabbed, shot and raped. *Culture, health & sexuality*, 22(6), 690-704.

Rathje, E., Bachhuber, J., Cox, B., French, J., Green, R. A., Olson, S., Rix, G., Wells, D., and Suncar, O., 2010. Geotechnical Engineering Reconnaissance of the 2010 Haiti Earthquake, GEER Association Report No. GEER 021, [http://www.geerassociation.org/GEER\\_Post%20EQ%20Reports/Haiti\\_2010/Cover\\_Haiti10.html](http://www.geerassociation.org/GEER_Post%20EQ%20Reports/Haiti_2010/Cover_Haiti10.html).

Rahill, G. J., Joshi, M., Lescano, C., & Holbert, D. (2015). Symptoms of PTSD in a sample of female victims of sexual violence in post-earthquake Haiti. *Journal of Affective disorders*, 173, 232-238.

Rahill, G. J., Ganapati, N. E., Clérismé, J. C., & Mukherji, A. (2014). Shelter recovery in urban Haiti after the earthquake: the dual role of social capital. *Disasters*, 38(s1), S73-S93.

Rahill, G. J., Ganapati, N. E., Joshi, M., Bristol, B., Molé, A., Jean-Pierre, A., et al. (2016). In their own words: Resilience among Haitian survivors of the 2010 earthquake. *Journal of health care for the poor and underserved*, 27(2), 580-603.

Rathje, E., Bachhuber, J., Cox, B., French, J., Green, R. A., Olson, S., Rix, G., Wells, D., and Suncar, O., 2010. Geotechnical Engineering Reconnaissance of the 2010 Haiti Earthquake, GEER Association Report No. GEER 021, [http://www.geerassociation.org/GEER\\_Post%20EQ%20Reports/Haiti\\_2010/Cover\\_Haiti10.html](http://www.geerassociation.org/GEER_Post%20EQ%20Reports/Haiti_2010/Cover_Haiti10.html).

Remington, C. L., & Ganapati, N. E. (2017). Recovery worker skills in post-earthquake Haiti: the disconnect between employer and employee perspectives. *Natural Hazards*, 87(3), 1673-1690.

Reuters (2021). Haiti since the assassination of President Moïse. Accessed on September 24, 2021, from <https://www.reuters.com/world/americas/haiti-one-month-without-assassinated-president-jovenel-moise-2021-08-06/>

Rivers, M. (2021). Amid a cascade of crises, Haiti's fuel shortage could be the worst. CNN. Accessed on November 10, 2021, from <https://www.cnn.com/2021/10/26/world/haiti-fuel-hospital-intl-latam/index.html>

Scherer, J., 1912, Great earthquakes in the Island of Haiti: *Bulletin of the Seismological Society of America*, v. 2, p. 161-180.

Schuller, M. (2017). Haiti's 'republic of NGOs'. *Current History*, 116(787), 68-73.

Sperling, D. (2017). In 1825, Haiti Paid France \$21 Billion To Preserve Its Independence -- Time For France To Pay It Back. *Forbes*.

Sovacool, Benjamin K. "Don't Let Disaster Recovery Perpetuate Injustice." *Nature (London)* 549.7673 (2017): 433-433.

Sontag, D. (2012). Years After Haiti Quake, Safe Housing Is a Dream for Many. *New York Times*. Accessed on September 23, 2021, from <https://www.nytimes.com/2012/08/16/world/americas/years-after-haiti-quake-safe-housing-is-dream-for-multitudes.html>

Shultz, J. M., Cela, T., Marcelin, L. H., Espinola, M., Heitmann, I., Sanchez, C., et al. (2016). The trauma signature of 2016 Hurricane Matthew and the psychosocial impact on Haiti. *Disaster health*, 3(4), 121-138.

Shultz, J. M., Marcelin, L. H., Madanes, S. B., Espinel, Z., & Neria, Y. (2011). The "Trauma Signature:" understanding the psychological consequences of the 2010 Haiti earthquake. *Prehospital and disaster medicine*, 26(5), 353-366.

Suleiman, L. (2013). The NGOs and the Grand Illusions of Development and Democracy. *Voluntas*, 24, pp. 241-261.

ten Brink, U. S., Bakun, W. H., & Flores, C. H. (2011). Historical perspective on seismic hazard to Hispaniola and the northeast Caribbean region. *Journal of Geophysical Research: Solid Earth*, 116(B12).

United Nations Conference on Trade and Development (2020). UN list of least developed countries. Accessed on October 22, 2021, from <https://unctad.org/topic/least-developed-countries/list>

United Nations Development Program (2010). 2010 Human Development Report: Latin America and Caribbean approaching EU, US levels in life expectancy, school. Accessed on October 21, from [https://www.europarl.europa.eu/meetdocs/2009\\_2014/documents/dlat/dv/hdr2010\\_undp/\\_hdr2010\\_undp\\_en.pdf](https://www.europarl.europa.eu/meetdocs/2009_2014/documents/dlat/dv/hdr2010_undp/_hdr2010_undp_en.pdf)

United Nations Development Programme (2015). Human Development Reports: Human Development Index (HDI). Accessed on September 24, 2021, from <http://hdr.undp.org/en/content/human-development-index-hdi>

United Nations Development Programme (2020). Human Development Report. The Next Frontier: Human Development and the Anthropocene. Accessed on October 23, 2021, from <http://hdr.undp.org/sites/default/files/Country-Profiles/HTI.pdf>

United Nations Integrated Office in Haiti (2021). Report of the Secretary General. Accessed on September 24, 2021, from [https://binuh.unmissions.org/sites/default/files/sg\\_report\\_on\\_haiti\\_binuh\\_e\\_11\\_june\\_2021.pdf](https://binuh.unmissions.org/sites/default/files/sg_report_on_haiti_binuh_e_11_june_2021.pdf)

United States Agency for International Development (USAID), 2010. Map of EarthquakeAffected Areas and Population Movement in Haiti, [http://www.usaid.gov/our\\_work/humanitarian\\_assistance/disaster\\_assistance/countries/haiti/template/maps/fy2011/haiti\\_10222010.Pdf](http://www.usaid.gov/our_work/humanitarian_assistance/disaster_assistance/countries/haiti/template/maps/fy2011/haiti_10222010.Pdf)

U.S. Agency for International Development (USAID). 2013. FACT SHEET#1: HAITI – HURRICANE SANDY. Retrieved from <https://www.usaid.gov/sites/default/files/documents/1866/02.15.13%20-%20Haiti%20Hurricane%20Sandy%20Fact%20Sheet.pdf>

U.S. Agency for International Development (USAID). 2017. FACT SHEET#19: CARIBBEAN – HURRICANE MATTHEW. Retrieved from [https://www.usaid.gov/sites/default/files/documents/1866/04.04.17\\_-\\_USAID\\_DCHA\\_Caribbean\\_Hurricane\\_Matthew\\_Fact\\_Sheet\\_19.pdf](https://www.usaid.gov/sites/default/files/documents/1866/04.04.17_-_USAID_DCHA_Caribbean_Hurricane_Matthew_Fact_Sheet_19.pdf)

United States Agency for International Development (USAID), 2015. Haiti Rural Livelihood Profiles. April 2015.

USGS, 2021. Magnitude 7.2 earthquake in Haiti website: Magnitude 7.2 Earthquake in Haiti ([usgs.gov](https://usgs.gov))

USGS, 2021 ground failure maps. Last updated 19 August 2021 <https://earthquake.usgs.gov/earthquakes/eventpage/us6000f65h/ground-failure/summary>

USGS, 2021 ground failure maps. Last updated 19 August 2021 <https://earthquake.usgs.gov/earthquakes/eventpage/us6000f65h/ground-failure/summary>

United Nations Office for Coordination of Humanitarian Assistance (n.d.). Haiti - Internally displaced persons - IDPs. Accessed on September 29, 2021, from <https://data.humdata.org/dataset/idmc-idp-data-for-haiti>

UN International Strategy for Disaster Reduction (UNISDR) | Department of Economic and Social Affairs. (2013). Retrieved from <https://sdgs.un.org/ar/node/8377>

United Nations Population Fund (2012). Gender-based Violence and Natural Disasters in Latin America and the Caribbean. Accessed on November 4, 2021, from <http://lac.unfpa.org/webdav/site/lac/shared/IMAGES/2012/Violencia%20de%20genero/UNFPA%20version%20ingles.pdf>

United Nations Security Council Report (2020). Chronology of Events. Accessed on September 29, 2021, from <https://www.securitycouncilreport.org/chronology/haiti.php>

Université Quisqueya (2021). Report #1 on the implementation of Quisqueya University's response to the earthquake. Accessed on September 10, 2021, from [uniq.edu.ht/soutenir-l-uniq-urgence-seisme-sud/](http://uniq.edu.ht/soutenir-l-uniq-urgence-seisme-sud/)

World Bank (n.d.). GDP per Capita (current US\$). Accessed on September 29, 2021, from [https://data.worldbank.org/indicator/NY.GDP.PCAP.CD?end=2020&locations=CO-BO-HT-MX-EC-CU-PE-HN-GT-NI&most\\_recent\\_year\\_desc=false&start=2010&view=chart](https://data.worldbank.org/indicator/NY.GDP.PCAP.CD?end=2020&locations=CO-BO-HT-MX-EC-CU-PE-HN-GT-NI&most_recent_year_desc=false&start=2010&view=chart)

World Bank (2011b). World Development Report 2011: Conflict, Security, and Development. Washington, DC: World Bank.

- World Bank (2019). Rebuilding Haitian Infrastructure and Institutions. Results Briefs. Accessed on October 23, 2021, from <https://www.worldbank.org/en/results/2019/05/03/rebuilding-haitian-infrastructure-and-institutions>
- World Bank (2021). Haiti Overview. Accessed on September 12, 2021, from <https://www.worldbank.org/en/country/haiti/overview>
- Willman, A., & Marcelin, L. H. (2010). "If they could make us disappear, they would!" Youth and Violence in Cite Soleil, Haiti. *Journal of Community Psychology*, 38(4), 515-531.
- Wdowinski, S. and Tsukanov, I., 2011, December. Disaster triggers disaster: Earthquake triggering by tropical cyclones. In AGU Fall Meeting Abstracts (Vol. 2011, pp. U53E-06).
- Woodring, W.P., J.S. Brown, and W.S. Burbank. Geology of the Republic of Haiti. Department of Public Works, Baltimore, Maryland: Lord Baltimore Press, 1924.
- Wald, D. J., & Allen, T. I. (2007). Topographic slope as a proxy for seismic site conditions and amplification. *Bulletin of the Seismological Society of America*, 97(5), 1379-1395.
- Witze, A. (2021). "Home seismometers provide crucial data on Haiti's quake," *Nature*, Vol. 597,18-19. doi: <https://doi.org/10.1038/d41586-021-02279-y>
- World Health Organization (2002). World Report on Violence and Health. Accessed on November 4, 2021, from [http://www.who.int/violence\\_injury\\_prevention/violence/global\\_campaign/en/chap6.pdf](http://www.who.int/violence_injury_prevention/violence/global_campaign/en/chap6.pdf)
- World Bank Group (2015). Haiti: Towards a New Narrative Systematic Country Diagnostic. Accessed on October 26, 2021, from Haiti - World Bank Documents <http://documents1.worldbank.org/curated/pdf>
- World Bank (2020). GDP per Capita (current US\$). Accessed on September 29, 2021, from [https://data.worldbank.org/indicator/NY.GDP.PCAP.CD?end=2020&locations=CO-BO-HT-MX-EC-CU-PE-HN-GT-NI&most\\_recent\\_year\\_desc=false&start=2010&view=chart](https://data.worldbank.org/indicator/NY.GDP.PCAP.CD?end=2020&locations=CO-BO-HT-MX-EC-CU-PE-HN-GT-NI&most_recent_year_desc=false&start=2010&view=chart)
- World Population Review. Haiti Population 2021. Accessed on September 12, 2021, from <https://worldpopulationreview.com/countries/haiti-population>.
- Xinhua (2010). Haitians face catastrophic situation, says ICRC. China Internet Information Center. Accessed on October 24, 2021, from [https://docs.google.com/document/d/1kHsDlGBI-AMtLSZXIvahu0dpnbP2dfIthry\\_f8IuyxU/edit](https://docs.google.com/document/d/1kHsDlGBI-AMtLSZXIvahu0dpnbP2dfIthry_f8IuyxU/edit)
- Zanotti, L. (2010). Cacophonies of Aid, Failed State Building and NGOs in Haiti: setting the stage for disaster, envisioning the future. *Third World Quarterly*, 31(5), 755-771.